

**A novel wearable electronic device for
treating neurogenic detrusor overactivity
by conditional neuromodulation**

by

Nuwani Ayantha Edirisinghe

A thesis submitted in accordance with the requirements of the
University College London for the
degree of Master of Philosophy

Department of Medical Physics and Bioengineering
University College London

October 2011

'I, Nuwani Ayantha Edirisinghe confirm that the work presented in this thesis is my own. Where information has been derived from other sources, I conform that this has been indicated in the thesis '

Abstract

Urinary incontinence is the involuntary leakage of urine and affects one in twenty of the population across all ages leading to poor quality of life and can be very high cost to the nation. It is possible to reduce these costs by accurate diagnosis and appropriate management of the condition. Urinary incontinence is often associated with an overactive bladder or urethral sphincter weakness, or both as a result of interrupting the pathway to nervous communication between the brain and the bladder leading to uncoordinated activity in the lower urinary tract.

Treatment options for overactive bladder include antimuscarinic drugs and implanted electrical stimulators. However these drugs have intolerable side effects, while implanting a stimulator is a surgical procedure which is associated with degree of risk and becomes ineffective due to habituation to the continuous stimulation.

The aim of the research was to develop a novel wearable anal device designed to deliver conditional neuromodulation. The device detects the electromyography activity in the lower urinary tract, and provides the transrectal stimulation to the Pudendal nerve when required, in order to suppress the bladder contractions while contracting the urethral sphincters.

The clinical study included designing and manufacturing patient compatible model and conducting a clinical study to measure the safety and the efficacy of the device. Electronics circuit design included amplifier, signal processing system and constant current stimulator based on the specification derived from the clinical study and finally focused on optimisation of the device electrodes for improving stimulating parameters.

Acknowledgements

I would like to thank my supervisors Prof. Michael Craggs and Prof. Nick Donaldson, who helped to make this project a reality and also for their invaluable guidance and technical assistance. It has been my privilege to have been supervised by two masters in the field.

Many thanks also to:

Dr. Brian Leaker for providing me with the much needed financial support.

Sister Judith Susser and Dr. Sarah Knight, clinical staff in the Royal National Orthopaedic Hospital, for their immense support as well as all the patients that participated in this study for donating their valuable time.

Dr. Upul Gamage, who helped to develop my knowledge on anatomy and physiology; also for his support and guidance throughout the writing of this thesis.

Tim Perkins, Kylie de Jager and Runhan Luo for their support and friendship, which always kept me going during the years of my research.

The Engineering and Physical Science Research Council (EPSRC) and the University College London for awarding the Dorothy Hodgkin postgraduate award to support my project.

My dearest parents, my mother-in-law, my brothers and sisters, whom always backed me up, when I was down and their support. My little Kalani, Chalani and Nikini for taking the stress away. This thesis would be just a dream, without the support of my eldest brother and his wife.

Finally, special thanks to my loving husband, for his words of encouragement in my endeavours and understanding during stressful times, without whom this thesis would have been impossible.

Table of contents

Abstract	- 3 -
Acknowledgements	- 4 -
Table of contents.....	- 5 -
List of abbreviations.....	- 9 -
List of figures	- 11 -
List of tables	- 17 -
Chapter 1 - Introduction.....	- 19 -
1.1 Background	- 19 -
1.2 Aim of the project.....	- 22 -
1.3 Publications	- 22 -
1.4 Thesis outline	- 23 -
Chapter 2 - Bladder inhibition – beyond nature	- 25 -
2.1 Introduction	- 25 -
2.2 Anatomy and physiology of the lower urinary tract.....	- 25 -
2.2.1 Anatomy of the lower urinary tract	- 25 -
2.2.2 Innervation of bladder and sphincter.....	- 26 -
2.2.3 Physiology of urination	- 29 -
2.3 Causes for bladder dysfunction	- 35 -
2.3.1 Supraspinal lesions.....	- 35 -
2.3.2 Spinal cord lesions.....	- 36 -
2.3.3 Peripheral nerve lesions.....	- 37 -
2.4 Treating and managing urinary incontinence.....	- 38 -
2.4.1 Medication.....	- 39 -
2.4.2 Absorbent products.....	- 40 -
2.5 Electrical stimulation for bladder inhibition	- 42 -
2.5.1 Neurostimulation and neuromodulation.....	- 42 -
2.5.2 History of neural prostheses.....	- 42 -
Chapter 3 - The project concept	- 49 -
3.1 Introduction	- 49 -
3.2 Background	- 49 -

3.3	Design requirements.....	- 50 -
3.3.1	Wearable device	- 50 -
3.3.2	Conditional stimulation	- 51 -
3.3.3	Warning indicator.....	- 52 -
3.3.4	Cost.....	- 52 -
3.4	Design principle	- 53 -
3.4.1	Detecting NDO.....	- 53 -
3.4.2	Treating NDO.....	- 56 -
3.5	The project concept	- 59 -
3.6	Study design	- 59 -
3.7	Other considerations.....	- 61 -
3.7.1	Clinical setting.....	- 61 -
3.7.2	Ethics approval	- 63 -
3.7.3	Diagnosing bladder dysfunction.....	- 63 -
Chapter 4 -	Realisation of the design.....	- 65 -
4.1	Introduction	- 65 -
4.2	Previous models	- 65 -
4.3	Shape consideration – anatomically	- 72 -
4.3.1	Anatomical stability of ACONTI.....	- 74 -
4.3.2	Effective recording of the EMG signals.....	- 75 -
4.3.3	Optimal stimulation to the Pudendal nerve	- 76 -
4.4	Material consideration	- 78 -
4.4.1	Device material.....	- 78 -
4.4.2	Electrode material.....	- 80 -
4.5	Manufacturing of the device.....	- 81 -
4.6	Conclusion.....	- 89 -
Chapter 5 -	Clinical efficacy of the ACONTI	- 90 -
5.1	Introduction	- 90 -
5.2	Background	- 90 -
5.3	Aim and objectives.....	- 91 -
5.4	Clinical set up.....	- 91 -
5.4.1	Participant selection	- 92 -

5.4.2	Experimental setup	- 95 -
5.5	Detecting NDO	- 100 -
5.5.1	Objective	- 100 -
5.5.2	Experimental protocol	- 100 -
5.5.3	Results and analysis.....	- 101 -
5.5.4	Discussion	- 115 -
5.6	Suppressing the detrusor overactivity through the device.....	- 117 -
5.6.1	Objective	- 117 -
5.6.2	Method.....	- 118 -
5.6.3	Experimental protocol	- 119 -
5.6.4	Results and analysis.....	- 120 -
5.6.5	Discussion	- 142 -
Chapter 6 -	Design and realisation of the electronic circuitry	- 144 -
6.1	Introduction	- 144 -
6.2	Aim and objectives	- 145 -
6.3	Amplification and signal processing	- 146 -
6.3.1	Background	- 146 -
6.3.2	System that is being used in clinical setting.....	- 149 -
6.3.3	Derivation of the required system	- 153 -
6.3.4	Realisation of the circuit.....	- 154 -
6.4	Stimulator design.....	- 183 -
6.4.1	Background	- 183 -
6.4.2	System that is being used in clinical setting.....	- 184 -
6.4.3	Derivation of the specification for the stimulator	- 186 -
6.4.4	Realisation of the stimulator.....	- 186 -
6.5	Overall system testing	- 204 -
6.6	Results and discussion.....	- 205 -
6.6.1	Power management	- 206 -
6.6.2	Other considerations.....	- 207 -
6.7	Conclusion.....	- 207 -
Chapter 7 -	Conclusions and future work.....	- 209 -
7.1	Summary	- 209 -

7.2	Achievements	- 211 -
7.3	Future work	- 212 -
7.3.1	Clinical testing.....	- 212 -
7.3.2	Optimising the device.....	- 212 -
7.3.3	Regulatory approval	- 214 -
	References	Error! Bookmark not defined.
	Appendix 1 – Patient consent form.....	- 232 -
	Appendix 2 – Multiple feedback filter design	- 234 -

List of abbreviations

ACONTI	Anal conditional neuromodulator for treating incontinence
AISI	American iron and steel institute
ARJ	Anal rectal junction
ASIA	American spinal injury association
BAN	Body area network
CAP	Compound action potential
CED	Cambridge electronic devices
CISC	Clean intermittent self catheterisation
CMG	Cystometrogram
CMRR	Common mode rejection ratio
CN	Conditional neuromodulation
DGN	Dorsal genital nerve
DH	Detrusor hyperreflexia
DSD	Detrusor sphincter dyssynergia
EAS	External anal sphincter
ECF	Extracellular field
EMG	Electromyogram
ES	Electrical stimulation
EUS	External urethral sphincter
FC	Foley catheter
ICF	Intracellular field
IP	Incontinence pad
LSR	Liquid silicone rubber
LUT	Lower urinary tract
M	Medication
MCC	Maximum cystometric capacity
MEP	Motor evoked potential
MHRA	Medicine and healthcare products regulatory agency
MS	Multiple sclerosis

NAFC	National Association for Continence
NDO	Neurogenic detrusor overactivity
NHS	National Health Service
NRES	National research ethics system
PCB	Printed circuit board
PMC	Pontine micturition centre
PTNS	Percutaneous tibial nerve stimulation
RNOH	Royal National Orthopaedic Hospital
SARSI	Sacral anterior root stimulator implant
SCI	Spinal cord injury
SENIAM	Surface electromyography for the non-invasive assessment of muscles
SWG	Standard wire gauge
UI	Urinary incontinence
US	Urethral sphincters
UTI	Urinary tract infections
VFC	Volume at first contraction

List of figures

Figure 2:1 - Coronal section of the male near urinary bladder.	- 26 -
Figure 2:2- Block diagram of the neural control of the lower urinary tract.....	- 28 -
Figure 2:3- Micturition cycle of a healthy adult.....	- 30 -
Figure 2:4 - Storage phase.....	- 32 -
Figure 2:5 - Voiding phase.....	- 34 -
Figure 2:6 - The lateral view of the spinal cord segments.	- 37 -
Figure 2:7 – Annual cost of conventional methods.....	- 41 -
Figure 2:8 – Cumulative bladder and bowel care cost.	- 41 -
Figure 2:9 – SARSI.....	- 47 -
Figure 3:1 – “InterStim” implant.....	- 53 -
Figure 3:2 - Anal (left) and vaginal (right) electrode carriers.	- 58 -
Figure 3:3 – The project concept.....	- 60 -
Figure 3:4 - Priorities of the spinal cord injured population – United States [57, 194].	- 62 -
Figure 4:1- (a) Anal plug used by Hopkinson and Lightwood. (b) and (c) show lateral and anterior view of the anal plug used in Brindley, Rushton and Craggs experiment [199].	- 70 -
Figure 4:2 - The x-ray of ‘Portex’ electric pessary [205].	- 70 -
Figure 4:3 – (a) The small portable electrical stimulator and range of five Hopkinson's intra-anal plugs to fit most patients [24]; (b) The external transrectal stimulator “Continaid” [206].	- 71 -
Figure 4:4 – (a) Sotiropoulos anal plug [207]; (b) The “Incontan” device with the top and the battery removed [187].	- 71 -
Figure 4:5 - Commercially available pelvic muscle toners.	- 72 -
Figure 4:6 – Coronal plane cross-section of the anus and the rectum of an adult [209].	- 73 -
Figure 4:7 - (a) Hopkinson's continence aid anal plug, (b) the modified plug introduced by Glen [212].	- 75 -

Figure 4:8 - Shows the transverse plane image of the male pelvis at the ano-rectal junction.	- 77 -
Figure 4:9 – Final shape of the ACONTI represent to a scale shown.	- 79 -
Figure 4:10 - The master model of the device.	- 81 -
Figure 4:11 – Sample electrodes.	- 83 -
Figure 4:12 – Shows how the electrode is connected when it is in the device, embedded in silicone rubber.	- 83 -
Figure 4:13 - The main mould for filling rubber.	- 84 -
Figure 4:14- Shows the design stages explained in the Table 4:3.	- 87 -
Figure 4:15 – ACONTI device in 3-dimensional plane	- 88 -
Figure 5:1 – Bladder and rectal lines.	- 96 -
Figure 5:2 - Cystometrogram set-up.	- 97 -
Figure 5:3 - Shows the laboratory equipment set-up.	- 99 -
Figure 5:4 – Standard CMG with external anal sphincter EMG	- 102 -
Figure 5:5 - CMG traces of the twelve subjects	- 106 -
Figure 5:6 - Shows the variation of the volume at first contraction.	- 109 -
Figure 5:7 - Shows the variation of the maximum cystometric capacity.	- 109 -
Figure 5:8 - Shows the intra subject change in bladder capacity due to repeated filling.	- 110 -
Figure 5:9 - Variation of the maximum detrusor pressure of each individual with error bars representing the standard deviation.	- 112 -
Figure 5:10 - Variation of the level of the processed signal of each individual.	- 114 -
Figure 5:11 – Motor evoked potential.	- 120 -
Figure 5:12- Shows the effect on detrusor contraction with and without stimulation.	- 123 -
Figure 5:13 - Shows the effect of single burst (60s) stimulation on detrusor pressure in each participant.	- 126 -
Figure 5:14 - Sample conditional stimulation fill, starting with an empty bladder. t_{1-n} represent the increase in catheterisation time as a result of neuromodulation.	- 128 -

Figure 5:15 - Time between suppressed hyperreflexic contractions during the continuous filling at 15ml/min.	- 129 -
Figure 5:16 - Average time between each contraction across all subjects. Error bars represent the standard deviation.	- 130 -
Figure 5:17 - Show the real time implementation of the conditional neuromodulation based on the level on processed signal to trigger the stimulation.	- 132 -
Figure 5:18 - Time taken to start the stimulation and the time taken to suppress the contraction.	- 135 -
Figure 5:19 - Correlation between the mean delay in stimulation, since detecting the contraction and the rise in the detrusor pressure during that time.....	- 137 -
Figure 5:20 - Maximum detrusor pressure during conditional neuromodulation of each individual, the error bars represent the standard deviation.	- 139 -
Figure 5:21- Change in mean peak detrusor pressure across all subjects with and without stimulation.	- 140 -
Figure 5:22- Change in maximum cystometric capacity across all subjects with and without stimulation.	- 141 -
Figure 6:1 – Shows the Lectromed 5361 differential amplifier,	- 149 -
Figure 6:2 – CED 1401 plus data acquisition system, act as an interface to the real time analogue signal and SPIKE digital signal [281].....	- 150 -
Figure 6:3 – Shows the EMG (green) and the detrusor pressure (blue) of a signal recorded through SPIKE programme.	- 150 -
Figure 6:4 – The raw EMG waveform shown in the Figure 6:3 is transformed in to frequency domain by 512 Hanning window in order to assess its frequency components.....	- 151 -
Figure 6:6 – Optimising the processing parameters.	- 152 -
Figure 6:8 - The bladder pressure is shown in Pves and the EMG signal recorded through ACONTI is shown in “Raw EMG” channel.	- 153 -
Figure 6:9 - The block diagram of the proposed circuit.	- 154 -
Figure 6:10 - Each electrode is connected to a buffer amplifier, so that the mismatch of the electrode impedance can be minimised.	- 156 -
Figure 6:11 - A simple circuit to provide the path for the bias current.	- 156 -

Figure 6:12- Shows the electrode impedance versus frequency, when the device is in a saline solution	- 157 -
Figure 6:13 - Instrumentation amplifier with non-infinite CMRR and non-infinite input impedance.....	- 159 -
Figure 6:14- An optimal biasing circuit with three resistors in a star configuration.	- 160 -
Figure 6:15 - AC coupled amplifier using simple RC filter.....	- 161 -
Figure 6:16 - Shows the circuit diagram of the pre-amplifier.....	- 162 -
Figure 6:17 - The gain vs frequency of the INA118 amplifier.	- 163 -
Figure 6:18 - DC offset values of the amplifier measured by the digital multi-meter.	- 165 -
Figure 6:19 - Active operational amplifier notch filter circuit [288].	- 168 -
Figure 6:20 - Active twin T notch filter circuit with variable Q [288].	- 169 -
Figure 6:22 - Shows the frequency response of the notch filter. The input to the notch filter is a sinusoidal wave with amplitude 10.2V.	- 170 -
Figure 6:23 - Multiple feedback high pass filter	- 172 -
Figure 6:25 - Shows the frequency response of the high pass filter with gain of 10.	- 172 -
Figure 6:26 - Multiple feedback low pass filter	- 174 -
Figure 6:28 - Shows the frequency response of the low pass filter with gain of 10.	- 175 -
Figure 6:29 - This precision rectifier requires two amplifier and the two resistors R1 and R2.	- 176 -
Figure 6:30 - (a) During the positive half of the cycle the circuit acts like a voltage follower. (b) During the negative half the circuit acts as a simple inverting amplifier.	- 176 -
Figure 6:31 - Shows the input and the output to the full-wave rectification circuit at different frequencies. (a) 10Hz , (b) 100Hz, (c) 250Hz and (d) 500Hz.	- 178 -
Figure 6:32 – In a RC filter, at position 1, the voltage across the capacitor is V_0 . .-	179 -
Figure 6:33 - 1st order passive low pass filter with cut-off frequency 5Hz, where $R1 = 90.9k\Omega$ and $C1 = 350nF$	- 180 -

Figure 6:35 - Shows the frequency response of the 1 st order passive low pass filter.	- 180 -
Figure 6:36 - 2nd order Sallen-key filter with cut-off frequency 7.2Hz.	- 181 -
Figure 6:38 - Shows the frequency response of the 2 nd order active low pass filter. The input to the filter is a sinusoidal wave with amplitude 1V.....	- 181 -
Figure 6:39 - Simple comparator circuit designed using TL082 amplifier and is powered by 5V.	- 182 -
Figure 6:40 – Spike software code for setting the stimulator parameters.	- 184 -
Figure 6:41 - Shows the Digitimer DS7A constant current stimulator.	- 185 -
Figure 6:42 – Logic circuit to adjust the stimulator duration.....	- 187 -
Figure 6:43 - The stimulation duration adjustor circuit.	- 188 -
Figure 6:44 - Shows the arrangement of falling-edge triggered non-retriggerable monostable circuitry.	- 189 -
Figure 6:45 – Monostable output - 1.	- 190 -
Figure 6:46 – Monostable output – 2.	- 191 -
Figure 6:47 - 200 μ s stimulation pulses.	- 192 -
Figure 6:48 - Output of the astable was inverted and multiplied with the 60s pulse in order to produce stimulation pulses with duty cycle of 0.3%.	- 192 -
Figure 6:49 - The stimulator pulse width adjustor circuit consists of NE555 astable and NAND gates.	- 193 -
Figure 6:50 – The output of the stimulation pulse width adjustor circuit.	- 194 -
Figure 6:51 - Isolation power supply circuit for the stimulation consist of two DC-DC converters and an optocoupler.	- 196 -
Figure 6:52 - LME0505SC 5V DC-DC converter. 5V _{is} is the isolated 5V output and GND _{is} is the isolated ground.....	- 197 -
Figure 6:53 - PICO5A200S 5V to 200V DC-DC converter. 200V _{is} is the isolated 200V output and GND _{is} is the isolated ground.	- 197 -
Figure 6:54 - HCPL2503 is an optocoupler consist of LED optically coupled to a high speed photo detector transistor.	- 198 -
Figure 6:55 - Blue waveform is the output of the astable and the purple waveform is the input to the optocoupler when the HCPL2503 is in place.	- 199 -

Figure 6:56 - An emitter follower circuit to boost the current entering the optocoupler. - 199 -

Figure 6:57 - Constant current stimulator circuit. - 200 -

Figure 6:58 – Stimulation pulsesThe orange wave shows the 60s pulse (2Q) and the blue shows the output of the astable (OUT). Purple waveform shows the output of the optocoupler and stimulator pulses with a frequency of 15Hz shown in the green waveform. - 202 -

Figure 6:59 – Shows the stimulating pulse of pulse width of 200 μ s. - 202 -

Figure 6:60 – Testing the processing circuit on thenar muscle EMG - 205 -

List of tables

Table 2-1 - Supraspinal lesion diseases and the effect on the bladder function [46-48].	- 35 -
Table 2-2 - Types of peripheral nerve lesions and their effect on bladder functions [56, 59, 60].	- 38 -
Table 2-3 – History of electrical stimulation for bladder dysfunction.	- 43 -
Table 3-1 - Methods for detecting detrusor contraction.	- 54 -
Table 3-2- Electrical stimulation treatment for NDO.	- 56 -
Table 3-3 - Bladder dysfunction diagnostic procedures [198]	- 63 -
Table 4-1 – Analyse some of the non invasive wearable devices used in the past to treat UI through electrical stimulation.	- 66 -
Table 4-2 - Desirable material properties for some metals commonly used as bio electrodes [222].	- 82 -
Table 4-3 - Highlights the problems faced in the previous approach and the solution to overcome them.	- 85 -
Table 5-1 - Patient details.	- 94 -
Table 5-2 - Volume at first contraction and the maximum cystometric capacity of the participants.	- 108 -
Table 5-3 - Maximum detrusor pressure during the control study.	- 111 -
Table 5-4 - Levels of the processed signal	- 113 -
Table 5-5 - Time difference in detecting contraction by processed signal and detrusor pressure as indicated in Figure 6:8.	- 115 -
Table 5-6 - Shows the sensory threshold and the stimulating current of each subject, which was utilised in delivering the stimulation.	- 121 -
Table 5-7 - Shows the time between each detrusor contraction of each individual.	- 129 -
Table 5-8 - Calculates the precision rate and the percentage of unwanted stimulation of a given threshold level for each patient.	- 133 -

Table 5-9 - The mean value of t_a , t_b , t_c and t_d (indicated in the Figure 5:18) - 136 -

Table 5-10 - Shows the rise in detrusor pressure due to the delay in commencing the stimulation. - 136 -

Table 5-11 - The maximum detrusor pressure of each successfully inhibited contraction of each individual. - 138 -

Table 5-12 - Shows the mean of the maximum detrusor pressure across each fill during control study and with conditional stimulation..... - 139 -

Table 5-13 - Shows the maximum cystometric capacity across each fill during control study and with conditional stimulation. - 141 -

Table 6-1 – The specification for the electronic circuitry - 144 -

Table 6-2 – The settings of the front end of the Lectromed amplifier [280] . - 149 -

Table 6-3 - The specification of the DS7A constant current stimulator [299].- 185 -

-

Table 6-4 - The specification for the simple stimulator circuit. - 186 -

Chapter 1 - Introduction

1.1 Background

Urinary incontinence (UI) is the involuntary loss of urine which is objectively demonstrable and a social or hygienic problem [1]. UI affects one in three of the population at some stage in their adult lives [2]. According to the National Association for Continence (NAFC) 200 million people worldwide suffer from this problem [3] and is thought to affect about six million adults in the UK [2]. Urinary incontinence is common as people get older and more common in women and double the incidence in women who have had vaginal deliveries [4]. For developing countries these figures increase rapidly due to the lack of people's health knowledge, embarrassment to discuss these issues with doctors and also insufficient health facilities [5].

Urinary incontinence can have devastating effects on the life of sufferers and their families and can be very high cost to the nation [5]. In adult women with urinary incontinence 60% avoid going away from their home, 50% feel odd and different from others, 45% avoid public transport while 50% report avoiding sexual activity through fear of incontinence [6].

The economic impact of incontinence on society is significant [7]. The cost includes medicine, absorbent products, catheters and loss of earnings. Also this needs to account the cost of primary and secondary care, nursing home and long term care. Between 2000 and 2003, the annual cost of incontinence to the NHS was £500 million and that is expected to rise to £2 billion by year 2020 [8]. It is possible to reduce these costs by accurate diagnosis and appropriate management of the condition.

There are four main types of urinary incontinence: stress incontinence, urge incontinence, overflow incontinence and mixed incontinence. Stress incontinence is the involuntary loss of urine during filling phase of the bladder when intravesical pressure exceeds maximal urethral closure pressure without any bladder contraction. Urge incontinence defined as the provoked or spontaneous detrusor contraction during the filling phase of the bladder when the individual is voluntarily inhibiting the micturition. When the urge incontinence is caused by neurogenic disorder, it is known as the neurogenic incontinence. Overflow incontinence results from over distension of the bladder due to bladder outlet obstruction or functional weakness of the bladder itself. Mixed incontinence is due to coexistence of bladder muscle overactivity and urethral sphincter weakness [9].

This research focused on a device for treating UI due to neurogenic incontinence, which affects nearly 16.6% of UI population aged ≥ 40 years [10]. Neurogenic incontinence occurs as a result of interrupting the pathway to nervous communication between the brain and the bladder leading to uncoordinated activity in the lower urinary tract (LUT). This can be due to a variety of reasons such as spinal injury, stroke, multiple sclerosis (MS) and Parkinson's disease. In neurogenic detrusor overactivity (NDO) also known as detrusor hyperreflexia (DH) the bladder contracts involuntarily during filling phase that leads to increase frequency and leakage of urine. This is often associated with detrusor sphincter dyssynergia (DSD), in which the bladder and sphincter contract together resulting voiding dysfunction. NDO together with DSD can cause high transient bladder pressure and may lead to vesicoureteric reflux, repeated bladder infections and renal failure if left untreated [11-15].

The standard method of treating NDO is antimuscarinic (anticholinergic) drugs to relax the detrusor muscle in order to prevent incontinence [16, 17]. Anticholinergic drugs, for example, Oxybutynin, Tolterodine are relatively

expensive and need lifelong treatment. Furthermore clinical experience shows that up to 50% of patients with NDO cannot tolerate the side effects of the drugs such as dry mouth, drowsiness, constipation, skin reactions and blurred vision [18-20].

For many years electrical stimulation (ES) has been a potential treatment to suppress detrusor contractions in patients with NDO [21-25]. The sacral anterior root stimulator implant (SARSI) has been proven to be an effective way of achieving good bladder emptying [26, 27]. Combining these two can replace the standard treatment.

Whilst implants are successful, these have disadvantages such as implantation of the stimulator is a surgical procedure and is associated with a degree of risk, also it cannot be serviced or removed easily [28]. Sometimes the lower urinary tract symptoms change over time; therefore non-invasive and non-destructive treatment is preferred until symptoms improve [29]. Further, most of the electrical stimulator treatments for bladder overactivity, provide continuous stimulation to the nerves that control the bladder. In these, stimulation becomes ineffective due to habituation and may increase the risk of tissue damage [28]. High energy consumption [12] and absence of warning time before the leak are also disadvantages of such systems.

A much better approach to this problem would be a wearable device, in which patients can experience the acute effect of stimulation before proceeding for an implantation and also to be used as a non-destructive treatment [29]. If the device can provide stimulation only when required, it will increase both battery and electrode life while reducing the effect of habituation [12, 28, 30, 30-32].

1.2 Aim of the project

The overall aim of the project is to develop a novel wearable anal device designed to deliver conditional neuromodulation¹ and ultimately prove its principle in a small scale clinical study. The device detects the electromyogram (EMG) activity in the lower urinary tract, and provides the transrectal stimulation to the Pudendal nerve when required, in order to suppress the bladder contractions while contracting the urethral sphincters [34].

1.3 Publications

The following work was published from the work mentioned in this thesis.

- Craggs M, Edirisinghe N, Leaker B, Susser J, Al-Mukhtar M and Donaldson N.; “Conditional neuromodulation using trans-rectal stimulation in spinal cord injury”, *Neurology and Urodynamics*; Vol. 28; pp. 836-837; 2009.
- Edirisinghe NA, Leaker B, Donaldson N. and Craggs MD; “A novel wearable medical device for controlling urinary incontinence by conditional neuromodulation”, *Proc. Conference organised by Institution of Mechanical Engineers (Incontinence: The Engineering Challenge VII)*, December 2009, London, UK.
- Edirisinghe NA, Leaker B, Susser J, Al-Mukhtar M, Donaldson N. and Craggs MD: “Assessment of a novel wearable conditional stimulation device for continence control”, *Annual Scientific Meeting of South East Division of Institute of Physics and Engineering in Medicine*, May 2009, Kent, UK.

¹ The influence of activity in one neural pathway modulates the pre-existing activity in another through synaptic interaction [33].

- Edirisinghe NA, Susser J, Al-Mukhtar M, Knight S, Leaker B, Donaldson N. and Craggs MD; “A novel wearable conditional neuromodulator for treating urinary incontinence in spinal cord injury”, *Proc. Conference organised by UK Continence Society (Broadening Horizons)*, April 2009, Swansea, UK.
- Edirisinghe NA, Donaldson N and Craggs MD; “A novel wearable medical device for controlling urinary incontinence by conditional neuromodulation”, *Graduate School poster competition, UCL*, March 2009, London, UK. Became the Runner-up in the Departmental category.
- Edirisinghe NA, Donaldson N and Craggs MD; “Neuromodulation Device for Pelvic Dysfunction”, *Graduate School poster competition, UCL*, March 2008, London, UK.

1.4 Thesis outline

The project is based on development and testing of the novel wearable conditional neuromodulation (CN) device. This thesis comprises eight chapters, which are:

Chapter 1 introduces the background problems, types of urinary incontinence and describes its severity. It briefly describes the current methods of treating UI and their drawbacks. Further the requirement of a new device to improve the quality of the life of the patients is described. Finally the chapter highlights the aim of the project.

Chapter 2 describes some basic understanding of the problem based on current findings. It briefly describes the anatomy and physiology of the lower urinary tract and then moves onto the causes and treatment of NDO and specially focuses on literature review on electrical stimulation as a treatment option.

Chapter 3 focuses on the study design. The chapter starts with a brief requirement of the device and then moves on to explaining the basic principle behind the operation of this device.

Chapter 4 describes the actual process of making the prototype device. It starts off with a previous model that is being used for similar applications and then talks about the design considerations based on biocompatibility and anatomy of the LUT. All the design steps involved are explained in detail within this chapter.

Chapter 5 explains the testing of the device within the clinical environment to find out its efficacy. It describes the patient selection, equipment setup and then a series of experiments that were carried out. These results were then analysed using statistics to assess its clinical significance.

Chapter 6 derives the specification for the required electronic circuitry to make this model as a stand alone device. Then it describes the building of the actual circuit and testing of the prototype system. Design considerations are mentioned for each part of the circuitry.

Chapter 7 summarises the work included in the thesis. The results presented in each chapter are analysed to see the direct benefit to the patient. Finally it finishes with a brief description of future work required for further development.

Chapter 2 - Bladder inhibition – beyond nature

2.1 Introduction

As explained in chapter 1, urinary incontinence is a wide problem to the society and treatment modification is required to increase the quality of life of the sufferers and also to reduce the cost to the NHS. In order to assess the problem of neurogenic detrusor overactivity, it is helpful to understand the basic mechanism of filling and emptying of the bladder.

This chapter provides some basic understanding of the term “urinary incontinence”, which is the main focus of the thesis. The discussion starts off by explaining the anatomy and the physiology of the lower urinary tract of a healthy adult. Then the explanation moves onto the causes for bladder dysfunction and to explain how it affects the physiology of the bladder. The latter part of the chapter talks about currently available treatments and special attention is given to past research based on electrical stimulation to treat bladder dysfunction.

2.2 Anatomy and physiology of the lower urinary tract

2.2.1 Anatomy of the lower urinary tract

The urinary bladder is a temporary store of urine from kidneys and empties through the urethra. The bladder varies in its size, shape and position according to the amount of urine it contains. When empty it lies entirely within the pelvis, but as it fills up it expands and extends upwards into the abdominal cavity [35].

The smooth muscle of the bladder is called the detrusor muscle (Figure 2:1) arranged in spiral, longitudinal and circular bundles. The contraction of the detrusor muscle is responsible for emptying the bladder during micturition [36].

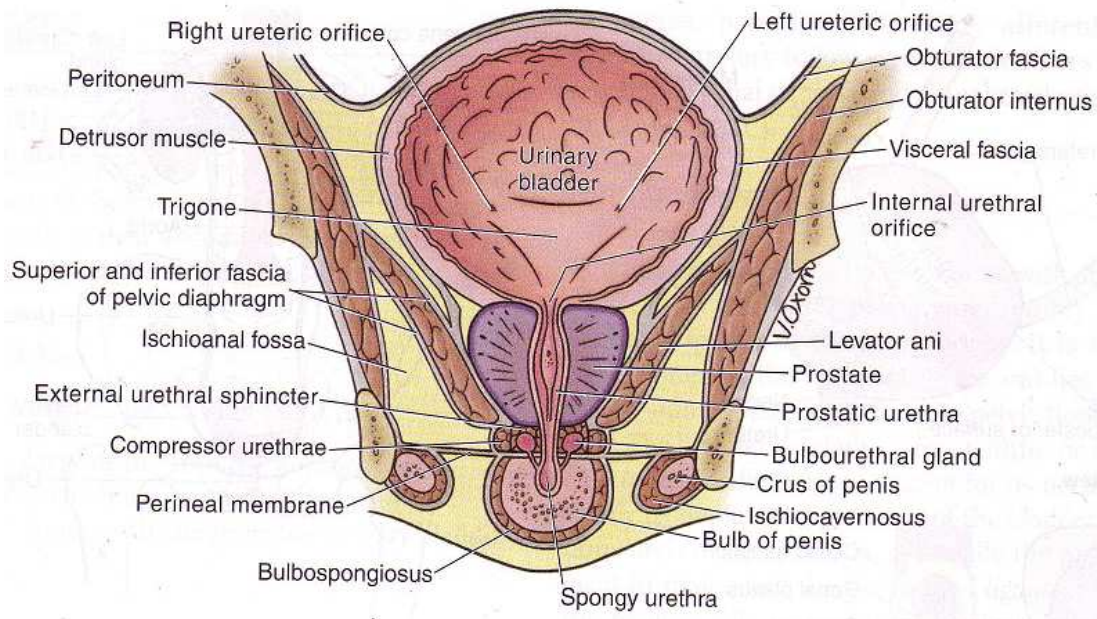


Figure 2:1 - Coronal section of the male near urinary bladder.

The bladder is formed from smooth muscle named detrusor muscle. External urethral sphincter provides continence during the filling phase of the bladder [37].

Muscle bundles pass either side of the urethra and formed internal urethral sphincters, which is involuntary. These fibres do not encircle the urethra. The function of these sphincters is to prevent retrograde ejaculation of the semen into the bladder [37]. Further along the urethra is a sphincter of skeletal muscle, the sphincter at membranous urethra is known as external urethral sphincter (EUS), which is mainly responsible for continence [35].

2.2.2 Innervation of bladder and sphincter

The lower urinary tract is supplied from the vesical plexus of nerves which is made up of parasympathetic, sympathetic and somatic systems. All of these

contain afferent (sensory) and efferent (motor fibres) and the innervations of the bladder and the sphincter are highlighted in Figure 2:2 [35].

Parasympathetic nerve supply

The parasympathetic system provides the major excitatory input to the detrusor muscle and is inhibitory to the urethral sphincters. These nerves arise from the pre-ganglionic neurons in the intermediolateral grey column of the S2-S4 sacral segments and travel in pelvic splanchnic nerves, synapse at the inferior hypogastric plexus and prostatic nerve plexus. Parasympathetic ganglionic cells are situated in the walls of the bladder and the ureter with postganglionic axons directly innervating the smooth muscle [38-41].

Afferent axons in the parasympathetic nerves travel back to the S2-S4 segments of the cord, and have their cell bodies in the sensory ganglia at those segments. These axons convey the information that is particularly important in producing the detrusor contraction in response to the bladder fullness [38].

Sympathetic nerve supply

The sympathetic efferent are said to be inhibitory to the detrusor and stimulatory to the smooth muscles of the bladder neck [35]. These nerves arise in the intermediolateral grey column of T10 –L2 of the cord. These pre-ganglionic axons travel via splanchnic nerves and synapse in lower prevertebral ganglia, especially the inferior mesenteric. From here, new axons form the hypogastric nerve, which runs on the posterior abdominal wall into the pelvis [38, 40].

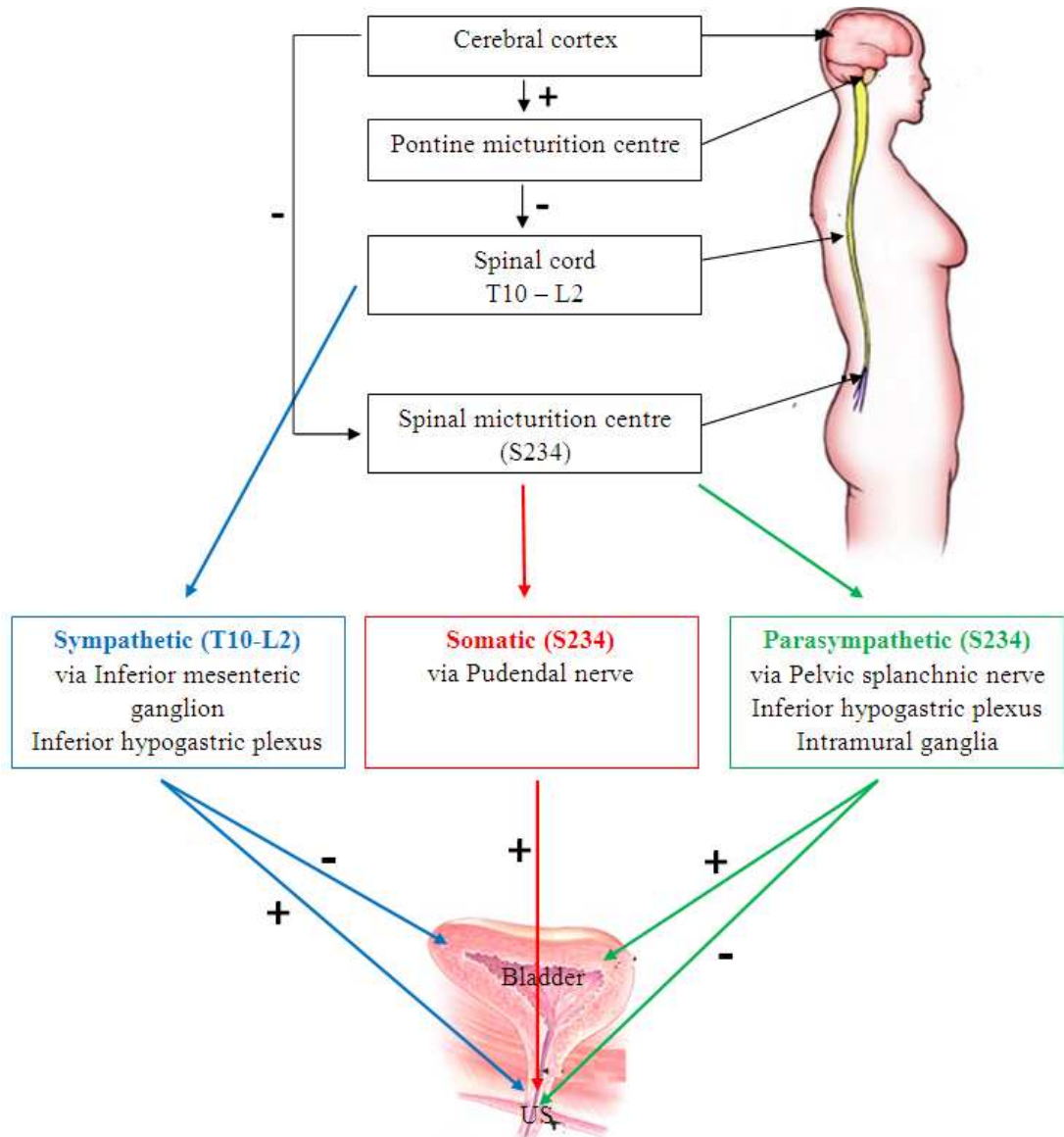


Figure 2:2- Block diagram of the neural control of the lower urinary tract.

The Innervation of the urinary bladder and urethral sphincters are from three types of nerves, which are parasympathetic (green), sympathetic (blue) and somatic (red). Contractions are shown as “+”, while inhibitions are “-“. Urethral sphincters represented as “US”.

Many axons in the hypogastric nerve are sensory. The afferent axons accompanying the sympathetic nerves are responsible for sensation of the bladder fullness. Cell bodies of these nerves are in the sensory ganglia of the lower thoracic spinal root [38].

Somatic nerve supply

Somatic nerves provide the voluntary control to the striated muscle of the external anal and urethral sphincters and pelvic floor muscles [38, 41]. These nerves arise from the motor neurons in Onuf's nucleus, a specialised group of anterior horn cells originating from S2-S4 segments [40]. After emerging from the pudendal (Alcock's) canal, this divides into the inferior rectal nerve, perineal nerve and the dorsal penile nerve [39].

The somatic afferent axons of the pudendal nerve have cell bodies in the sensory ganglia of S2-S4. These sensory fibres convey the sensation of urine passing through the urethra, felt at the conscious level [38].

2.2.3 Physiology of urination

In healthy individuals, the lower urinary tract has two discrete functions.

- A storage function is brought about by autonomic bladder relaxation and tonic contraction of the external urethral sphincter.
- Micturition is brought about by voluntary relaxation of the external urethral sphincter and pelvic floor, along with reflex contraction of the detrusor muscle.

The urinary pathways that control these two functions have two states [42]. This analogy is illustrated in Figure 2:3.

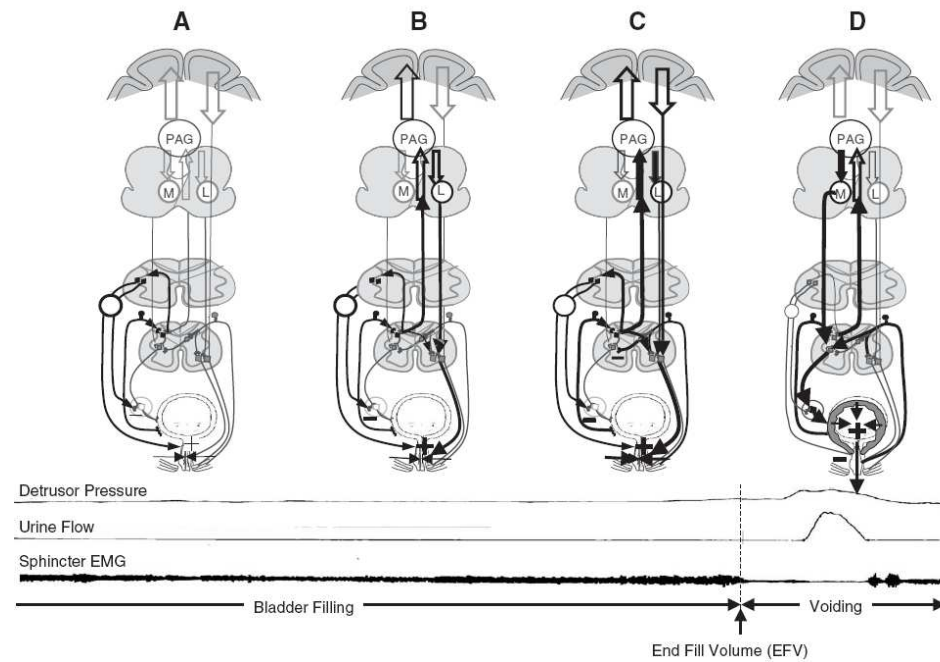


Figure 2:3- Micturition cycle of a healthy adult.

The filling and voiding events are recorded by cystometry and sphincter EMG traces as shown in the diagram. (A) As the bladder fills sympathetic reflexes suppress the parasympathetic pathways to the detrusor muscle while increasing the tone of bladder neck and the urethra. (B) By the time first desire to void, the “guarding reflex” begins and increases the tone of the sphincter (electromyography) further. (C) As the desire to void increases further, the voluntary contraction increases the tone of the sphincters to its maximum. (D) At an appropriate social condition the voiding reflex begins by opening the sphincters and contracting the detrusor muscle [43].

Storage phase (The guarding response)

According to law of Laplace, as the bladder accumulates increasing volume of urine, the tension to the bladder wall increases so does the radius of the bladder; resulting low intravesical pressure until the bladder is well filled [36]. The extent to which the change in volume (δV) occurs in relation to a change in intravesical pressure (δP), is known as the bladder compliance ($\delta V/\delta P$). The factors that contribute to this are the visco-elasticity of the bladder and the inhibition of parasympathetic nerves [14, 44].

As the bladder fills, sympathetic nerves inhibit the parasympathetic nerves from triggering bladder contractions. Sympathetically mediated reflexes cause the suppression of detrusor activity and contract the smooth muscle of the bladder neck and proximal urethra [14].

In the mean time urethral sphincters also contract via pelvic afferents to pudendal efferent reflex in order to prevent the leakage. This mechanism is known as “guarding reflex”, which generates the sphincter EMG during bladder filling [45]. Contraction of external urethral pressure coupled with that of internal urethral sphincter, maintains the urethral closure pressure. As long as the maximum urethral closure pressure is higher than the intravesical pressure, the continence is maintained [40, 43, 46].

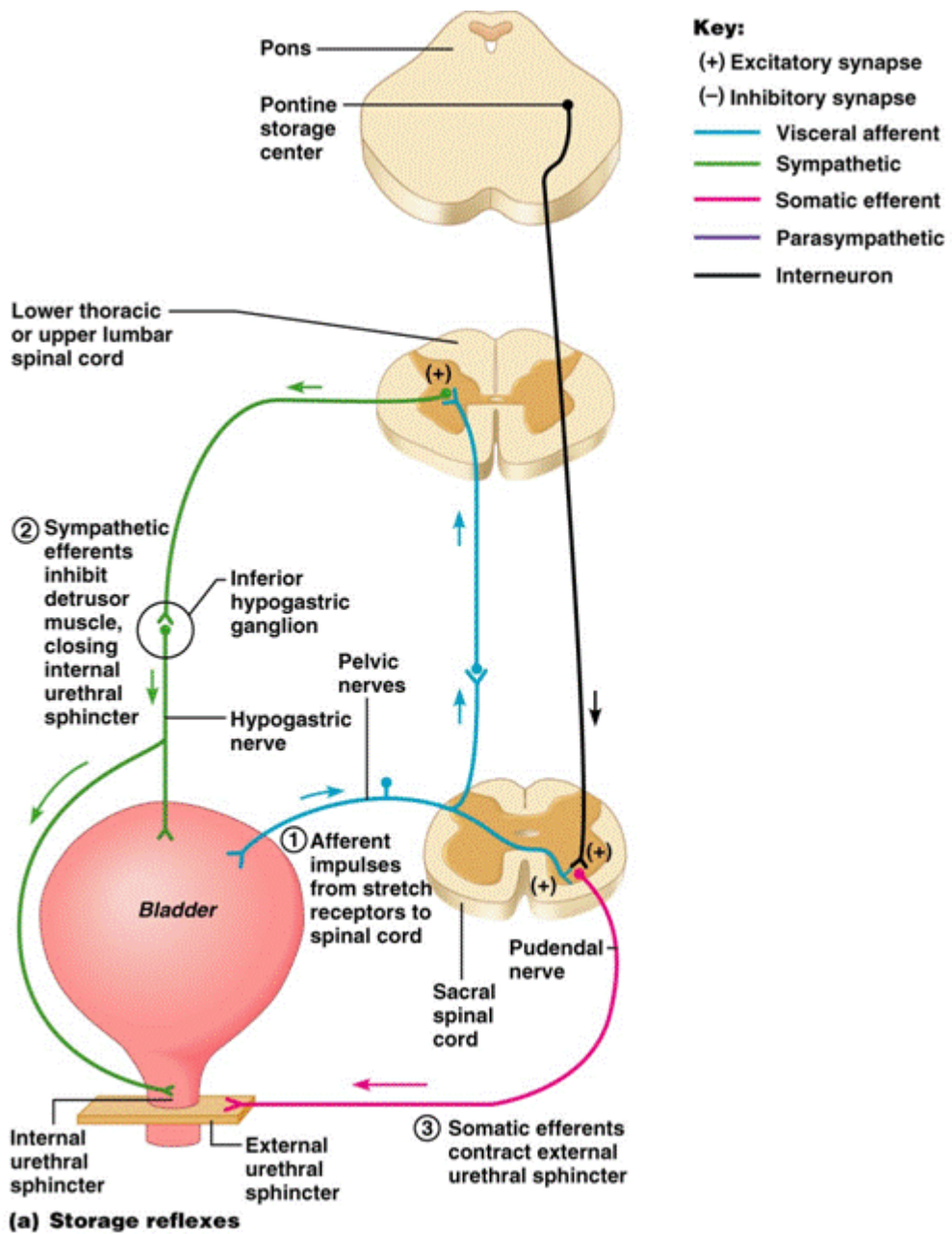


Figure 2:4 - Storage phase

As urine accumulates, distension of the bladder activates stretch receptors, which trigger spinal reflexes, resulting in storage of urine [47].

Voiding phase

It is through the learnt ability to postpone the micturition until the socially acceptable conditions are present [33, 36]. Once the bladder reaches its full capacity, stretch receptors within the bladder wall trigger micturition reflexes, resulting in excitation of the parasympathetic pathways, while inhibiting sympathetic and somatic pathways. At this point the Pudendal nerve causes relaxation of the levator ani so that the pelvic floor muscle relaxes. This causes a downward tug on the detrusor muscle to initiate its contraction. Efferent fibres conduct the signal for sphincter relaxation, which results in lowering of the urethral pressure.

Signals from parasympathetic nerve triggers the detrusor contraction and results the increase in intravesical pressure above the maximum urethral closure pressure. Thus the micturition process is initiated. The flow of urine can be interrupted at any point, by contracting the sphincters voluntarily through the somatic pathways [40, 43].

The bladder can be made to contract voluntarily when it contains only few millilitres of urine. This is done by voluntary contraction of the abdominal muscle, which aids the expulsion of urine by increasing the intra-abdominal pressure [36, 46].

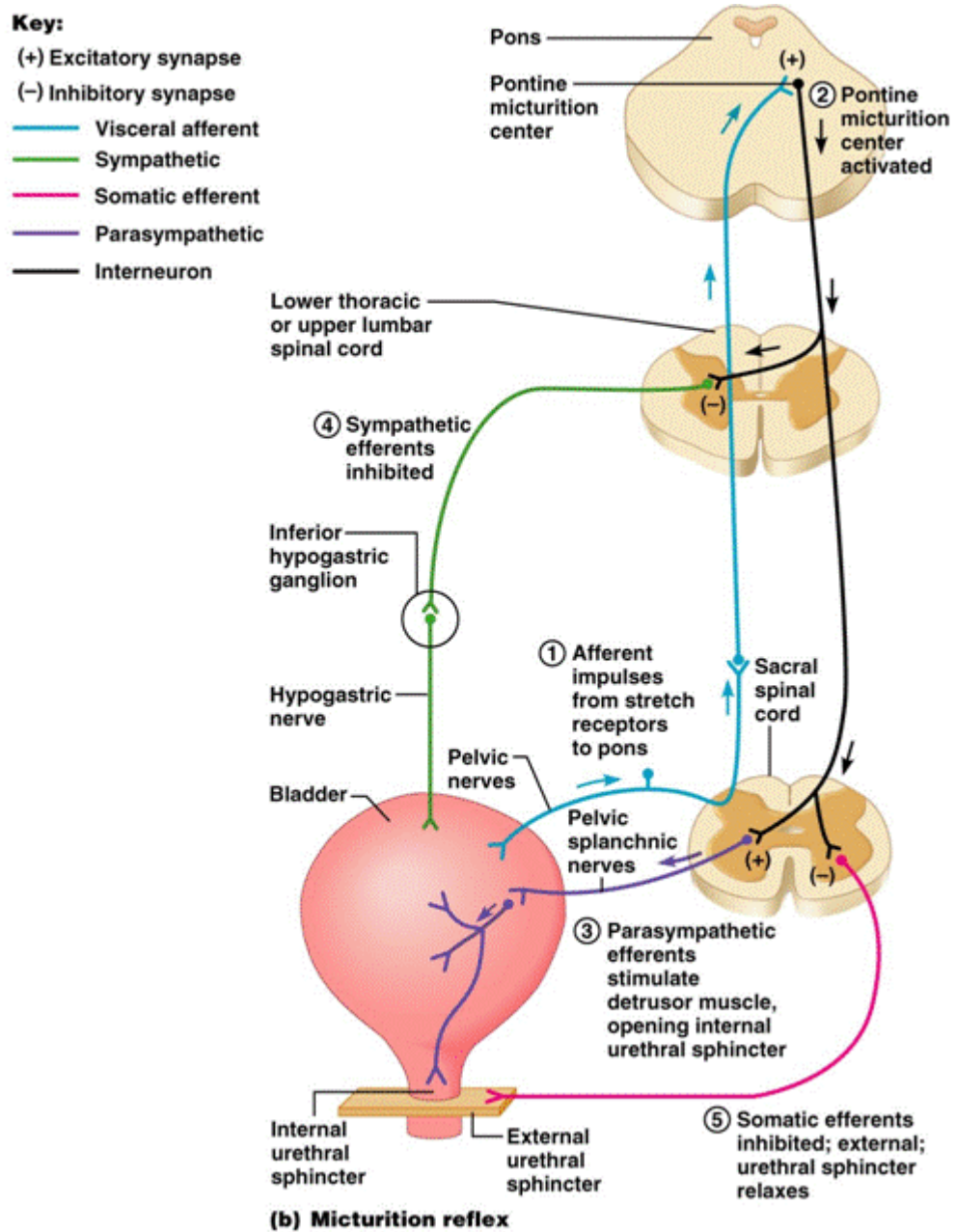


Figure 2:5 - Voiding phase

Voluntary inhibition of voiding reflex results in activation of the micturition centre of the PMC, which signals parasympathetic motor neurons that stimulates the contraction of the detrusor muscle and relaxation of the urinary sphincters [47].

2.3 Causes for bladder dysfunction

Continence is maintained by the coordinated action of the brain, spinal cord and the innervated nerves of the bladder as well as proper integrity of the detrusor muscle, the urethra and the sphincter. If a problem arises in any one of these bladder may become dysfunctional.

2.3.1 Supraspinal lesions

Lesions that are occurred in the central nervous system and involve the pontine micturition centre are known as supraspinal lesions. Symptoms of these diseases and their effect on bladder function are listed in Table 2-1.

Table 2-1 - Supraspinal lesion diseases and the effect on the bladder function [46-48].

Disease	Effect on bladder
Dementia	Incontinence may be caused due to both loss of judgement due to frontal lobe atrophy as well as loss of volitional control of detrusor reflex function.
Parkinson's disease	Overactive bladder can be present due to increase in cholinergic activity in the brain as a result of deficiency of dopamine.
Cerebrovascular accident	After cerebral shock phase wears off, the bladder demonstrates detrusor hyperreflexia with coordinated urethral sphincter activity due to focal neurologic deficit.
Multiple sclerosis	Due to focal demyelinating lesion of the brain or the spinal cord or the axons, the nerves that control the continence mechanism can be blocked or delayed. The effect of this may be temporary or permanent and can be detrusor

	hyperreflexia or detrusor areflexia.
Brain tumors	If the tumor is located closer to the pontine micturition centre, the detrusor areflexia or hyperreflexia can occur.

2.3.2 Spinal cord lesions

With spinal cord injury, there is sudden (spinal shock phase) partial or complete loss of voluntary movements below the level of lesion associated with partial or complete abolition of sensation. As the spinal shock phase (6-12 weeks) wears off, the reflex activity increases [48].

If the injury is above the sacral division (Figure 2:6) of the spinal cord, the individual may experience detrusor hyperreflexia together with detrusor sphincter dyssynergia. Even though the bladder is trying to force out the urine, the sphincters remains contracted which prevents flow.

Injuries occurring to the nerves which arise from the sacral cord may prevent the bladder from emptying. If the sensory fibres are damaged, the individual may not feel the bladder fullness or, if the motor fibres are damaged, the person feels the bladder is full, however the detrusor may not contract. This is known as detrusor areflexia.

The most common cause for spinal cord lesion is road traffic accidents [49].

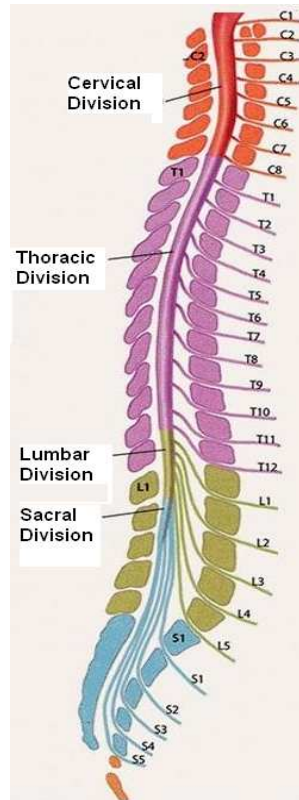


Figure 2:6 - The lateral view of the spinal cord segments.

The spinal cord segments can be divided into four main sections as Cervical (red), Thoracic (purple), Lumbar (green) and Sacral (blue) [50].

2.3.3 Peripheral nerve lesions

The most common types of peripheral nerve lesions and their effect on bladder functions are highlighted in Table 2-2.

Table 2-2 - Types of peripheral nerve lesions and their effect on bladder functions [48, 51, 52].

Disease	Effect on bladder
Diabetic cystopathy	After ten or more years of diabetes mellitus causes segmental demyelination and impaired nerve conduction. As symptoms arise by losing bladder filling sensation and motor function, the result is detrusor areflexia.
Herpes zoster	This causes inflammation of posterior nerve roots and may block nerve conduction. During the inflammation, detrusor areflexia may occur and normal bladder function will return once the infection is cleared.
Pelvic surgery	Bladder dysfunction may result from pelvic surgeries such as removal of prostate glands, hysterectomy and child birth injuries. Most commonly these patients experience temporary detrusor areflexia, which fades away with recovery from the surgery.

2.4 Treating and managing urinary incontinence

Neurogenic bladder dysfunctions may lead to irreversible renal damage and bladder wall destruction before incontinence becomes an issue. Therefore it is important to treat this condition at an early stage [53]. Although many different types of treatments are available in managing urinary incontinence, none has proved universally satisfactory. Some of the most common treatments and management methods are discussed in this section.

2.4.1 Medication

For the vast number of people who suffer from urinary incontinence, drugs are the initial treatment. There are many drugs available on the market and all owing the same effects [19].

If the problem is detrusor overactivity, the rational treatment is to give a medication that is capable of reducing the detrusor overactivity, possibly by blocking the parasympathetic transmission such as using anticholinergic drugs. Oxybutynin chloride and Tolterodine are two of the most commonly prescribed drugs. These drugs increase bladder capacity, decrease bladder filling pressure and improve compliance [53]. However the main problem of these is the short duration of action, therefore when the patient stops the medication, the symptoms return [18].

However clinical evidence shows that up to 50% of patients with NDO cannot tolerate the side effects of the drugs such as dry mouth, drowsiness, constipation, skin reactions and blurred vision [19, 54].

Recently a treatment known as botulinum toxin-A (“Botox”) was introduced to inhibit detrusor overactivity, which has effects lasting for about a year [55]. Botox inhibits the neurotransmitter release at the nerve endings, suppressing bladder contractions [56]. However the long-term effects of this injection are not yet known [41].

2.4.2 Absorbent products

These are the garments designed to absorb urine to protect the skin and clothing, and are mostly used as a temporary method until a permanent solution become available.

There are two major types of absorbent products, which are body-worn products and bed pads. They come in many shapes and sizes. These also can be divided into disposable and washable products. Washable products are unsuitable for heavy leaking but generally provide better protection; whereas the disposable products are less vulnerable for urinary tract infections (UTI) but high in cost [5].

Improper absorbent products may contribute to skin breakdown and urinary tract infections. Furthermore absorbent products are generally not recommended for the spinal cord injured patients, which might lead to pressure source due to the lack of mobility.

All the treatment and management methods described in section 2.4 are associated with their own side effects. They do not provide permanent solution to the problems associated with the bladder. In 2001 Creasey and Dahleberg concluded that the neural prosthesis² for bladder and bowel management is less costly than the conventional methods (Figure 2:7 and Figure 2:8) [58].

² A neural prosthesis is a device or technique used to supplement or replace lost or missing function in neurologically impaired individuals [57].

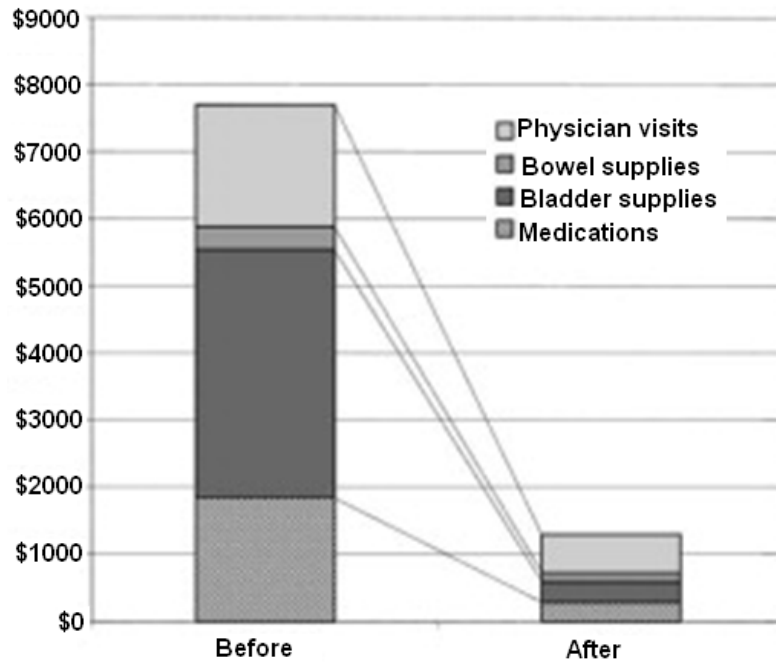


Figure 2:7 – Annual cost of conventional methods

Mean cost of conventional methods of bladder and bowel care before and after using electrical stimulation as a treatment was calculated using a sample size of 12 [58].

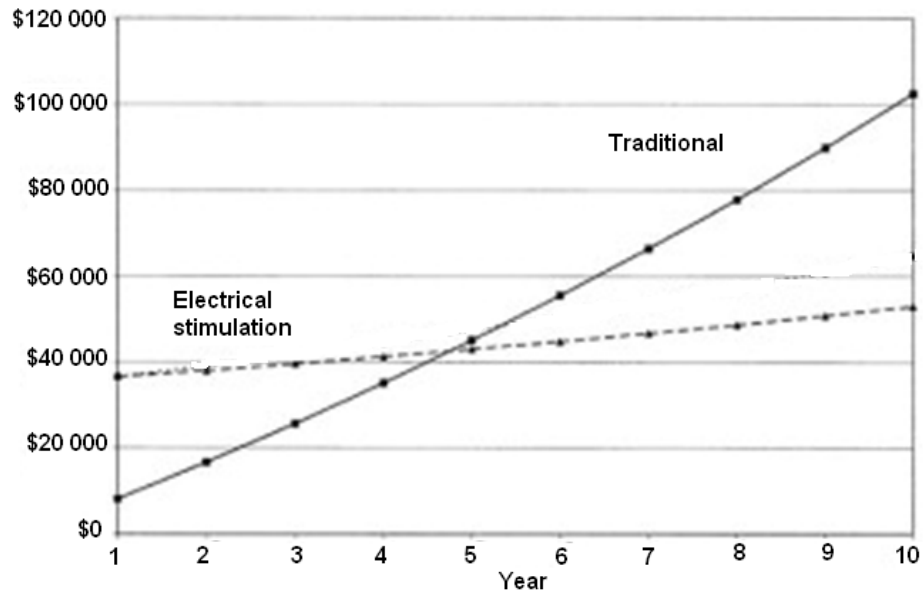


Figure 2:8 – Cumulative bladder and bowel care cost.

Estimated cumulative cost over ten years of person using conventional bladder and bowel care methods or electrical stimulation [58].

2.5 Electrical stimulation for bladder inhibition

For many years electrical stimulation has been a successful treatment for problems of the lower urinary tract, especially urinary incontinence caused by sphincter weakness or bladder overactivity [32, 33, 59].

In humans, stimulation of the sympathetic nerves arising from T10-L2 spinal levels (Figure 2:2) results in relaxation of detrusor muscle and contraction of urethral sphincters causing inhibition of urination. Stimulating the parasympathetic pathway arising from S2-S4 (Figure 2:2) has the opposite effect [60].

2.5.1 Neurostimulation and neuromodulation

Electric stimulation can be mainly divided into two categories as neurostimulation and neuromodulation. In neurostimulation nerves or muscles directly stimulated to achieve immediate responses [60]; whereas in neuromodulation the influence of activity in one neural pathway modulates the pre-existing activity in another through synaptic interaction (alters the neurotransmission process) [33].

2.5.2 History of neural prostheses

The first reported case of attempted neuromodulation in patients with bladder dysfunction is by the Danish surgeon Saxtroph in 1878 to treat urinary retention [60, 61]. Since then there have been many discoveries in this field and some of them are highlighted in this table.

Table 2-3 – History of electrical stimulation for bladder dysfunction.

Table shows the discoveries by scientists regarding electrical stimulation to treat bladder dysfunction over the past century.

Year	Scientist	Discovery
1895	M.H. Saxtroph	Intravesical stimulation of the bladder to treat urinary retention [60, 61].
1895	J. Griffiths	Electrical stimulation of proximal stump of the cat’s pudendal nerve resulted in a pronounced relaxation of the bladder, if its wall is in the contracted state [62].
1937	Langworthy and Hesser	Detrusor inhibition on vaginal or anal dilatation has been observed [25, 63].
1954	Boyce	Bladder wall stimulation implant was developed to induce bladder emptying [61, 64].
1955	Ingersoll	Pelvic nerve stimulation studies on cats and dogs [65].
1963	Caldwell	Electrodes implanted in urethral and anal sphincters to deliver electrical stimulation. This is reported as the first attempt in management of incontinence [66].
1963	Kock and Pompeius	Vesical motor activity has been inhibited by anal stimulation [67].
1963	Habib	Electrical stimulation of the sacral anterior roots of human and animal study [68].
1964	Rossier and Bors	Detrusor inhibition in human by pin-prick stimuli applied in the perineal region [69].
1968	Alexander and Rowan D	Radio controlled implant and also external electrode systems with vaginal and anal

		electrodes that stimulated the anal sphincters, pelvic floor muscles and pelvic nerves to control incontinence. The stimulation increased the urethral resistance and inhibited the bladder [22].
1969	Brindley	Finetech-Brindley sacral anterior root stimulator first tested on animals [26].
1969	DeGroat and Ryall	Demonstrated inhibitory postsynaptic potentials and inhibition of discharges of parasympathetic neurons due to spinal reflex with a pudendal afferents of a cat. Also reported that stimulation of these somatic afferents may have both excitatory as well as inhibitory influence on the bladder depending on the intravesical pressure low or high [70].
1972	Sundin and Carlsson	Stimulation of pudendal afferents was shown to induce bladder inhibition due to pudendal to hypogastric spinal reflex [71].
1974	Sundin	Stimulation of pudendal afferents was shown to induce bladder inhibition due to pudendal to pelvic spinal reflex. Assumed to be of main importance for detrusor inhibition in humans [72].
1975	Godec	First use of electrical stimulation explicitly for bladder inhibition using functional electrical stimulation applied to the anal sphincters [73].
1978	Brindley	Sacral anterior root stimulator first implanted on patients [26].

1978	Fall	The pudendal to spinal reflex mechanism was activated by intravaginal electrical stimulation in cats [74].
1979	Janez	Urethral and bladder response to anal electric stimulation were evaluated by cystometry in 55 patients with bladder dysfunction [24].
1982	Kondo	Mechanical stimulation (squeeze) of the penis for bladder inhibition [75].
1983	McGuire	Bladder inhibition was achieved through tibial nerve stimulation [76].
1983	Lindstrom	Showed the activation of sympathetic vesicoinhibitory neurons and inhibit the parasympathetic vesical motor neurons. Also shown the sphincter muscle contraction is not necessary to achieve detrusor inhibition by afferent stimuli in animals [77].
1984	Nakamura and Sakurai	Detrusor activity was suppressed using transcutaneous electrical stimulation applied to the penis [78].
1985	Brindley and Donaldson	An implantable system, where pudendal nerve stimulation was controlled by detrusor pressure was tested for six months [41].
1986	Vodusek	It was shown that, in human the bladder inhibition can be achieved by stimulating the pudendal afferents of the dorsal penile stimulation and showed that all that is required for bladder inhibition is depolarising the

		<p>pubudal afferents. Furthermore detrusor inhibition was achieved by direct pudendal nerve stimulation using needle electrode and using low currents [79].</p>
1988	Schmidt	<p>Implantable stimulator connected to an electrode making contact with S3 nerve root [33].</p>
1991	Fall and Lindstrom	<p>Concluded that dorsal penile/clitoral nerve stimulation activates inhibitory sympathetic bladder pathways and inhibits the preganglionic bladder motor neurons through a direct route of sacral cord [80].</p>
1996	Sheriff	<p>Neuromodulation of detrusor hyperreflexia by multi pulse magnetic stimulation of the sacral roots [81].</p>
1996	Hansan	<p>Transcutaneous electrical stimulation of the sacral dermatomes to treat idiopathic detrusor instability [82].</p>
2000	Grill and Craggs	<p>First implantation of “BION” micro stimulator, which delivers chronic stimulation of the pudendal nerve. This can be implanted using minimally invasive techniques [83].</p>

The attempts to use electrical stimulation for the treatment of bladder dysfunction have found their way into clinical practice [61]. One of the best examples is the Finetech-Brindley stimulator (Figure 2:9), that so far has been implanted in more than 2500 patients over the last twenty years [84]. The implant is very reliable

and there was an average one fault in the implant for every 19.6 implant-years and some patients having the implant for more than twenty three years [27].

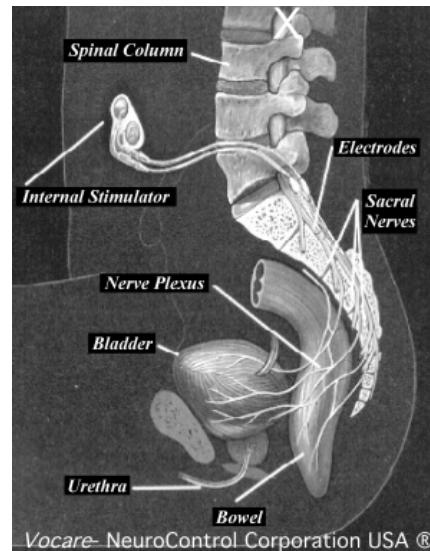


Figure 2:9 – SARSI

The Finetech-Brindley Sacral Anterior Root Stimulator Implant. The implantable receiver (Internal Stimulator) is connected by cables to electrodes placed next to the sacral nerves carrying motor fibers to the bladder detrusor muscle [83].

Electrical stimulation is recommended prior to any other treatment for bladder dysfunction provided the following criteria are met [25].

- Underlying conditions should be treated accordingly prior to electrical stimulation treatment.
- Conditions such as urinary tract infections, vaginal discharge should be treated prior to stimulation.
- Patient's cooperation and ability to manipulate the device is essential.
- Neuromuscular structure involved in urinary storage must be at least partially preserved.

Short term electrical stimulation is non-invasive, practical and generally well accepted by the patient, the devices are reasonable costly and the risk for the patient is negligible [25].

Although electrical stimulation methods are widely accepted, these treatments still have greater potential for use of urology than currently realised [85].

Chapter 3 - The project concept

3.1 Introduction

The chapter initiates by showing the background leading to a requirement of a new device and highlights its advantages. Section 3.4 discusses the different detection and treatment methods that can be used. The basic principles behind the project are explained in section 3.5. The chapter describes the overall thesis hypothesis and introduces the basic principle of the device operation. The chapter finishes with a discussion of how this “proof of principle study” can be realised with the available facilities.

3.2 Background

Urinary incontinence is a major medical and social problem, which affects nearly 200 million people worldwide [3]. Approximately 16% of the urinary incontinence population suffers from incontinence as a result of detrusor overactivity [10]. Urinary incontinence has devastating effects on the life of sufferers and their carers as well as enormous cost to the nation [5] and the cost of incontinence to the NHS is expected to reach £2 billion by year 2020 [8]. The conventional treatment for overactive bladder is anti-muscarinic drugs [17, 19, 43, 86]. However research has shown that nearly 50% of neurogenic patients can become refractory to these oral agents [20, 87] or cannot tolerate the side effects [12, 19]. Therefore improved management and treatment methods are required to reduce the long-term cost.

3.3 Design requirements

The conventional management and treatment methods described in chapter 2 have their own disadvantages [58]. Even though electrical stimulation for bladder overactivity is a better treatment than conventional methods [58], further modifications are required in order to be accepted by the wider community. These modifications are addressed as design requirements of the novel device described in this thesis.

3.3.1 Wearable device

Most of the currently acceptable electrical stimulation devices for achieving good bladder capacity, deliver stimulation through implanted electrodes [88] and have certain disadvantages.

- Implanting electrodes is a surgical procedure and associated with degree of risk [61].
- Reliability of the implantable system is an issue and repair requires another operation [61].
- Implants cannot be used on children due to their rapid growth.
- Some bladder dysfunction symptoms change over time and non-destructive treatment is preferred [89].
- Unpublished data of a recent study suggested that electrical stimulation as a treatment option for women with overactive bladder reduces their infertility rate [90]. In such a condition this would be an ideal treatment.
- Sometimes patients prefer to experience the acute effect of stimulation, before making the decision to have an implant.

- Some women experience mild incontinence due to overactive bladder during their menstrual cycle. For such a condition, a wearable device would be an advantage.

All of these points lead to the requirement for a non-invasive device.

3.3.2 Conditional stimulation

Electrical stimulation can be applied in two different ways, continuous [91] or conditional [31, 32]. In continuous mode, the stimulation is applied throughout filling of the bladder while in conditional mode the stimulation is applied only when a hyperreflexic contraction occurs [92]. Current systems for long term stimulation use the continuous mode [31]. Although a continuous stimulation system is easy to design [31], it would have many disadvantages when compared to conditional stimulation [92].

- The effectiveness of bladder inhibition may be limited by habituation resulting from repetitive activation of spinal reflexes [12, 30-32, 86, 93, 94].
- On average conditional stimulation increases the bladder capacity by 6% to 18% when compared to continuous stimulation [92, 94, 95, 95].
- Also conditional stimulation has been shown to increase the bladder capacity by 79% to 250% over no stimulation [31, 92, 96, 97].
- It may cause tissue and neural damage [12, 32, 86, 98].
- It reduces electrode life [31, 32, 61, 86].
- As the stimulator be switched on throughout the day power consumption is high, therefore low battery life [12, 30, 31, 61, 86]. Recent study showed that

the conditional stimulation reduces the stimulation time by 73%, when compared to continuous stimulation [95].

In principal detrusor inhibition is only necessary during an involuntary contraction and thus stimulation can be turned off between contractions [30]. Studies have proved, applying stimulation at the start of a contraction can completely suppress it, while increasing the bladder capacity [94].

The above factors suggest that conditional stimulation has more benefits over continuous stimulation. Therefore the novel device explained in this thesis will provide stimulation upon satisfaction of a condition related to detrusor contraction.

3.3.3 Warning indicator

Most neurogenic patients with urge incontinence have little or no sensation prior to a detrusor contraction [41]. By using a conditional stimulation system, it is possible to inform the patient when the stimulation is applied [31, 61], using body area network (BAN) or wireless communication link. In this way patient is aware about the status of the bladder and can determine when to empty [12, 30, 86].

3.3.4 Cost

The cost of electrical stimulation devices is a strong limiting factor for patients using the therapy. The currently commercially available systems such as Medtronic “InterStim” (Figure 3:1) device costs around £10,000 [87]. In this project, the device is designed to keep the cost as low as possible so that it can be used widely in the health system.

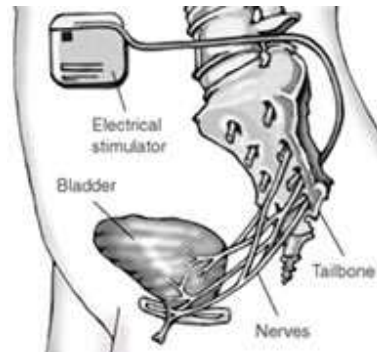


Figure 3:1 – “InterStim” implant.

“InterStim” is an implantation neurostimulation system that sends mild electric pulses to the sacral nerve, the nerve near the tailbone that influences bladder control muscles [99].

3.4 Design principle

The novel device has incorporated all the features described in the design requirements in section 3.3 to become more user-friendly. The design principles behind this device for detecting and treating detrusor overactivity are discussed in this section.

3.4.1 Detecting NDO

As this is a conditional neuromodulation system a certain condition needs to be satisfied in order to deliver the stimulation. This condition should relate to detrusor contraction and over the past few years many methods have been demonstrated to be related. Some of these are highlighted in the Table 3-1.

Table 3-1 - Methods for detecting detrusor contraction.

This table compares the detection methods suggested by researchers and remarks the outcome of the study in order to determine a reliable method.

Detection	Method	Remarks
Patient activation [12, 100, 101]	Allowing patients to switch on the stimulation when a contraction is felt.	During ambulation, the mean detection is about 23% and stimulation was switched on after mean delay of 57s since the start of contraction. Is not suitable method for activating stimulation as the reliability is highly limited.
Electroneurography of sacral roots [92, 94, 102, 103]	Recorded afferent nerve activity related to mechanical activity of the bladder by placing nerve cuff electrodes on the S3 roots.	Requires a surgical procedure, thus associated with risk. Improvements in recording quality and sophisticated signal processing methods are required.
Measuring detrusor pressure [12, 30, 31, 100]	By placing catheters in the bladder and the rectum to obtain the pressure difference. A contraction was identified when detrusor pressure exceeds 8-12cmH ₂ O.	Patient's mobility is restricted due to this method. This cannot be used as a chronic solution.
External urethral	Record the electrical activity	Provides a reliable method for

sphincter EMG [86]	of the muscles which correlate with pelvic floor by inserting fine wire electrodes.	detecting contractions, but may not be feasible for everyday use.
External anal sphincter (EAS) EMG [59, 95, 104]	Record the electrical activity of the sphincters through needle electrodes inserted 2-3cm deep into EAS.	Provides a reliable method for detecting bladder contractions; however this can only be used as a temporary method due to the usage of invasive electrodes.

Considering the tabulated information, the method for recording EMG from urethral or anal sphincters could be modified to be non invasive and practical method for daily use. Considering these two sphincters, it is hard to place electrodes of a wearable device adjacent to the urethral sphincters; therefore the better option appears to be the external anal sphincters.

The external anal sphincters, which are also innervated by the pudendal nerve exhibits bursts of activities associated with bladder contractions in cats, rats as well as in humans [104-106]. In 1981, Blaivas concluded that during dyssynergia, the increase in activity in the sphincters occur coincident or immediately after the onset of the detrusor contraction [107]. These studies suggest that EMG of the external anal sphincters is robustly modulated during NDO and thus can be utilised as the trigger signal for conditional stimulation.

3.4.2 Treating NDO

As explained in section 2.5, electrical stimulation has been shown as an effective treatment to inhibit the detrusor contraction.

Table 3-2- Electrical stimulation treatment for NDO

The table compares some currently available electrical stimulation treatments, in order to determine the best method for the novel device.

Treatment	Method	Remarks
Dorsal genital nerve (DGN) stimulation [12, 30, 31, 91, 95, 100, 108, 109]	Placing cutaneous electrodes over the dorsal base of penis [110] in males and just cranial to clitoris [111] in females.	Simple, effective and non-invasive. However not reliable methods as placement of electrodes are difficult and is not a practical solution.
Intravesicular stimulation [60]	Direct stimulation of the bladder via a catheter with a special stimulation electrode. The intravesicular electrode is a cathode.	Higher current intensities are required, thus it is painful.
Magnetic stimulation [81]	A specially designed coil (9cm focal point) placed over the sacrum and connected to a high frequency stimulator.	Produces consistent and predictable acute inhibition of detrusor hyperreflexia. It's a non invasive, but due to placement of a coil on the pelvis, the practicality of the device will be limited. Also chronic effects are not yet know.

<p>Percutaneous Tibial nerve stimulation (PTNS) [60, 112-114]</p>	<p>A stainless steel needle electrode is inserted approximately 3-4cm into medial malleolus. A stick-on electrode is placed on the same leg near the arch of the foot. These are connected to a low voltage stimulator.</p>	<p>Provides a reliable treatment option for NDO, however regular visit to the clinics are required because the patient cannot perform the procedure by himself.</p>
<p>Vaginal electrical stimulation [115-117, 117]</p>	<p>The vaginal device shown in (Figure 3:2) was inserted to the vagina of the female patient and constant voltage stimulation was applied.</p>	<p>Showed significance increase in bladder capacity with minimal supervision. High currents are required for the stimulation and also the treatment is limited to females.</p>
<p>Intra-anal stimulation [23, 115, 116, 118]</p>	<p>The anal device shown in (Figure 3:2) was inserted to the anus of the patient and constant voltage stimulation was applied.</p>	<p>Long lasting bladder inhibition was recorded and the treatment can be used for both male and female. Minimal supervision is required. However high stimulating currents are required.</p>



Figure 3:2 - Anal (left) and vaginal (right) electrode carriers.

Shows the intra-anal and intra-vaginal electrodes used by Ohlsson and Fall, to study the effect of external and direct pudendal nerve maximal electrical stimulation [115].

According to Table 3-2, there are many methods available for treating NDO of which the dorsal genital nerve stimulation is the most used due to the non-invasive procedure. However dorsal genital nerve stimulation, PTNS and magnetic stimulation limits the mobility of the patient. Therefore the methods that can be incorporated into a wearable device that can be used by the patient daily is intra-vaginal and intra-anal stimulation.

In 1989, Ohlsson compared the intra-anal and intra-vaginal stimulation and showed that long lasting bladder inhibition can be achieved with a device delivering intra-anal stimulation [115, 116]. Furthermore intra-anal stimulation can be used for both male and female patients. Therefore in this study trans-rectal stimulation to the Pudendal nerve is applied through intra-anal device.

3.5 The project concept

Based on the detection and treatment methods discussed in section 3.4, a closed loop electrical control system to treat urinary incontinence can be realised as shown in the Figure 3:3.

3.6 Study design

With the concept of the project being set, the overall hypothesis of the project can be described as “the novel wearable conditional neuromodulation device can be used to treat urinary incontinence” and the device can be named as “ACONTI” (**A**nal **C**onditional **N**euromodulator for **T**reating **I**ncontinence).

There are certain design steps involved in proving this hypothesis.

- First, is to come up with a suitable design of the plug, based on the anatomy of the anal canal and an evaluation of previous models, that had been designed for this purpose.
- Test the method on people with NDO and to see whether the detrusor contractions can be detected and the continence be maintained as a result of trans-rectal stimulation through the device.
- Design, build and test the required electronic circuitry for data processing, which can then be integrated to the device.
- Finally, evaluate whether the device delivers optimum stimulation to the nerves of interest.

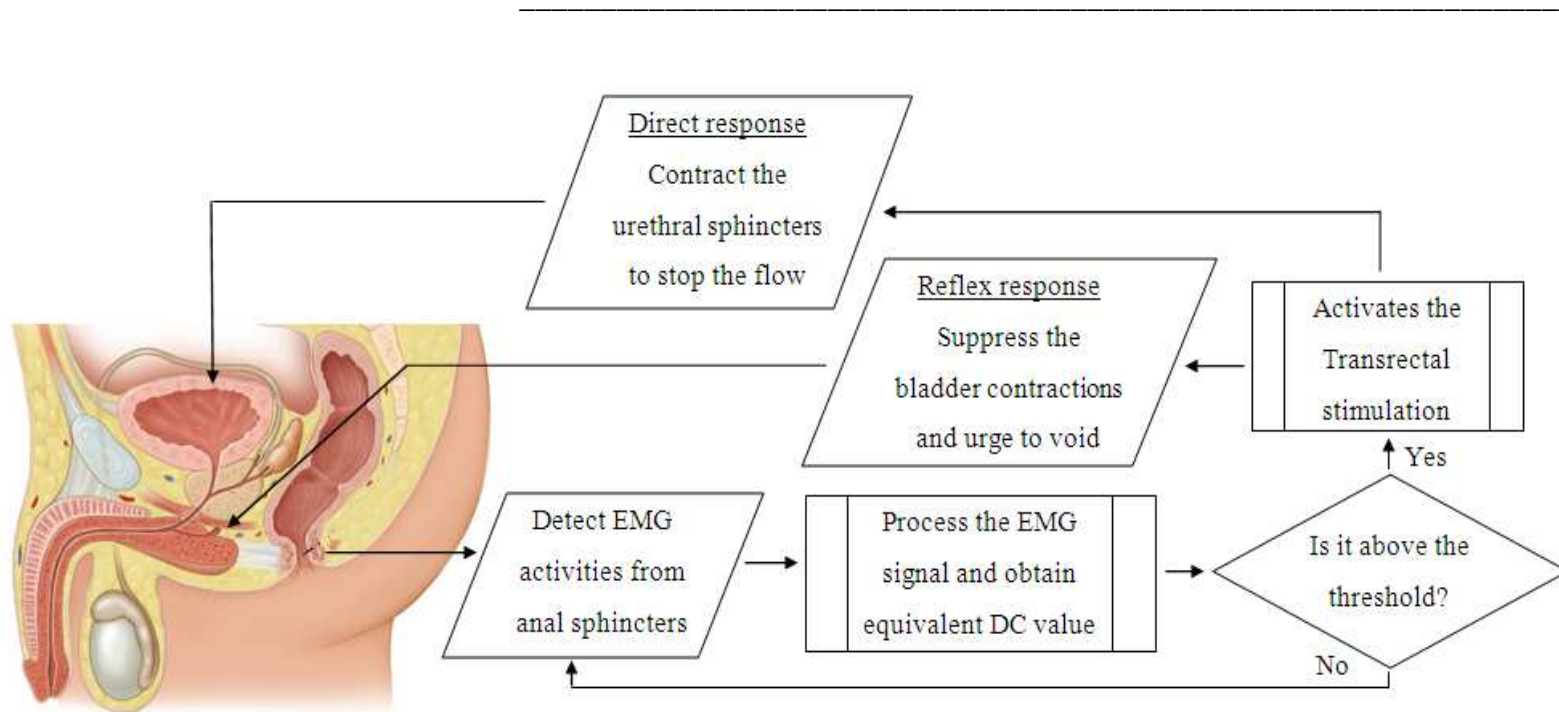


Figure 3:3 – The project concept

Electrodes of the device detect the EMG signals from the anal sphincters, acting as a surrogate to the urethral sphincters. The signal is then processed and when it exceeds the predetermined threshold, activates the stimulation of the pudendal nerve to suppress the bladder and to contract the sphincters [119].

3.7 Other considerations

3.7.1 Clinical setting

Even though the device is designed for all types of neurogenic incontinence such as multiple sclerosis, Parkinson's disease etc, the initial experiments were carried out mainly on spinal cord injured people. The reason for this was the easy access to the facilities and the patients, in the Royal National Orthopaedic Hospital (RNOH) and the involvement of the principle supervisor Prof. Michael Craggs and the assisted nurse Judith Susser being a part of the hospital research staff.

Acute traumatic spinal cord injury (SCI) remains a costly problem to the society. A report published in 2005, showed that nearly 131,623 SCI cases reported worldwide each year [120] and in UK it is estimated nearly 40,000 people living with chronic SCI [121]. Approximately 54% of this population has some degree of urinary incontinence [122]. A recent survey showed that, among the SCI community bladder, bowel and sexual dysfunction was their primary concern to be resolved [49, 123]. Chronic renal failure was the most common cause of death following SCI [81, 124]. Figure 3:4 shows the priorities of the spinal cord injured people.

Even though the device was designed for both men and women, the experiments were carried out only on men. This is because there is higher percentage of men (81%) with SCI compared to women (19%) [125] and the easiness of carrying out the procedures in men, such as collection of urine.

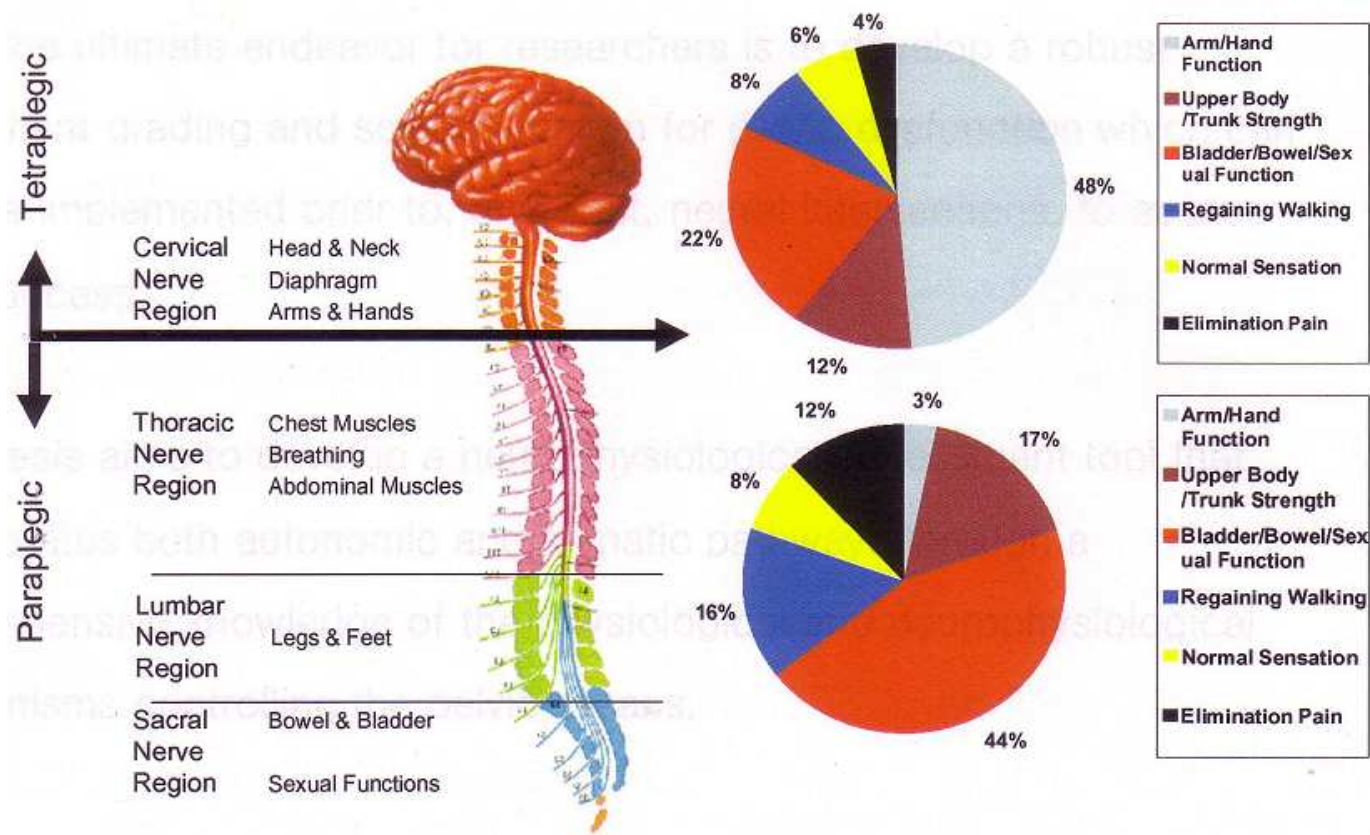


Figure 3:4 - Priorities of the spinal cord injured population – United States [49, 123].

3.7.2 Ethics approval

All research projects involving data collection from human participants require prior ethics approval. This is to ensure the safety, rights, dignity and well-being of the participant and those of the researcher. This study has received approval from the Local Research Ethics Committee of the Royal National Orthopaedic Hospital NHS Trust via the National Research Ethics System (NRES). Participants were invited for the assessment through an official invitation letter together with the patient information sheet. Patient involvement required fully signed informed consent. The patient consent form is attached in the Appendix 1.

3.7.3 Diagnosing bladder dysfunction

Although history and physical examination are used for the initial evaluation of patients with NDO, more exact measurement is required to identify the nature of the bladder dysfunction [126]. Some of the diagnostic methods are detailed in the Table 3-3.

Table 3-3 - Bladder dysfunction diagnostic procedures [127]

Diagnosing method	Remarks
Postvoid residual urine (PVR)	If the PVR is high, the bladder may be acontractile or the bladder outlet may be obstructed.
Uroflow rate	Uroflow rate is the volume of urine voided per unit time and mainly uses to evaluate bladder outlet obstruction.
Subtracted cystometrogram	Assess the bladder capacity, integrity of the sphincter mechanism and the presence of detrusor instability while filling the bladder with a liquid

	(mostly sterile saline) and measuring the bladder and rectal pressure.
Urethral pressure profilometry	Measure functional urethral length and maximal urethral closure pressure to determine the presence of stress incontinence. By combining static and voiding cystogram, the degree of urethral motion, bladder neck and urethral sphincter function during filling and voiding can be assessed.
Electromyography	Helps to identify the presence of coordinated and uncoordinated activity in the sphincters. EMG allows accurate diagnosis of detrusor sphincter dyssynergia, which is common in SCI.
Cystoscopy	Used to evaluate any bladder lesions or bladder stone.
Videourodynamics	Is the standard evaluation of patient with incontinence. This allows to visualise vesicoureteral reflux as well as the pressure-flow relationship between the bladder and urethra.

Considering the methods mentioned above, in order to evaluate the efficacy of the “ACONTI”, cystometrogram combined with electromyography were used to evaluate neurogenic detrusor overactivity.

Chapter 4 - Realisation of the design

4.1 Introduction

Having revealed the concept of the project and explained why the specific approach was taken when compared to the currently available methods, the next step is to find out how the design can be achieved practically. The previous chapter highlighted the requirements of a wearable device, which delivers stimulation upon satisfaction of a certain condition. In this case the condition is to detect bladder contractions related to the detrusor overactivity. Another requirement of the design is low cost. Major design requirements of the device are it should consist of electrodes for detecting bladder contractions, a signal processing unit and electrodes to deliver the stimulating current.

This chapter starts by discussing the models that were used in the past, which was the foundation of the new development. Section 4.3 illustrates how the shape of ACONTI was obtained considering the anatomical structure of the pelvis. Having obtained the required shape, the next step was to determine the materials for the body and the electrodes. Once all the design factors are collected the actual building of ACONTI is described in the section 4.5 and the chapter finishes with a summary.

4.2 Previous models

Table 4-1 analyses advantages and disadvantages of the anal and vaginal devices that have been used over four decades to treat urinary incontinence.

Table 4-1 – Analyse some of the non invasive wearable devices used in the past to treat UI through electrical stimulation.

Device	Design	Advantages and disadvantages
<p>“Anal continence aid”</p> <p>Hopkinson and Lightwood 1967</p> <p>[25, 128]</p>	<p>Made by Cardiac Recorders Limited and shown in Figure 4:1(a)</p>	<p>When the device is in place and the stimulation turned to full strength motor fibres of the pudendal nerve do not stimulate; only reflex activity is detected with latency of 65ms.</p>
<p>“Portex” pessary</p> <p>(Figure 4:2)</p> <p>Alexander and Rowan 1968</p> <p>[128, 129]</p>	<p>Pessary is modified to carry two stainless steel wire wound (10 turns, 25 SWG) stimulating electrodes, which lie anteriorly in the vagina. The electrodes mid-point subtends at an angle of $60^{\circ} - 70^{\circ}$ to the centre of the pessary. These wires are then led within the pessary, in zig-zag to a midpoint of the electrodes and connected to a miniature stimulator under the axilla through a conventional cable. Devices Implants Ltd designed this pessary.</p>	<p>The method of construction ensures that the leads can withstand the mechanical stresses which take place within the pessary, particularly during insertion. Normally the stimulator is switched on and only switched off to permit micturition. However it failed to produce maximal contraction of the relevant muscles and hardly obstruct the micturition at the greatest strength of the stimulation. Out of 28 patients, the success rate was 46% [130].</p>

<p>Vaginal device Soldenhoff and McDonnell 1969 [25, 128, 131]</p>	<p>An electrode pessary similar to tampon inserted into the vagina and connect it to the stimulator box, which is powered by 9V battery. This system was made by Vitalograph Limited.</p>	<p>Voluntary micturition in all subjects is unimpeded or nearly so by these when they are fully switched on. Reported 80% success rate on 28 women with stress incontinence [130].</p>
<p>Intra-anal plug Hopkinson 1972 [23]</p>	<p>The shape of each patient’s anal canal was determined by using soft wet plaster of Paris inside the finger-piece of a thin plastic glove. A Perspex plug was made to the determined shape with two parallel circumferential electrodes 1cm apart, placed to lie above and below the neck of the plug (presumed site of recto-pubalis).</p>	<p>Five different sizes were used (Figure 4:3a). The plug needs to be manoeuvred to obtain the best possible contraction. The success rate was greater in children as the plug fits better. The plug has not proved a better treatment as most of the patients cannot keep it in. Success rate of 57% on 63 patients [130].</p>
<p>Anal plug Brindley, Rushton and Craggs 1975 [128]</p>	<p>The device (Figure 4:1b and Figure 4:1c) has two internal electrodes arranged to lie near the pudendal nerve (at the anorectal junction) and two external electrodes.</p>	<p>Stimulation caused only slight or no pain. Voluntary perineal contraction caused no visible movement of the device. Direct stimulation of the motor fibres activated external urethral sphincters as well as left or right</p>

		(independently) of the ischiocavernosus muscle and caused maximal contraction through both sexes, sustaining continence against 110mm of Hg.
<p>“Continaid” (Figure 4:3b) Merrill, Conway and DeWolf 1975 [132]</p>	<p>The transrectal stimulator consists of bipolar rectal tampon, a flexible cord and a small plastic case containing the 9V battery. The tampon is inserted so that the bulbous portion of the tampon lies within the rectal sphincter.</p>	<p>The device is switched off during micturition. In some patients the device caused abdominal cramps and mild diarrhoea. It was proved to be a good method of assessing a requirement for a chronic stimulator.</p>
<p>Anal plug (Figure 4:4a) Sotiropoulos 1975 [133]</p>	<p>The stimulator can be kept inside a pocket or attached to the belt and powered by a 9V battery. There are two parallel electrodes which are 1cm apart on the surface of hour glass shaped Perspex plug. Once the device is positioned inside the anal canal electrodes rest in close contact with the anal wall above and below the level of the pubo-rectalis</p>	<p>Plugs are commercially produced in four different sizes: 25mm (large), 24mm (medium), 20mm (small) and 15mm (infant) in diameter. The product showed better response among the younger ones.</p>

	muscle.	
<p>“Incontan” device (Figure 4:4b) Eriksen 1987 [116]</p>	<p>The complete system consists of 12V battery, electronics and electrodes integrated in plastic plug housing. The stimulator is automatically activated when the ring electrode touches the wall of the anal canal.</p>	<p>The device is intended to strengthen pelvic muscles by continuous stimulation. The device caused anal soreness and changes in bowel function in some of the patients. However the device fits the anal canal well, making it possible for the patient to sit in comfort and move around normally with the stimulator in place.</p>

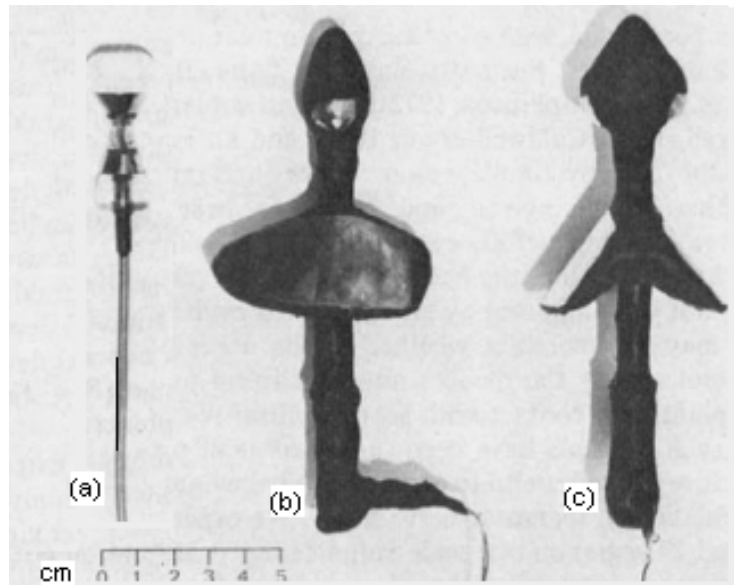


Figure 4:1- (a) Anal plug used by Hopkinson and Lightwood. (b) and (c) show lateral and anterior view of the anal plug used in Brindley, Rushton and Craggs experiment [128].

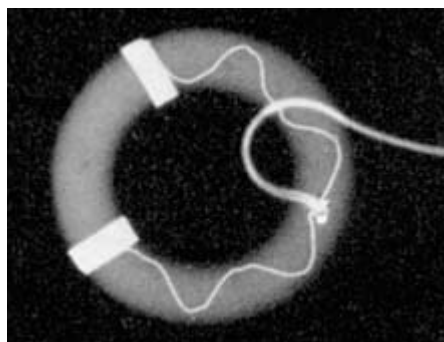


Figure 4:2 - The x-ray of 'Portex' electric pessary [134].

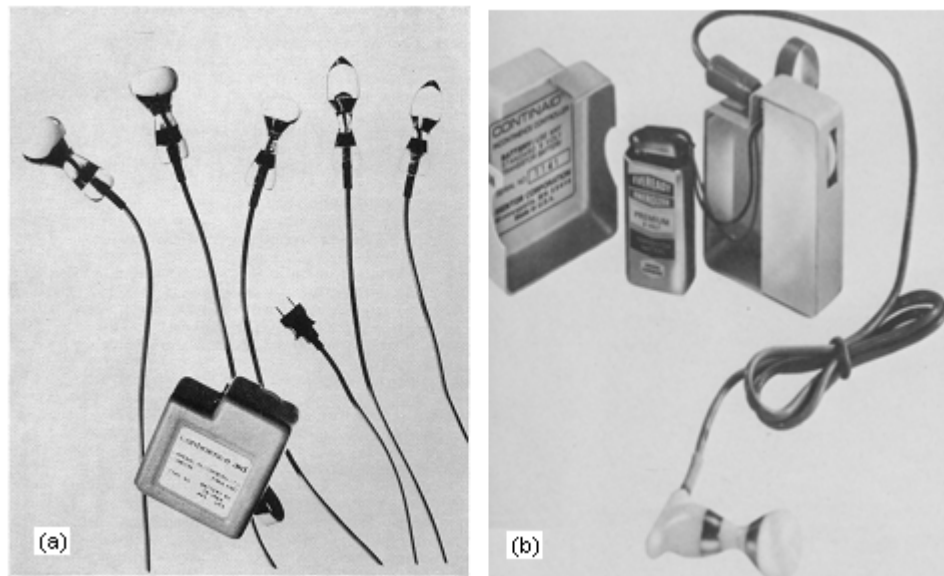


Figure 4:3 – (a) The small portable electrical stimulator and range of five Hopkins' intra-anal plugs to fit most patients [23]; (b) The external transrectal stimulator “Continaid” [132].

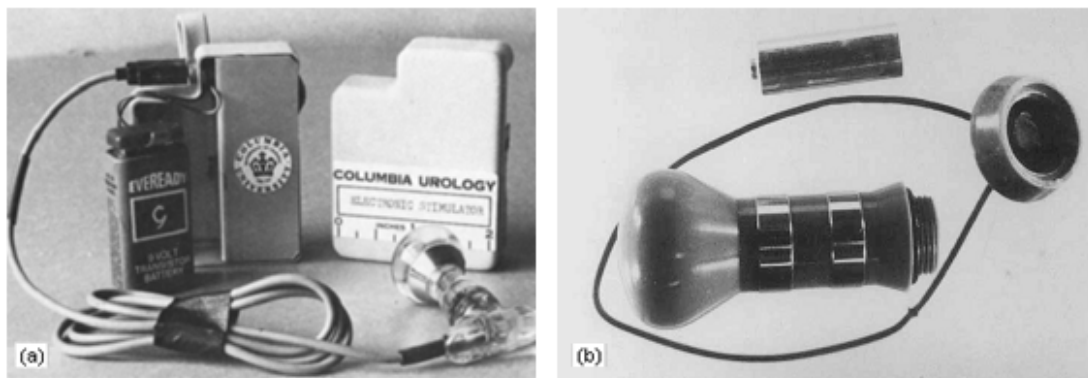


Figure 4:4 – (a) Sotiropoulos anal plug [133]; (b) The “Incontan” device with the top and the battery removed [116].

Since the 1970's there has not been major development of the anal devices to treat urinary incontinence through electrical stimulation. However some devices have been developed as pelvic muscle toners (Figure 4:5) in which some ideas can be utilised in the design of ACONTI.



Figure 4:5 - Commercially available pelvic muscle toners.

(a) Anuform, (b) Liberty electrode, (c) Anal electrode PR13. The body of these devices made out of GE plastic MG47 and the electrodes are made out of stainless steel [135].

Hopkinson's anal device provides the foundation in designing ACONTI. Over the years some modifications have been made to this, however the basic shape remains the same. Whatever the design, it should be easy to manipulate and should be well accepted by patients. Furthermore it should provide satisfactory retention in the anal canal during stimulation.

4.3 Shape consideration – anatomically

The device is to be inserted into the anal canal. In order to deliver successful neuromodulation three main criteria need to be satisfied. Those are;

- anatomical stability of the device during patient's activity.
- effective recording of EMG signals from the external anal sphincters.
- optimal stimulation to the Pudendal nerve.

In order to derive the shape of ACONTI, it is better to understand the structural anatomy of the anus and the rectum (Figure 4:6).

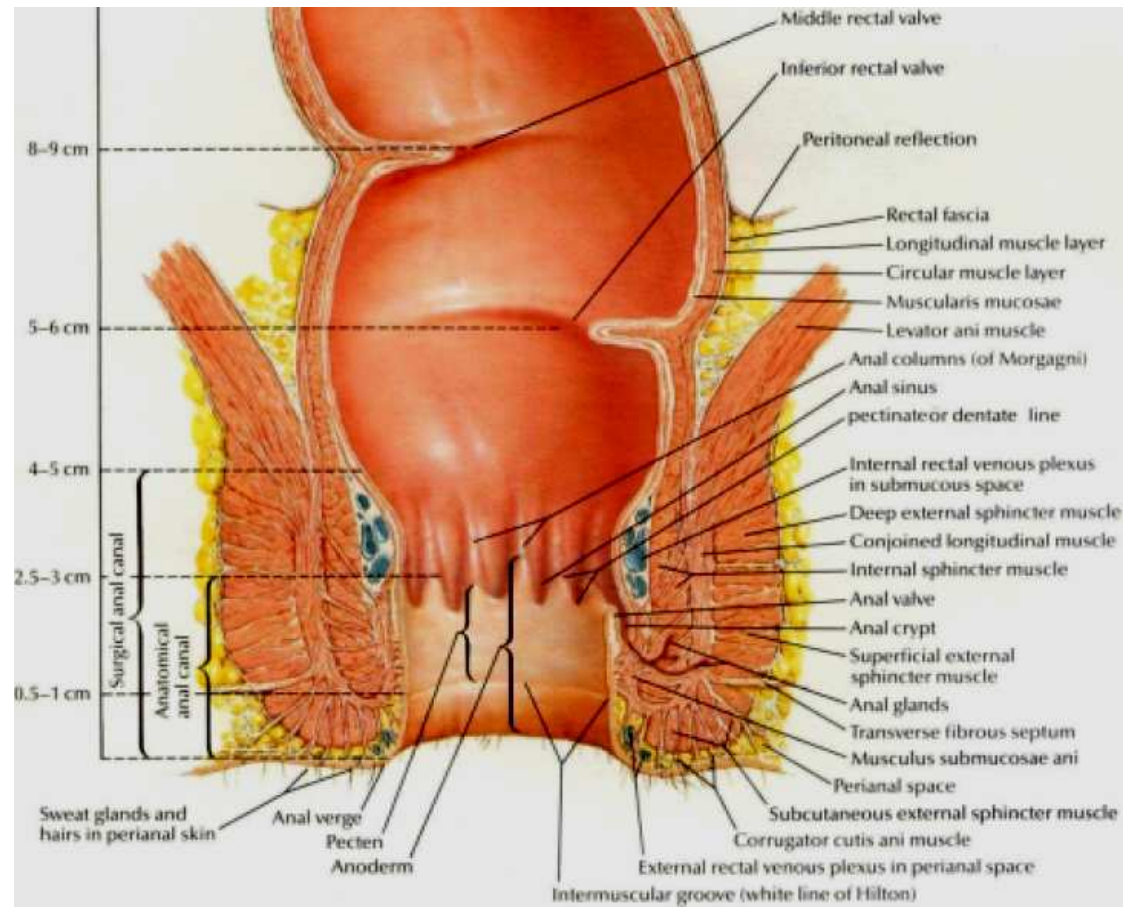


Figure 4:6 – Coronal plane cross-section of the anus and the rectum of an adult [136].

The anal canal is about 4cm long and passes downward and backward from the rectal ampulla to the anus. The anal canal is a narrower, tubular structure and it continues to the wider muscular tube called the rectum [35].

4.3.1 Anatomical stability of ACONTI

The ACONTI has to be easy to insert, without causing much pain. Once in place it should be secure and should not move due to movement or stimulation. The points that should be considered in designing its shape relate to stability. These are listed below.

- The head of ACONTI should be narrow and the diameter should gradually increase (similar to the anal plug used in Brindley’s experiment in the Figure 4:1b and Figure 4:1c) to provide easy insertion.
- The device should be flexible in order for it to follow the $4.12^{\circ}/\text{mm}$ curvature of the ano-rectal junction [137].
- The part of the device that sits on the anal canal (stem) should be narrow to be held easily without applying much pressure to the walls of the anus, in order to minimise discomfort.
- To stop ACONTI moving during stimulation, an approach similar to “Anuform” (Figure 4:5a) can be adopted; by making an isthmus near the end of the device so that the anal verge can be made to sit around it.
- To prevent the device sliding further in to the orifice, a small guard can be introduced at the end of ACONTI similar to the modification Glen [138] introduced to the Hopkinson device (Figure 4:7). This also makes the device easy to remove and as a support for holding the cables.

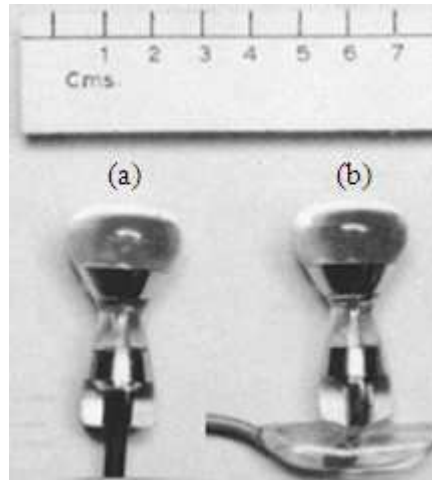


Figure 4:7 - (a) Hopkinson's continence aid anal plug, (b) the modified plug introduced by Glen [138].

4.3.2 Effective recording of the EMG signals

The effectiveness of conditional neuromodulation depends on how well the condition for stimulation is detected. The main consideration is how specific muscle signal currents can be recorded without significant interference unrelated to the function is required.

The lateral wall of the anal canal is kept in apposition by the levator ani muscle and the anal sphincter. The anal canal comprise of inner longitudinal muscle layer as an internal anal sphincter enclosed by external sphincter [139]. The external sphincter is formed with three main parts (shown in the Figure 4:6). A subcutaneous part which encircles the lower end of the anal canal, a superficial part which is attached to the coccyx posteriorly and perineal body anteriorly and finally the deep part of the anal sphincter encircles the upper end of the anal canal [140].

During bladder filling, the activity in the longitudinal muscle increases, therefore it is accepted that bipolar surface electrodes for recording striated muscle EMG

are usually placed in the direction of the muscle fibre [141]. Due to the structural anatomy the recording electrodes should be constructed considering the following factors.

- The two recording electrodes should be placed along the axis of ACONTI and should be equally separated on the circumference.
- Recording end of the device should be wider than the stem in order to push the electrodes towards the wall of the anal sphincters as similar to the “Anuform” (Figure 4:5a).
- The reference electrode should be placed somewhere electrically inactive such as the stem, therefore the stem should be wide enough to hold the ground electrode.

4.3.3 Optimal stimulation to the Pudendal nerve

It is important to ensure that when a nerve is stimulated, that electrical current is delivered to the nerve in an adequate amount to generate an action potential as well as the stimulating currents be focused such as to minimise unwanted stimulation of other nerves.

The ano-rectal junction is the closest part of the gastro intestinal tract to the Pudendal nerve. Therefore if the stimulating electrodes can be made to sit on the ano-rectal junction, the stimulating current can be directed to Alcock’s (Pudendal) canal. As the Pudendal nerve runs bilaterally at 10 o’clock and 2 o’clock position (Figure 4:8), it will be beneficial if there are two sets of stimulating electrodes.

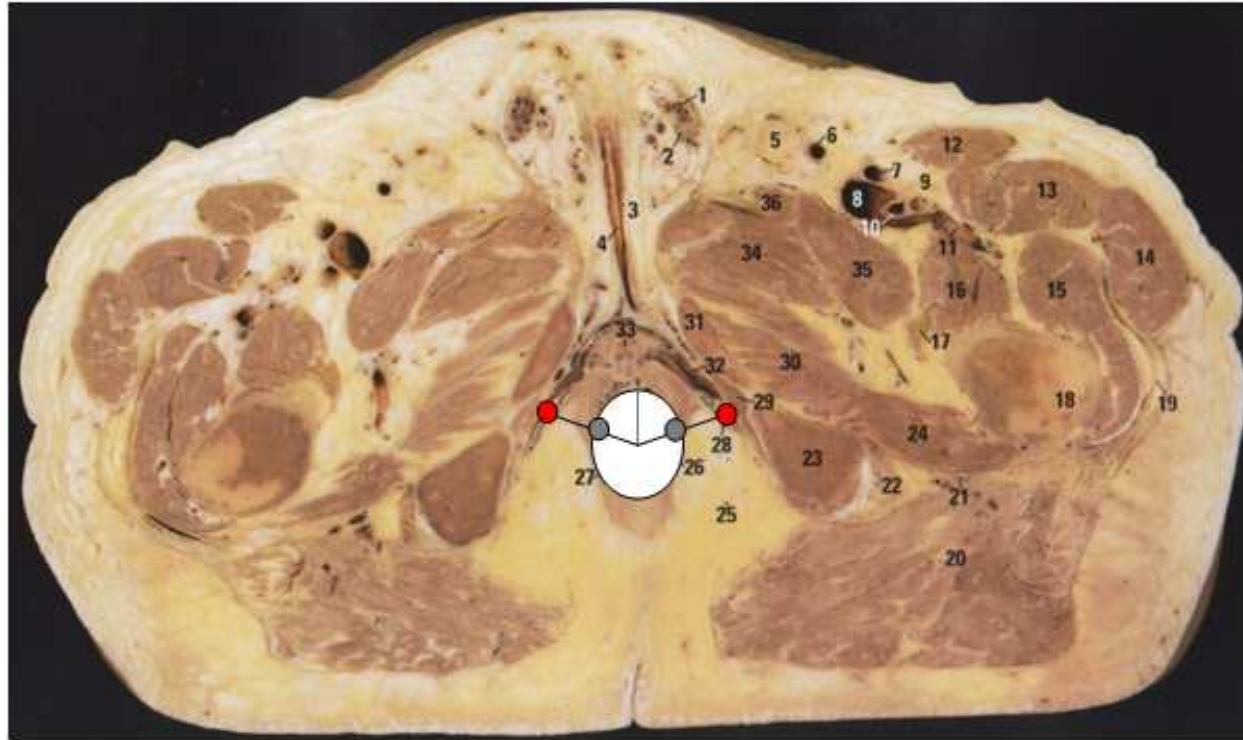


Figure 4:8 - Shows the transverse plane image of the male pelvis at the ano-rectal junction.

Pudendal canal is marked in red circles, and for optimal stimulation the stimulating electrodes ideally be located in grey circles [142].

As the rectum is much wider than the anus, the stimulating head can be made wider too, giving more space to place the embedded electronics as well as to push the stimulating electrodes more towards the Pudendal canal. The anode can be made bigger than the cathode, to increase the current density near the cathode as the stimulation occurs close to the cathode.

Based on these considerations, the shape of ACONTI can be derived and is shown in Figure 4:9.

4.4 Material consideration

Having derived the shape of ACONTI based on anatomy, the next step is to determine the suitable material for the device and the electrodes. The main factors that need to be addressed in determining the materials are bio-compatibility within the body and patient compliance.

4.4.1 Device material

The anal and vaginal devices discussed in Table 4-1, use perspex for the device body. As ACONTI is to be non-implanted, the material does not have to be implant grade, but should be biocompatible. Due to its elastic nature (availability of different grades), silicone rubber is a better choice than perspex and this will make the device easier to follow the curvature of the anal canal. In addition to the elastic nature, silicone also has low surface tension, chemical and thermal stability which made it to be used widely in the healthcare [143]. As the silicone polymers are structured with an inorganic backbone, which minimise the chemical reaction with living organic system, good biocompatibility results in devices in this nature [144].

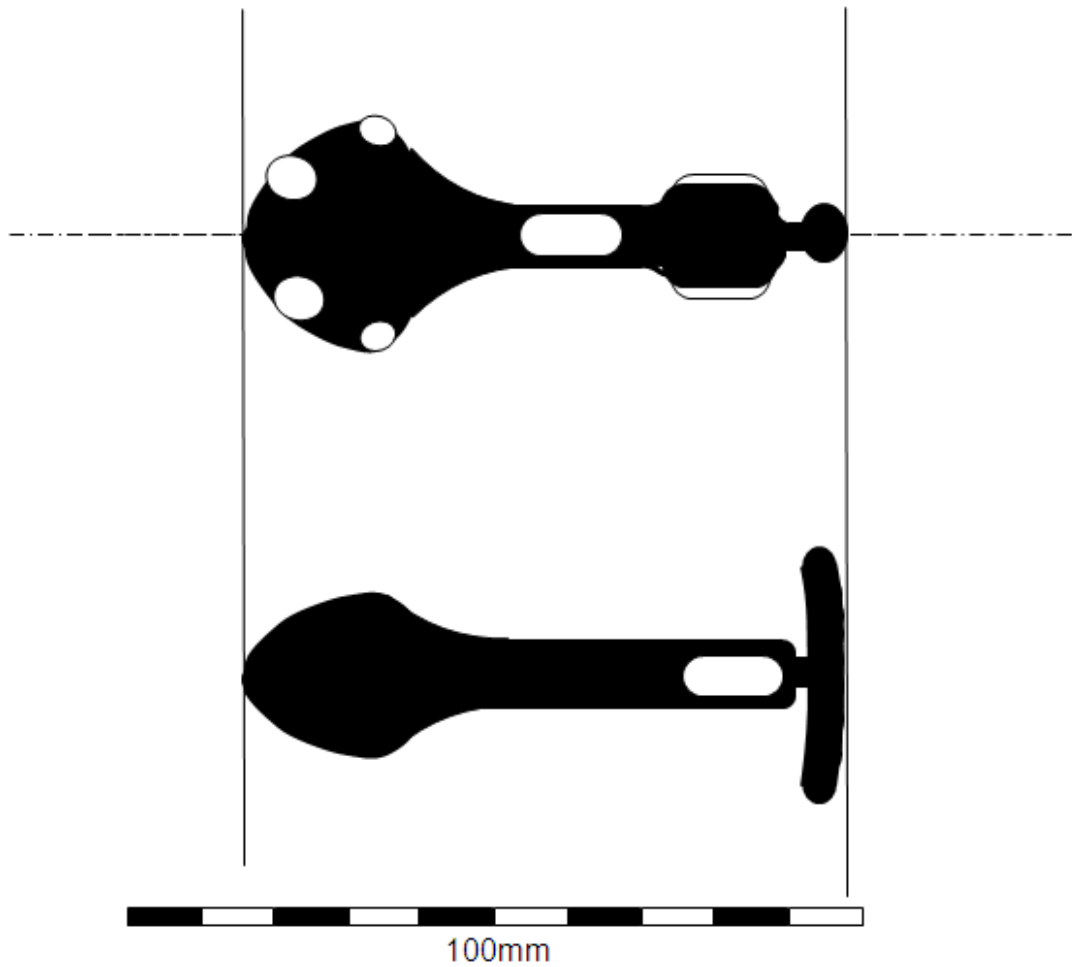


Figure 4:9 – Final shape of the ACONTI represent to a scale shown.

The top figure shows the axial view while the bottom figure shows the longitudinal view. Small circular dots represent the cathodes; large circular dots show the position of the two anodes. Round rectangular electrode on the stem is the ground electrode, and that near the end is one of the two recording electrodes.

The silicone rubber that is available in liquid form is widely used in injection moulding applications and available in different grades with a range of hardness of the cured rubber. In order to determine the suitable grade cylinders with dimensions 5cm in length and 1cm in diameter was made in LSR10-LSR90. These cylinders were then analysed for their elasticity and the ability to hold electrodes. Based on this analysis it was concluded that LSR40 is the best grade for ACONTI. Therefore MED-4940³ two part liquid silicone rubber from NuSil Technology was used in this application. This is restricted rubber, which can be used on external devices or implantation for less than 29 days [145].

4.4.2 Electrode material

Most electrodes that are used for electrical stimulation are polarisable electrodes. However to reduce the complexity of using two electrode materials; the same material is used for both recording and stimulating electrodes. Polarizable electrodes are either made of noble metals like platinum, iridium, gold or non-noble metals/alloys such as titanium or stainless steel [146].

Table 4-2 highlights material properties of some commonly used bio electrodes.

³ This is the medical grade (restricted) silicone rubber, which has the hardness grade similar to as LSR40.

In the devices mentioned in Table 4-1 and the pelvic muscle toners in the Figure 4:5 the choice of electrode material is medical grade stainless steel. Stainless steel is a cost-effective engineering material with good corrosion resistance and a range of mechanical and physical properties coupled with inert, easily cleaned surfaces that are well suited to a wide variety of medical applications, where hygiene is a major requirement. AISI-316 (medical grade) stainless steel is specially produced with enhanced chemical composition in order to be suitable for close and prolonged contact with human tissue [147]. Therefore medical grade stainless steel was used as the choice of material for both recording and stimulating electrodes.

4.5 Manufacturing of the device

With the basic shape of the device being derived based on the previous devices described in Table 4-1, the next stage was to make some devices to be tested in clinical studies. In order to have a repeatable design with accurate measurement and method of filling with liquid silicone rubber, it was decided to produce a mould. This procedure was handed over to pattern maker.

In order to design the mould for filling the rubber, a prototype device was made using epoxy which is shown in Figure 4:10.

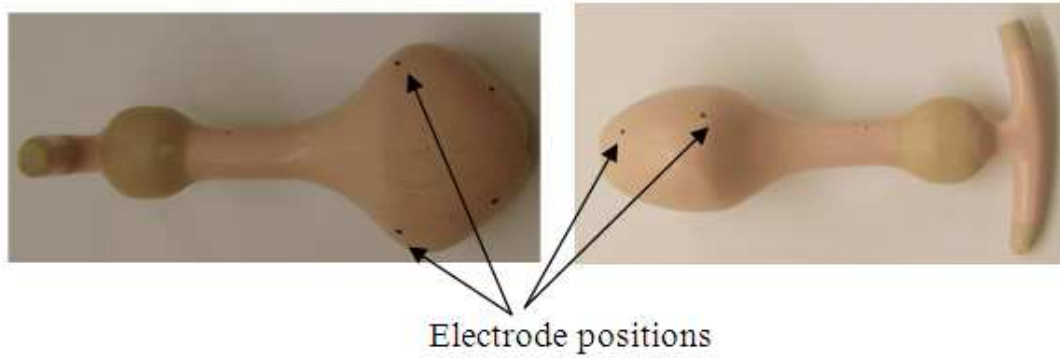


Figure 4:10 - The master model of the device.

The master model was made by the pattern maker using epoxy to the exact measurement shown in Figure 4:9.

Table 4-2 - Desirable material properties for some metals commonly used as bio electrodes [148].

	Platinum	Iridium	Gold	Silver	Tantalum	Titanium	Stainless steel
Corrosion resistance	X	x	x		x	x	x
Biocompatibility	X	x	x		x	x	x
Electrical conductivity			x	x			

In determining the size and the shape of the electrodes, the surface area of the recording electrode should be made to the maximum allowable size to minimise the electrode impedance. As explained in section 4.3.3, a pair of stimulating electrodes will be added to the device for bilateral stimulation and the anode was made bigger than the cathode. Sample electrodes produced by the pattern maker are shown in the Figure 4:11.

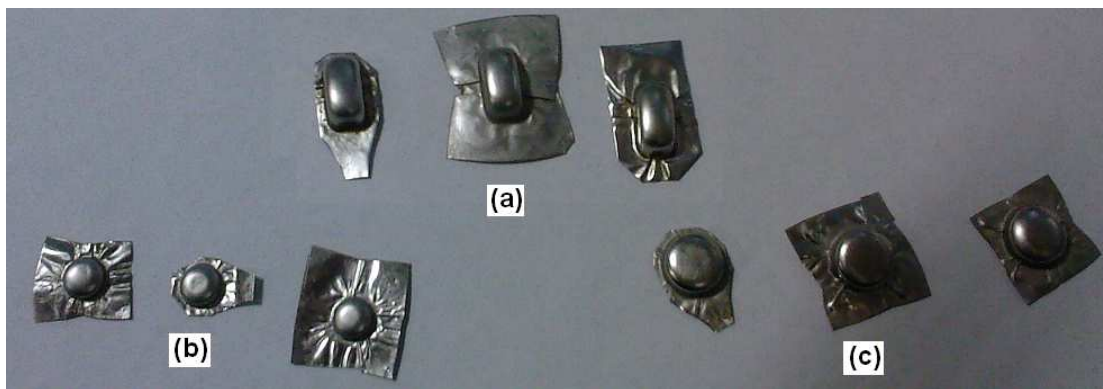


Figure 4:11 – Sample electrodes.

The electrodes are made out of medical grade stainless steel. (a) recording electrodes are round rectangular shape of 5mm x 10mm, (b) circular shape cathode electrodes of diameter 5mm and (c) circular shape anode electrodes of diameter 8mm.

The electrode connection in the device is shown in the Figure 4:12.

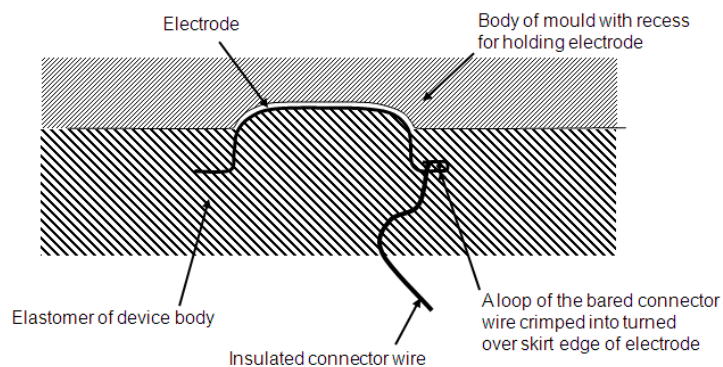


Figure 4:12 – Shows how the electrode is connected when it is in the device, embedded in silicone rubber.

Using the master model shown in the Figure 4:10, a mould was made out of aluminium loaded epoxy (Figure 4:13).

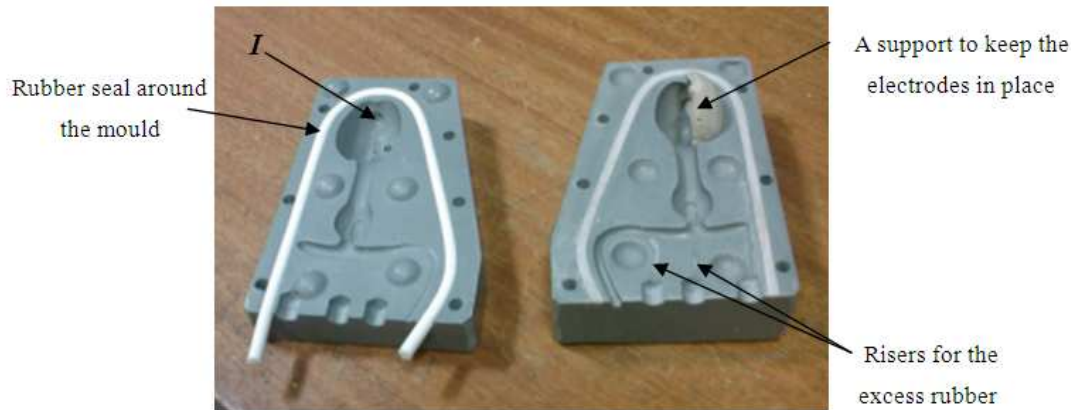


Figure 4:13 - The main mould for filling rubber.

The two halves of the mould will be screwed together before filling. The rubber will be injected into the mould from I. The electrodes were glued to the mould temporarily.

A two part liquid silicone rubber (MED-4940) was mixed 1:1 and then injected to the mould. The mould was then put into the oven and left for more than 24 hours at 70⁰C. When the mould was checked, the rubber was not cured. It was left in the oven further 2 days, but still the rubber was not cured properly. Therefore this approach failed for the following reasons.

- The rubber was inhibited by the mould material
- The cables used for connecting the electrodes had an overall diameter of 5mm. Due to this cable and the support to hold the electrodes injection of the rubber was hard.
- It was difficult to keep the electrodes in place by using temporary glue.

In order to overcome these problems a new method was developed: the design stages are described in Table 4-3.

Table 4-3 - Highlights the problems faced in the previous approach and the solution to overcome them.

Stage	Problem faced in the previous design	Solution	Design procedure
(a)	Rubber was not curing due to the reaction of rubber with epoxy and not enough heat transferred to the inside of the mould.	Made the mould out of heat transferrable material.	Melted metal was poured over the master model when it is resting inside a block.
(b)	It was hard to push the rubber because the mould was blocked by the cable and the support to hold the electrodes in the opposite side.	Kept all the electrodes on the same half, so they can be held using the mould itself.	Orientation of the device in the mould was changed and the recording electrodes that were 180 ^o apart were brought to 120 ^o (4 and 8 o'clock positions).
(c)	Keeping the electrodes steady during the filling.	Attached the electrodes to the mould using fishing line: and can be cut at the end to release the electrodes.	A hole of 1mm was made in each electrode, through which can pass a fishing line and tie on the other side, so that it stops the electrode moving.

(d)	Wires touching the wall of the mould so they are not embedded in the device.	<p>Wrapped the wires around rubber tubing in the middle.</p> <p>Used enamelled copper wires of thickness 0.125mm.</p>	<p>The wires were soldered to the electrodes (using phosphoric acid to dissolve the oxide layer). These were wrapped around the silicone rubber tubing, which was held using 1mm rod passing through the middle of the mould. When the rubber is set this rod can be pulled out.</p>
(e)	Curing the rubber and preventing air bubbles.	Used the pressure chamber and the hot plate.	<p>The rubber was then vacuum centrifuged and then injected into the mould. This mould was kept inside a pressure chamber at a pressure of 1atm. This system was then kept overnight on a hot plate.</p>

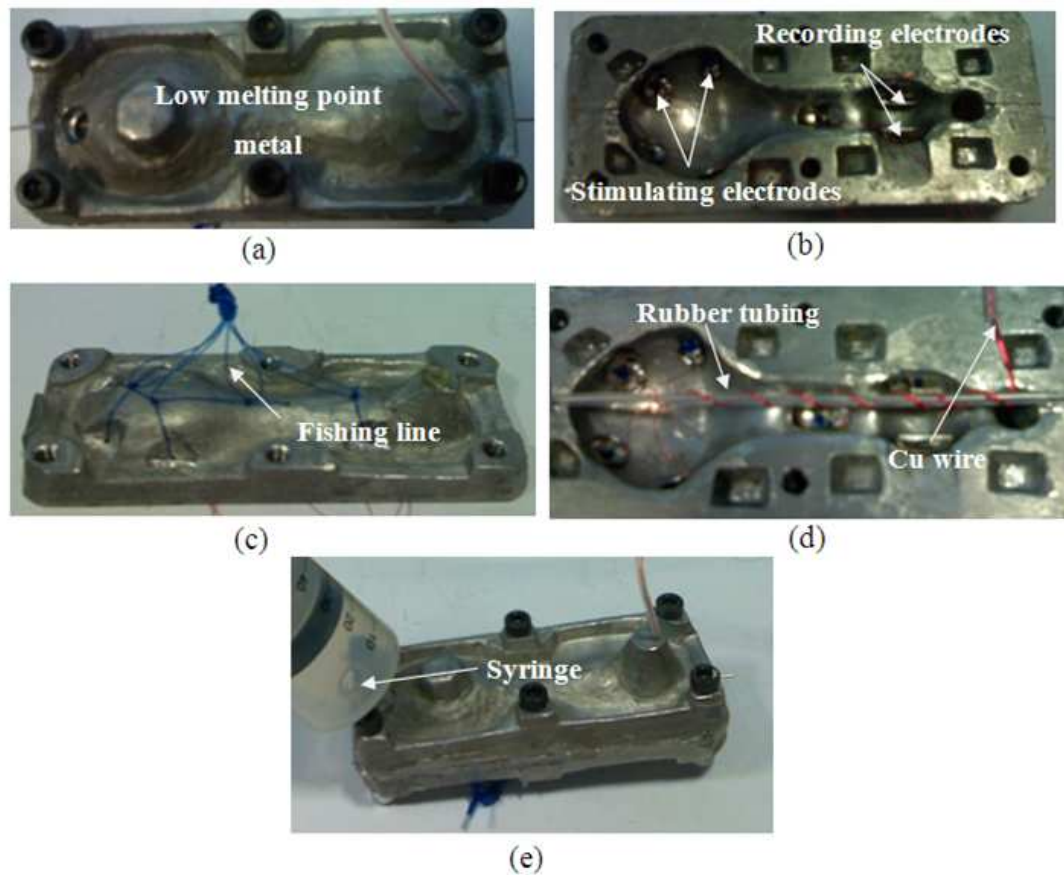


Figure 4:14- Shows the design stages explained in the Table 4-3.

(a) The mould which is made out of low melting point metal. (b) All the electrodes are in the same plane. (c) Electrodes are held in place using a fishing line. (d) The copper wires are connected to the electrodes and wrapped around the rubber tubing. (e) The rubber free from air bubbles was injecting through the inlet.

The resultant device (shown in the Figure 4:15) is up to expectation. This new version of ACONTI was tested clinically, and gave promising results which will be described in chapter 5.

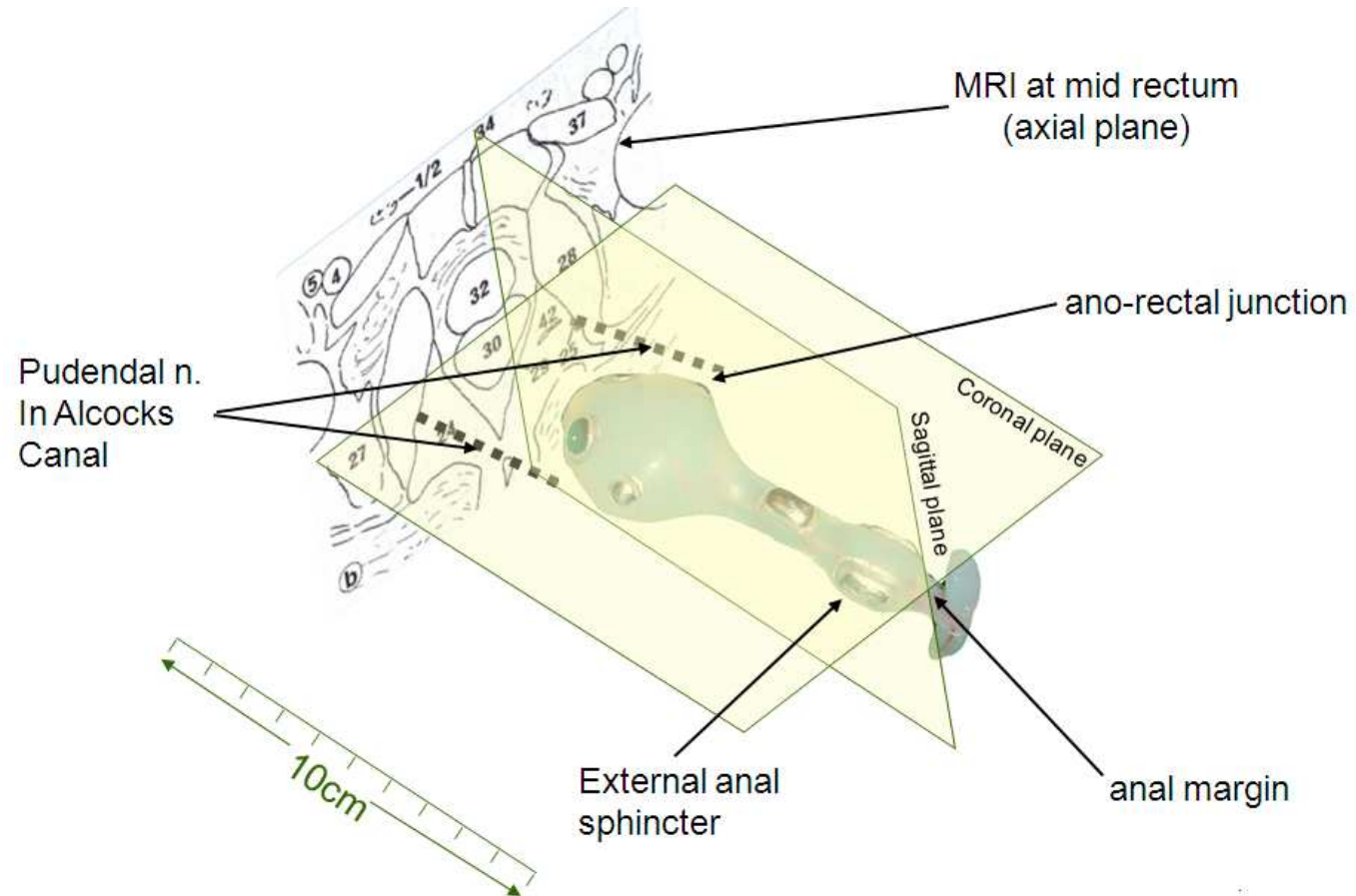


Figure 4:15 – ACONTI device in 3-dimensional plane

4.6 Conclusion

The foundation for the design of the novel wearable bladder control device was derived from the Hopkinson's anal device. The electrodes position of ACONTI was based on the anatomy and neurophysiology of the ano-rectal region.

The chapter described the actual manufacturing of the device together with the problems faced thus led to design limitations such as increasing the distance between the recording electrodes. These limitations can be overcome by using more sophisticated method.

Based on the anatomy and practical experience, it was assumed that the stimulating head of ACONTI sits on the ano-rectal junction. However precise measurements have not been taken. The position could be measured by taking MRI images of ACONTI when it is in the pelvic orifice of a patient. Once those images are produced further details regarding positioning electrodes can be analysed. An experiment to optimise the stimulating electrodes of ACONTI is described in the chapter 7.

With these two results ideal positions for the electrodes can be obtained. Once all the relevant information is known, this device will be redesigned to be built using an industrial method.

Chapter 5 - Clinical efficacy of the ACONTI

5.1 Introduction

Once a satisfactory design was obtained, as described in chapter 4, the next stage is to perform some clinical studies to determine the efficacy of the design. This chapter starts by recapping the background leading to the clinical experiments and then moves onto describing the aim and the objectives of these experiments. Section 5.4 explains the patient selection and the equipment set-up. Then the chapter divides into two main sections based on the experiments, where section 5.5 describes detecting NDO and 5.6 describes treating NDO. Each of these sections talks about the objective, method, results and analysis and discussion.

5.2 Background

Urological problems following SCI, mainly neurogenic detrusor overactivity and/or detrusor sphincter dyssynergia, cause severe urinary incontinence [12, 32, 49, 95, 101, 122]. Approximately 54% of the SCI community suffer some degree [122] of incontinence and restoring bladder, bowel and sexual function is their main priority [40, 49]. Even though anti muscarinic drugs remain the common management [5, 12, 17, 20, 28, 43, 86, 95], 50% of neurogenic patients cannot tolerate the side effects of these drugs and have poor compliance [20, 87]; leading to a need for alternative treatment modalities such as electrical stimulation [12, 28, 95].

Most of the currently available devices were set to deliver continuous stimulation [31, 100]. The principle of conditional neuromodulation was introduced in order to overcome some of the problems associated with continuous stimulation such as stimulation becoming ineffective due to habituation and high power consumption [12, 28, 31, 33, 86]. Accordingly, a condition must be satisfied to deliver the stimulation. Most previous studies used rise in intravesical pressure as the trigger for the stimulation [30-32, 41, 92, 149]. As explained in chapter 4, ACONTI sits in the anal canal and monitors the muscle activity of the external anal sphincters, which act as surrogates for the urethral sphincter during DSD to trigger the stimulation of the pudendal nerve [40].

5.3 Aim and objectives

The aim of the research is to develop a wearable conditional neuromodulator device to treat NDO and restore continence for the people with neurogenic incontinence. This aim can be divided into two main questions as objectives, which are:

- Does the device detect the surrogate external anal sphincter EMG with related to the detrusor activity during NDO?
- Does the device stimulate the pudendal nerve suppressing NDO, leading to increase in bladder capacity?

The two experiments described in the sections 5.5 and 5.6 are intended to answer these questions.

5.4 Clinical set up

As explained in 3.7, the study was conducted in the spinal injury unit of the RNOH. In order to commence the study appropriate patient group and the

necessary equipment must be set up as described in this section. The patients participated in the study required a fully informed consent. The study was conducted in the context of good clinical practice.

5.4.1 Participant selection

Twelve complete and incomplete SCI men were selected for the study based on appropriate inclusion and exclusion criteria.

Inclusion criteria

- Participants must be aged between 18 years to 75 years due to their independence in taking decision.
- Participants must have had their injury at least twenty-four months prior to the study. This is to ensure that the time for natural recovery and physiological instability has finished.
- Individuals must have a complete or incomplete supra-sacral spinal cord injury at upper motor neurone because lesions at the vertebrae below T10 may have denervation [150].
- Participants must have proven NDO and/or DSD as indicated by previous urodynamics studies.
- For the practical reasons and to improve the acceptability as well as to avoid any confounding errors during analysis, only men were considered at this stage.

Exclusion criteria

- Patients with any other neurological disorder.

- If the patient had a history of any implanted device for bladder function, or if they had a surgical intervention at any time to the bladder, sphincters or any infection in the rectum.
- To minimise autonomic dysreflexia during cystometry, patients with any past or present cardiovascular conditions.
- Also if the patient gets recurrent resistant urinary tract infection or reported any of the symptoms on the day, patient was excluded from the study until they are positively treated.
- Patients who had botulinin toxin interventions to either bladder or bladder outlet [151].
- If the patient is participating in any other drug study they were excluded in order to avoid conflicting drugs.

In addition to these, the participant will be requested to stop anti-cholinergic drugs or other drugs being taken for their bladder condition (such as oxybutynin, toltarodene or detrunorn) for a period of 5 days (7 days if it is x1⁴) prior to the assessment. If the subjects proved to have history of UTI, a single dose of Genitamicin (80mg) was given intramuscularly against any possible UTI caused by the repeated catheterisation.

Those who met these criteria and were included in the study are listed in the Table 5-1. These details were extracted from the patient's notes and by further discussion with them. All subjects who participated in the study signed a consent form having first been fully briefed and given the opportunity to have their questions answered.

⁴ Modified release version of the drug.

Table 5-1 - Patient details.

CISC = intermittent self catheterisation, M = medication, FC = Foley catheter, IP = incontinence pad

Patient	Level of injury	Complete/ Incomplete	ASIA grade	Date of injury	Bladder management
P1	T11-T12	Incomplete	-	May 2006	CISC, M
P2	T10-T11	Complete	A	March 2005	CISC, M
P3	C3-C7	Incomplete	D	October 2002	CISC, M
P4	T4	Complete	A	September 2007	CISC, M
P5	T12	Incomplete	D	April 1998	M, FC
P6	L5-S1	Complete	-	1992	CISC, IP
P7	T11-L1	Complete	-	August 2005	CISC, M
P8	C4-C6	Incomplete	-	September 1997	CISC, M
P9	C6-C7	Incomplete	D	2000	CISC, M
P10	T6	Incomplete	C	June 2007	CISC, M
P11	T3-T4	Complete	-	January 2001	CISC
P12	T2	Complete	-	1987	CISC, M

In the Table 5-1, the injury levels of the patients are shown according to the relevant vertebral level. In some of these patients, multiple vertebral sites are shown either due to the several injury sites of the spinal cord or due to the fact injury is located in between the particular vertebrae.

One of the inclusion criteria of the selection of the patients was that the injury should be above T10. However patients P1, P2, P5, P6 and P7 have their injury below T10. The reason for including them for the study was, these patients were taking oxybutynin for bladder control and previous urodynamics investigations have shown hyperreflexic bladder.

5.4.2 Experimental setup

The experiments were carried out in the Royal National Orthopaedic Hospital (RNOH) in Stanmore. The experiment session was supervised by Professor Craggs (consultant clinical scientist) and the clinical work with regards to the patient was carried out by a specialist urology nurse.

Performing cystometrogram

According to the bladder dysfunction diagnostic methods, described in chapter 3, it was concluded that standard cystometrogram proved to be the best method for assessing the efficacy of the device. Cystometry is a method to obtain pressure/volume curve by filling the bladder with physiological saline at a constant rate while monitoring changes in intravesical pressure. Any detrusor contractions greater than 15cmH₂O are considered abnormal [152]. Detrusor pressure is obtained by standard subtraction cystometry, which is the subtraction of the abdominal (rectal) pressure from the intravesical (bladder) pressure [153].

First of all, the patients were laid flat on the bed in a comfortable position. In order to measure the bladder pressure, standard 4.5Fr blue catheter (Figure 5:1a) inserted into the bladder through the urethra, and a 4.5Fr rectal line inserted through the hole at the midline of ACONTI (Figure 5:1b) was used to measure the rectal pressure.

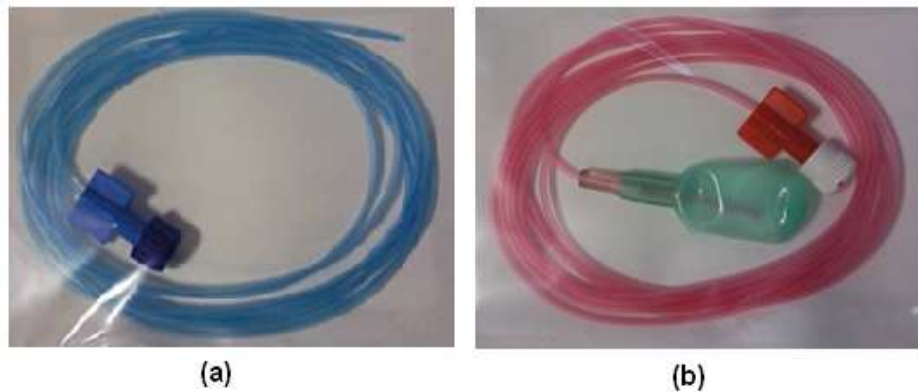


Figure 5:1 – Bladder and rectal lines

Shows the 4.5Fr (a) bladder line and (b) rectal line to measure the intravesical and the abdominal pressure respectively.

The other ends of these catheters were connected to the Digitimer pressure transducers, which then were connected to 10ml syringe containing sterile saline to flush the pressure lines. These lines were calibrated (zeroed to the air), before connecting to the Lectromed amplifier system. Subtraction of these two pressure values (showed the detrusor pressure) was done in the software.

Volume assessment involved filling the bladder with saline via the filling line. The filling line was 10Fr catheter and was connected to the pump with sterile saline infusing at room temperature. This filling line was also used for catheterising the subject by connecting to a two way tap system. The filling line was connected to a pump (Lectromed, UK) with the room temperature sterile saline as the infusion fluid.

At the end of each filling a rest period of at least five minutes was obeyed, in order for the patient to change his position to minimise any tendency for pressure sores.

This set up is shown in the Figure 5:2.

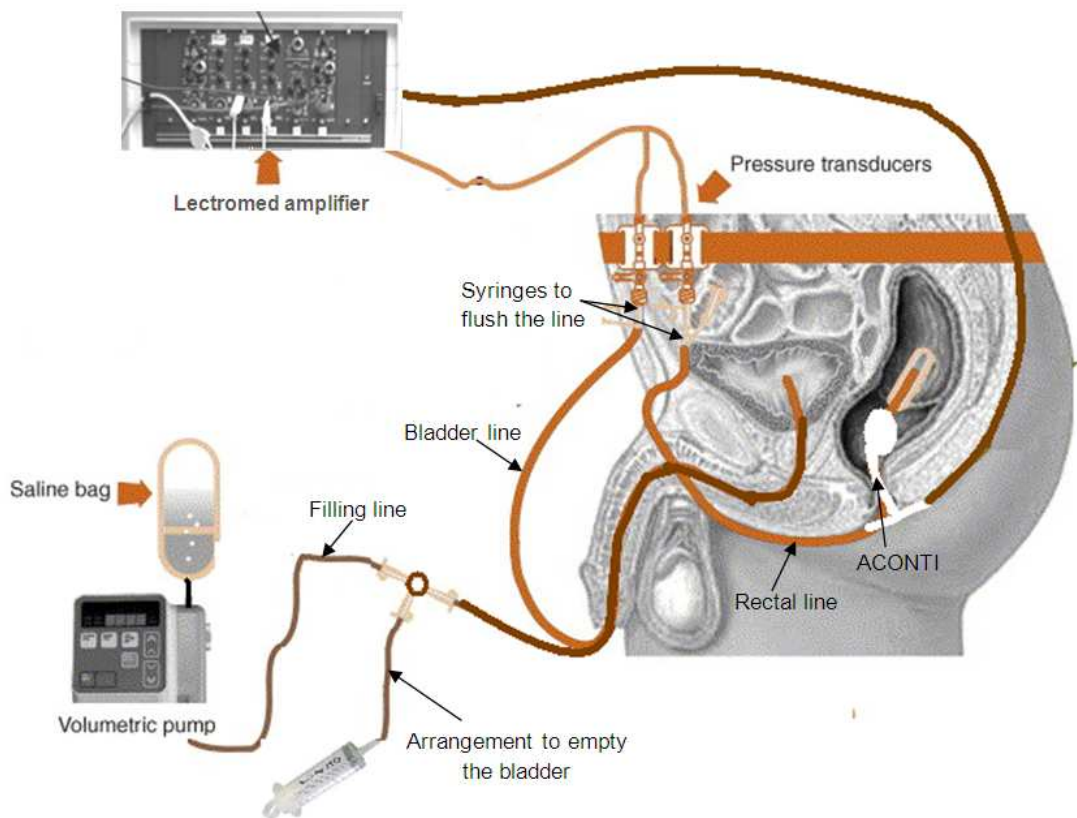


Figure 5:2 - Cystometrogram set-up

The figure shows the setup of the catheters to measure the abdominal (rectal line) and intravesical (bladder line) pressure. The other ends of these catheters are connected to pressure transducers. The filling line and the attachment to empty the bladder are connected to a two way tap system.

ACONTI was inserted to the anal canal (facing the electrodes anterior) using KY gel. The cable of the device was connected to the amplifier through a connector box. Each individual has their own device and at the end of the experiment. At the end of the experiment this was washed and cleaned with Milton solution.

Signal processing

For the purpose of clinical study, the EMG signal detected by the recording electrodes of the device was then passed onto the Lectromed amplifier. The 5361 amplifier is a general purpose isolated preamplifier mainly intended for bio potential signals [154]. The input signal is AC coupled with a time constant of 0.03s.

This analogue signal is then passed to the data acquisition system by Cambridge Electronic Devices (CED), which was set to allow a pass band of 20 Hz to 10 kHz and a sweep time of 200ms. This signal is post processed using SPIKE software also from CED. This software gives the freedom of post processing easily such as for filtering, rectifying etc; which simplifies the signal analysis.

The final part of the system is a Digitimer DS7 electrically isolated constant current stimulator. This can deliver current up to 100mA with stimulus pulse duration varying from 50-2000 μ s. The triggering signal for stimulation is provided through the Spike [155].

All of these systems are fully approved by the European EMC directive “89/336/EEC”. Arrangement of this system is shown in Figure 5:3.

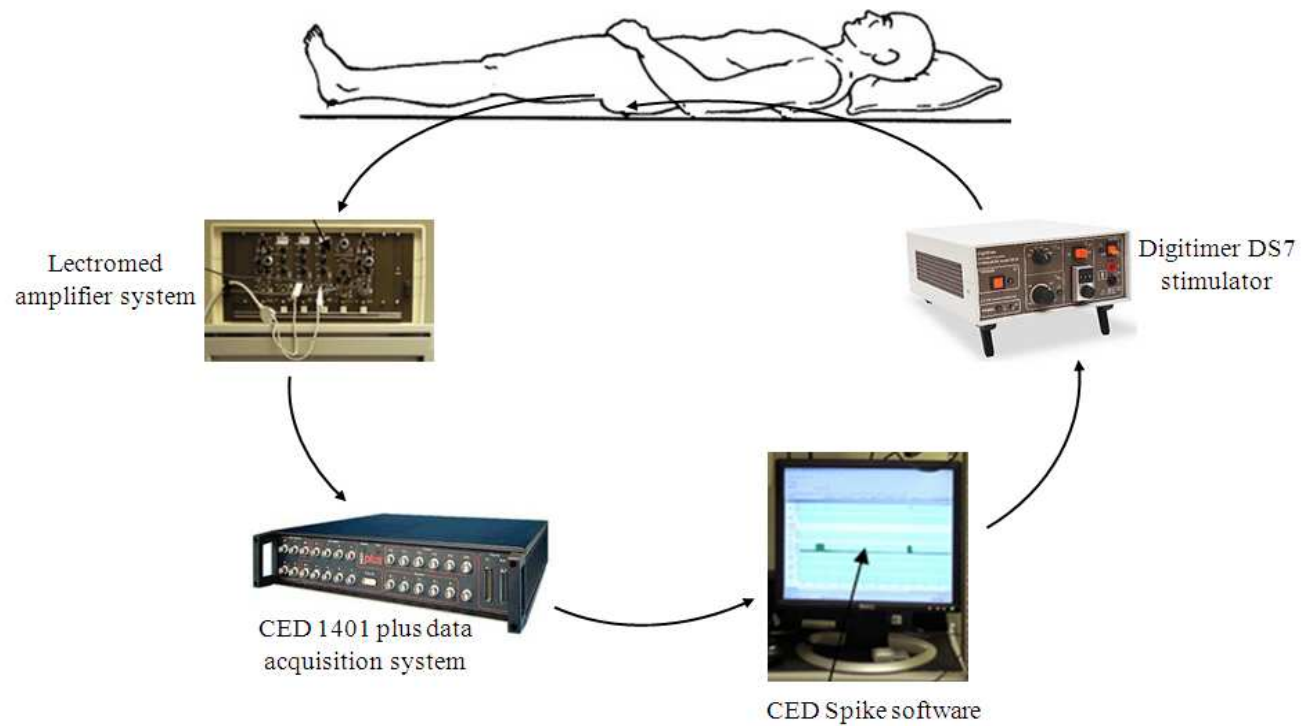


Figure 5:3 - Shows the laboratory equipment set-up.

The two pressure transducers and the EMG signal are connected to the Lectromed amplifier. These signal then converted to digital signals using CED 1401 data acquisition system, which then pass these information these information to Spike software for graphical user interface and for further signal processing. Finally this sends the signal to activate the stimulation pulses.

When recorded the raw EMG signal consists of the actual anal sphincter EMG as well as interference from other sources such as from mains. Therefore this raw EMG signal is first filtered using digital band pass filter with cut off frequencies 60Hz – 500Hz, then this signal is full wave rectified and smoothed with a time constant of 1s. The reasons for using these parameters for processing the signal will be explained in chapter 6.

5.5 Detecting NDO

In order to suppress the detrusor contraction, it is important to start the stimulation early. Therefore, when using conditional neuromodulation the contraction should be identified easily and early, to prevent the leakage.

5.5.1 Objective

The objective of this experiment is to assess the relationship and its reliability of the EMG signals recorded from the external anal sphincters through the device, to the detrusor contraction.

This part of the study measures the bladder capacity of the individual and helps to conform the presence of NDO. Further it analyses the level of the external anal sphincter EMG signal, which will be used as the trigger for conditional stimulation.

5.5.2 Experimental protocol

The bladder was drained of urine before each bladder fill. Once all the filling lines, catheters and the device were in place as explained in 0 and the informed consent was obtained, the standard cystometrogram was performed at non-

physiological rate of 60 ml/min while recording anal sphincter EMG. At the start of the experiment the subject was asked to cough to ensure that the equipment was positioned and recording correctly [156]. Blood pressure monitoring was not carried out during cystometry, but signs or symptoms of autonomic dysreflexia were monitored. Maximum cystometric capacity (MCC) was established when there is leakage, patient discomfort or when 500ml volume was reached [157]. The volume at first sustained contraction (VFC) (when the $P_{det} > 15\text{cmH}_2\text{O}$ above the baseline for at least 10s [40, 41, 95]), MCC and the maximum P_{det} were recorded. This procedure was repeated three times in order to determine the repeatability of the results. For the patients with no observed NDO present, the experiment was terminated at this point.

5.5.3 Results and analysis

Standard CMG with anal sphincter EMG and the processed signal are shown in Figure 5:4 and the urodynamics traces of each individual showing the detrusor pressure, raw EMG signal and the processed signal illustrated in the Figure 5.4. The pressure, volume data and the level of processed signal during DSD of each subject is shown in the Figure 5:5.

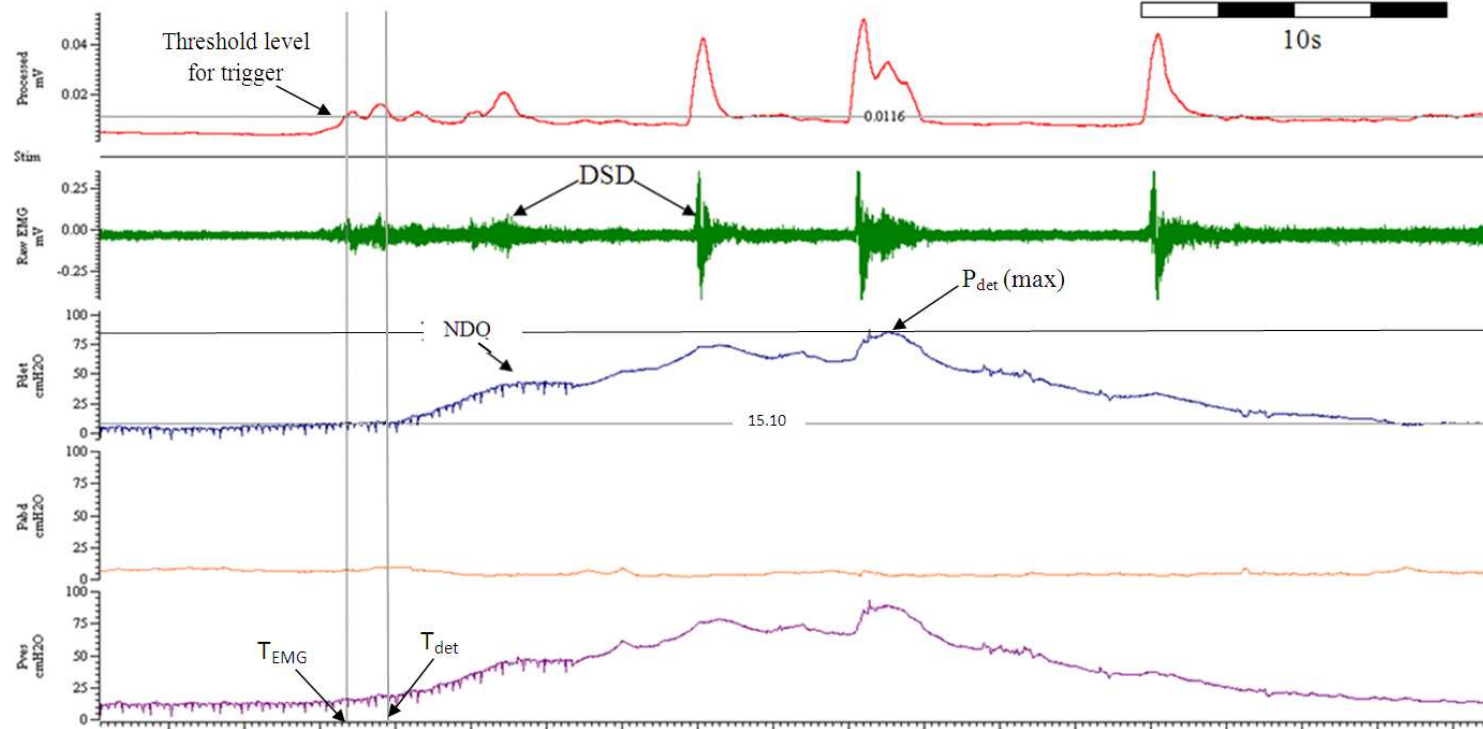
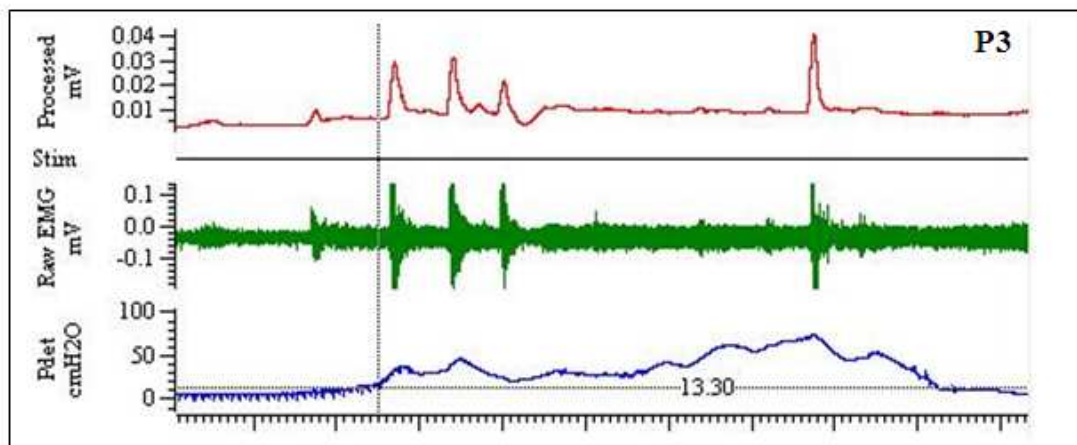
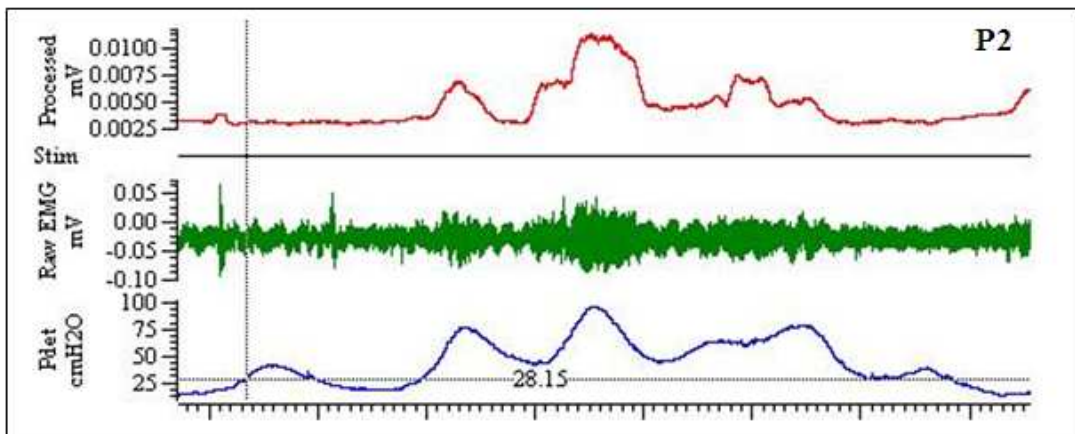
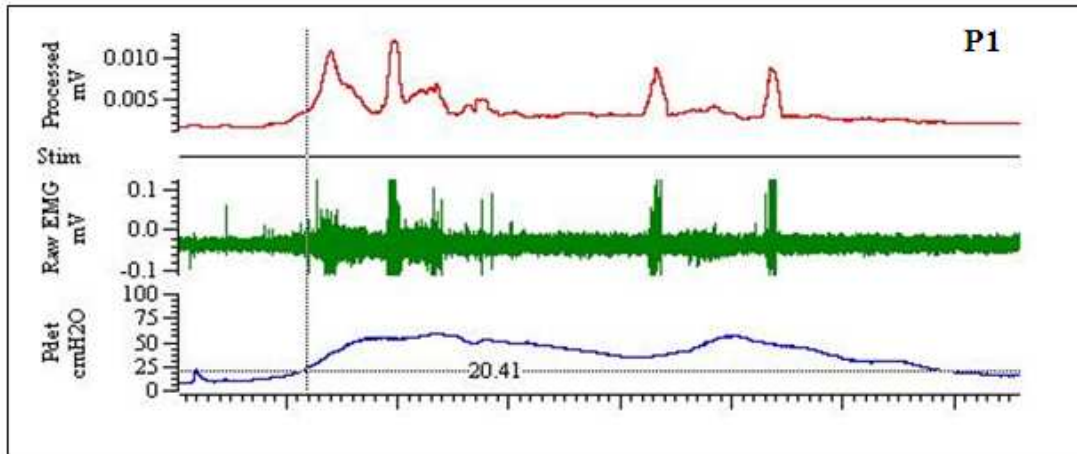
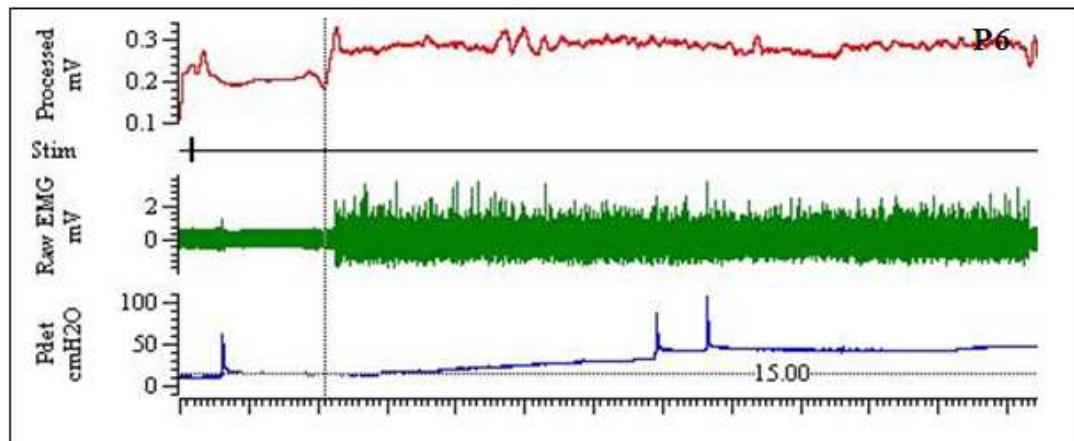
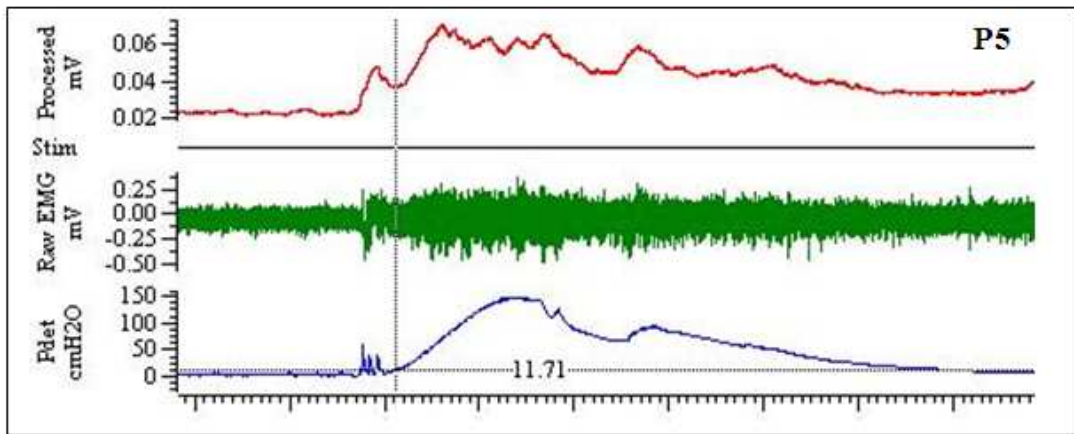
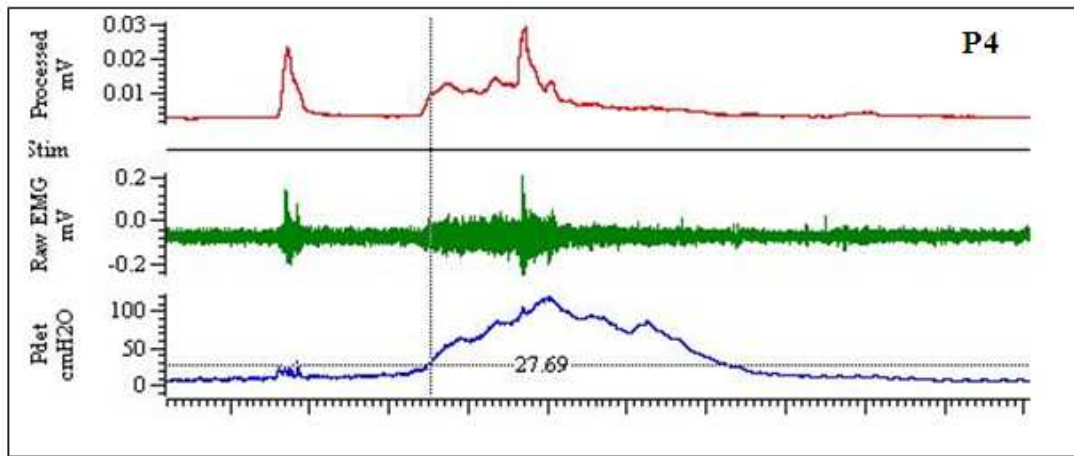
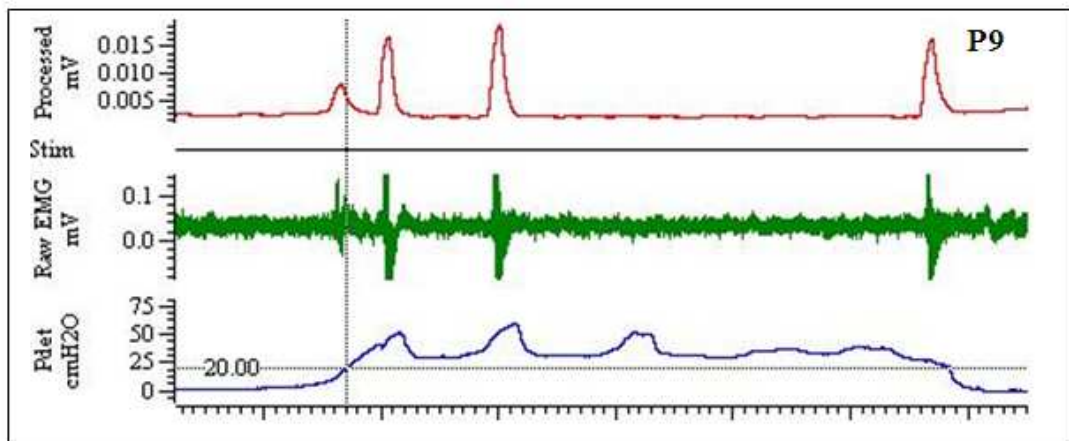
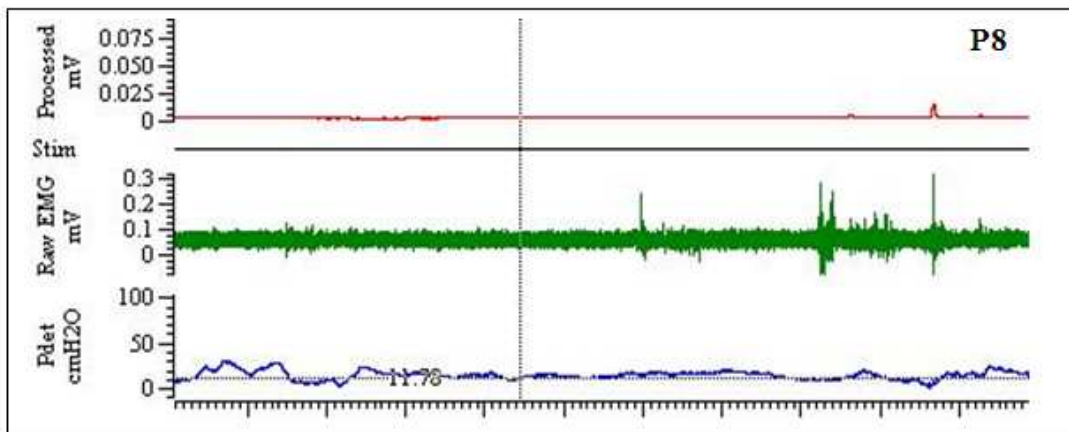
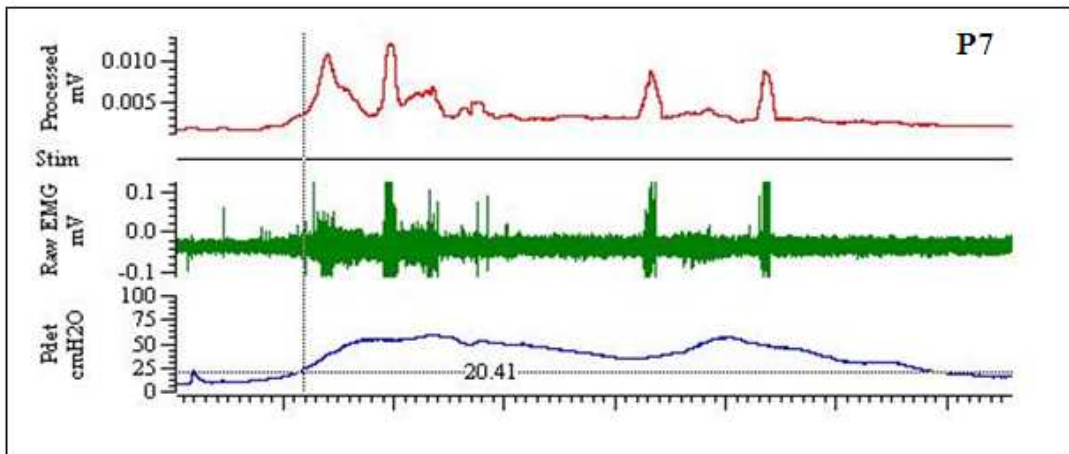


Figure 5:4 – Standard CMG with external anal sphincter EMG

P_{ves} , P_{abd} and P_{det} represent the bladder, abdominal and detrusor pressures (by subtracting P_{abd} from P_{ves}) respectively. EMG of the anal sphincters represents in “Raw EMG” and the waveform used for triggering is filtered, rectified, smoothed EMG shown as the “processed” signal. T_{EMG} = time at which the processed signal crossed the threshold line, T_{det} = time at which the detrusor pressure reached above 15cmH₂O the baseline.







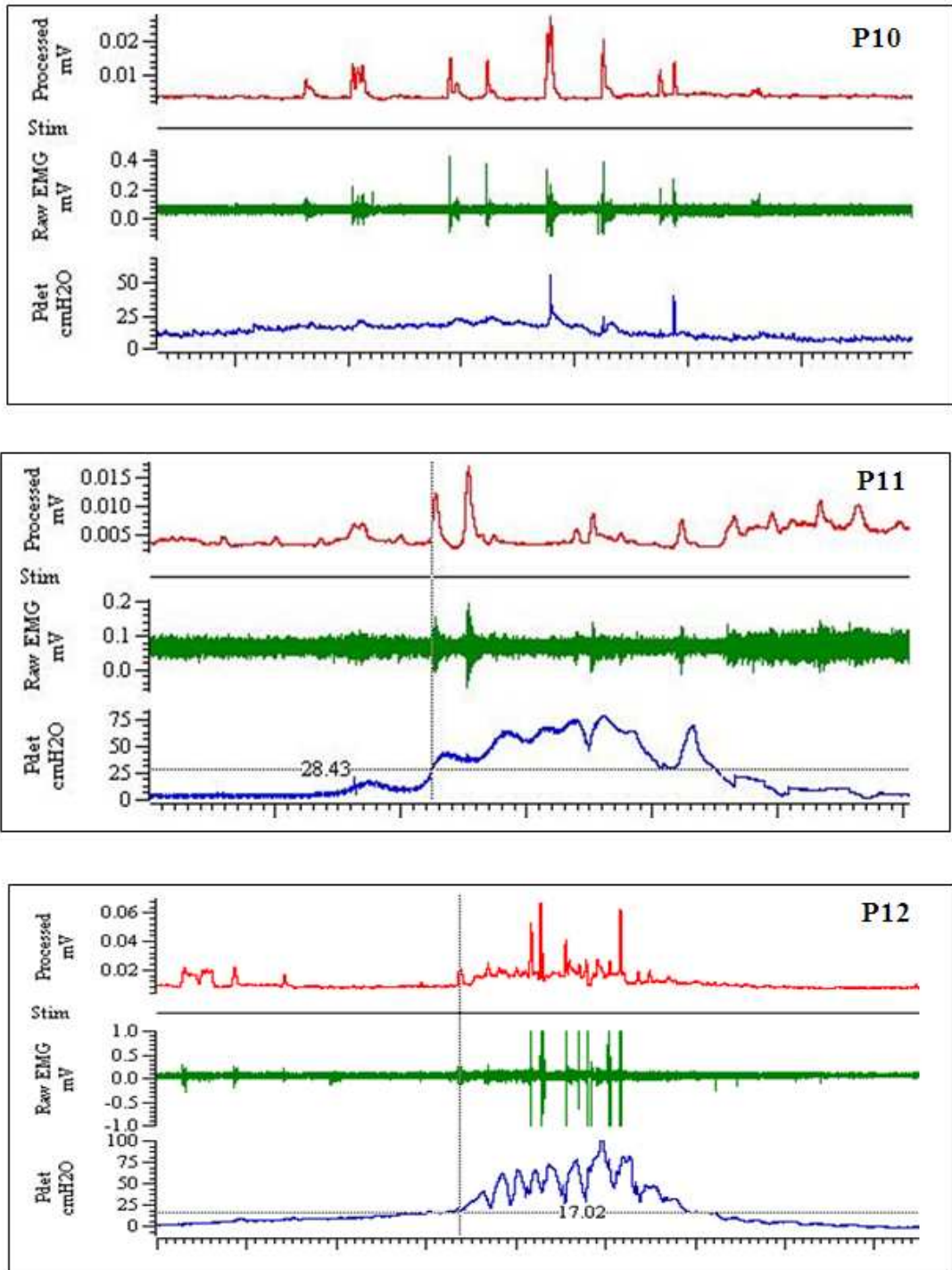


Figure 5:5 - CMG traces of the twelve subjects

These graphs are source scaled and only the important signals (related to setting the stimulation threshold) are shown to highlight the detrusor contraction.

Out of the twelve patients that participated in the study four had to be turned down due to absence of NDO. Subject P6 had a low compliant bladder, in which the detrusor pressure increased with the filling; however the MCC reached at 300ml. For the subjects P7 and P10, filling of the bladder was terminated when the pump infused 500ml and 450ml respectively. The MCC were 550ml and 450ml including the natural filling. For these two subjects there were no high pressure present and the bladder can accompany any volume of saline. This might be due to the fact that all the neural pathways to the bladder may have damaged as a results of injury. Furthermore they had no NDO but instead acontractile bladders and show signs of overflow incontinence. Patient P8 did not show any increase in detrusor pressure or guarding reflex, however there was leakage and the MCC was approximately 300ml. This may be due to weak urethral sphincters. Considering all these observations P6, P7, P8 and P10 will not benefit from this study.

Bladder capacity

One of the objectives of this experiment was to measure the bladder capacity of each individual, so that it is easy to know when to expect a dyssynergic response in the next part of the study and also to conform the presence of NDO. Figure 5:6 and Figure 5:7 show the bladder volume at first sustained contraction and the mean variation of the maximum cystometric capacity respectively.

Table 5-2 - Volume at first contraction and the maximum cystometric capacity of the participants.

The volume at first contraction was obtained by measuring time and multiplying it by the fill rate. The maximum cystometric capacity was obtained by measuring the amount of fluid withdrawn from the bladder after each fill.

Subject	Volume at 1 st contraction (ml)			Max. cystometric capacity (ml)		
	Fill 1	Fill 2	Fill 3	Fill 1	Fill 2	Fill 3
P1	138	140	-	150	155	-
P2	72	40	83	100	87	105
P3	109	118	118	145	145	175
P4	73	45	39	105	82	55
P5	175	234	278	180	235	280
P6	122	66	50	370	300	300
P7	-	-	-	550	-	-
P8	133	157	91	245	307	370
P9	231	205	246	257	212	255
P10	300	300	-	466	425	-
P11	283	330	291	410	395	355
P12	279	307	205	450	500	337

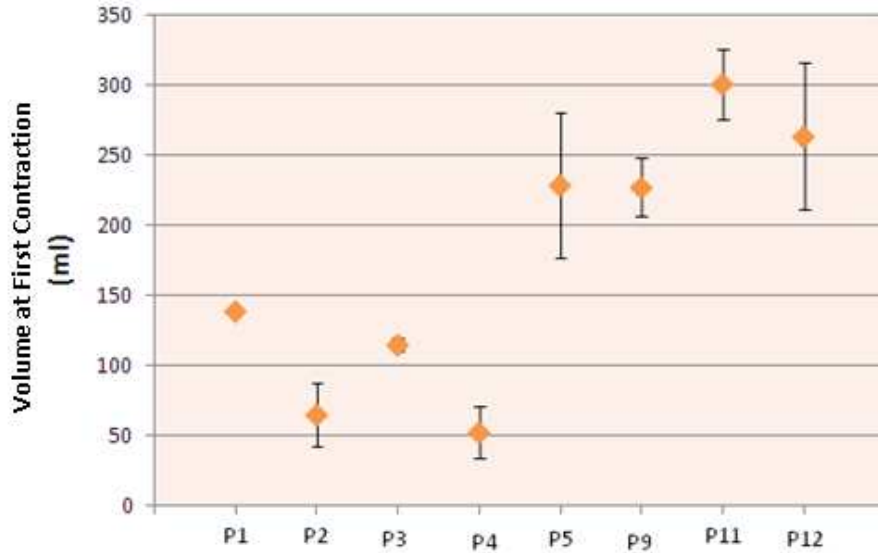


Figure 5:6 - Shows the variation of the volume at first contraction

The volume shown is the mean of the three fills of each individual and error bars represent the standard deviation.

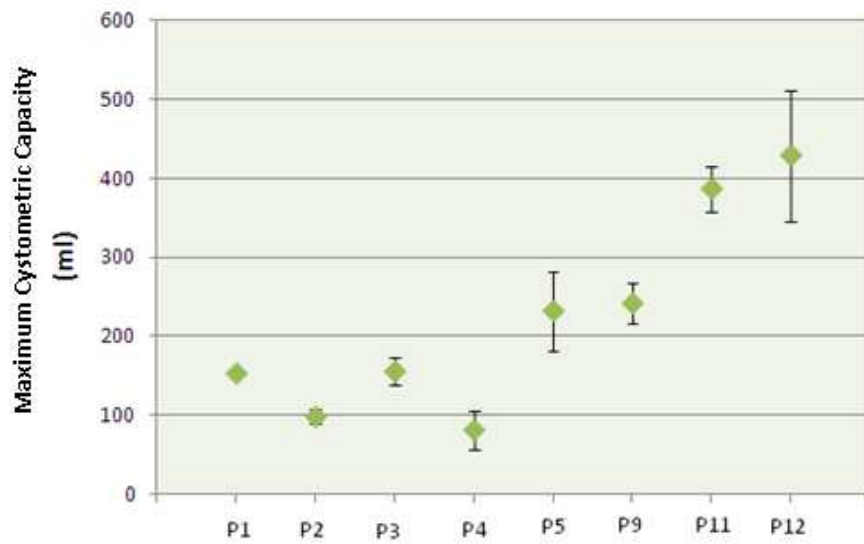


Figure 5:7 - Shows the variation of the maximum cystometric capacity

Capacity shown is the mean of the three consecutive fills on each individual and error bars represent the standard deviation.

The maximum cystometric capacity of each individual varied from 55ml to 500ml and the mean MCC was 221 ± 128 ml. When bladders are filled artificially, there is a tendency for the detrusor muscle to stretch and accommodate more volume at each time. Figure 5:8 highlights the increase in bladder capacity of each subject on each consecutive fill.

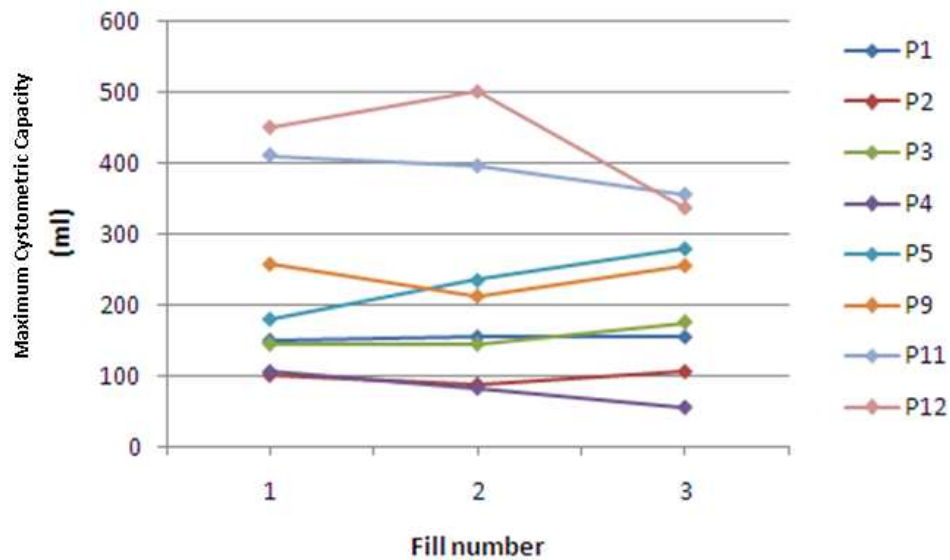


Figure 5:8 - Shows the intra subject change in bladder capacity due to repeated filling.

These data were analysed with Friedman test (used to detect differences in treatments across multiple test attempts [158]) in order to determine the significance in increase in the bladder capacity across the fills. The results were $p = 0.9048$ across all three fills, showing that increase in bladder capacity across each fill was not statistically significant.

Maximum detrusor pressure

Another problem of NDO is high detrusor pressure, which may lead to vesicoureteric reflux, repeated bladder infections and renal failure if left untreated. Figure 5:9 shows the variation of the maximum detrusor pressure of each individual during detrusor sphincter dyssynergia [13].

Table 5-3 - Maximum detrusor pressure during the control study

The maximum detrusor pressure is the highest peak recorded in the control study.

Subject	Maximum P _{det} (cmH ₂ O)		
	Fill 1	Fill 2	Fill 3
P1	59	55.54	-
P2	78	83	97
P3	99	110	93
P4	118	116	84
P5	148	167	99
P6	57	48	27
P7	13	-	-
P8	53	61	46
P9	60	63	50
P10	10	14	-
P11	75	80	83
P12	96	69	72

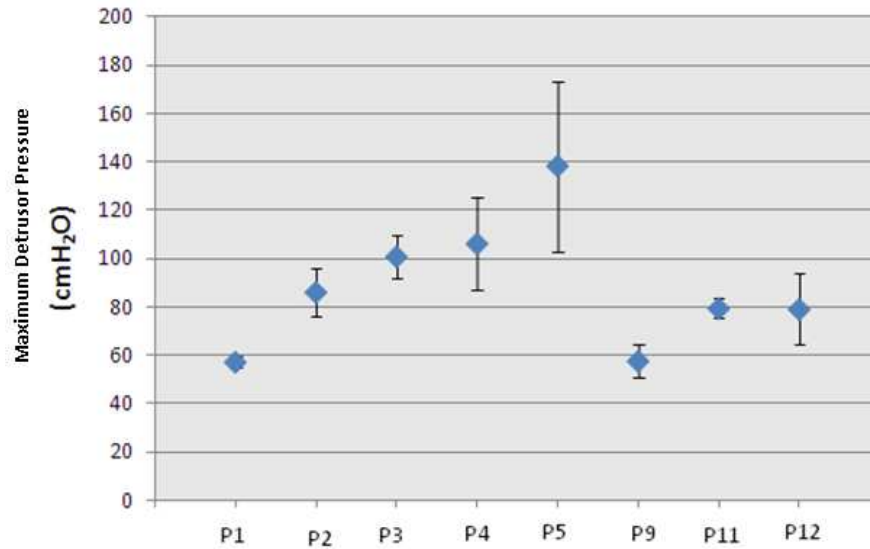


Figure 5:9 - Variation of the maximum detrusor pressure of each individual with error bars representing the standard deviation.

The maximum detrusor pressure varied from 50 cmH₂O to 167 cmH₂O across all subjects and the mean pressure was 88 ± 27 cmH₂O.

Level of processed signal

The main reason for carrying out this experiment is to determine the level of the processed signal during DSD of the neurogenic patients, so that it can be used as the trigger in conditional neuromodulation. Figure 5:10 shows the level of the processed signal of each individual at the start of the first sustained contraction at which the stimulation should be applied in order to suppress the contraction.

Table 5-4 - Levels of the processed signal

These results were obtained by reading the level of the processed signal when a sustained contraction occurred (time at which detrusor pressure crosses 15cmH₂O).

Subject	Level of processed signal (μV)		
	Fill 1	Fill 2	Fill 3
P1	5.15	10.99	-
P2	2.25	4.17	3.7
P3	15.2	9.08	8.31
P4	3.8	3.45	9.1
P5	36.5	32.4	35.6
P6	283	280	254
P7	-	-	-
P8	4.1	5.0	3.6
P9	25.4	33.5	35.5
P10	4.9	3.3	-
P11	7.6	5	4.6
P12	8.1	10.6	10.7

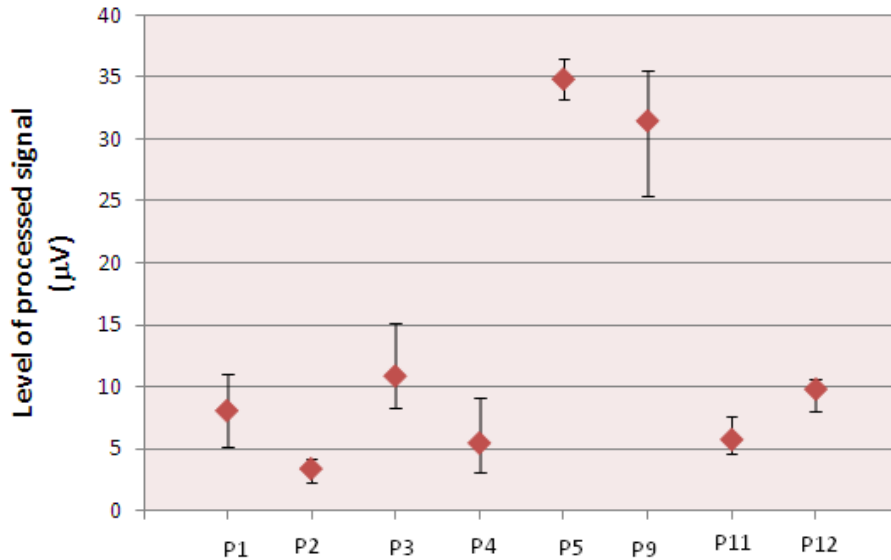


Figure 5:10 - Variation of the level of the processed signal of each individual.

Error bars representing the minimum and maximum recorded values at the start of first contraction.

The level of the EMG signal varies $2.25\mu\text{V}$ to $36.5\mu\text{V}$ on each individual depending on their lesion and the state of their sphincters. However for stimulation it is necessary to avoid any false negative situation, therefore the minimum level of the processed signal identified on this experiment will be used as the trigger level for each of the subject.

Relationship of the processed signal to the detrusor contraction

One of the objectives of this study is to determine whether the external anal sphincter EMG can be used as a reliable trigger signal with relation to detrusor contraction. For all the eight subjects with NDO, the time at which the rise in detrusor pressure and the time as which the there is a significant change in the processed signal were noted.

Table 5-5 - Time difference in detecting contraction by processed signal and detrusor pressure as indicated in Figure 6:6.

Patient	$T_{EMG} - T_{det}$ (s)
P1	15
P2	12
P3	0.1
P4	- 0.6
P5	- 2.09
P9	1.5
P11	-1.8
P12	3.2

According to the data shown in the Table 5-5; on average, using an EMG threshold is 3.4s faster than setting the trigger level on the detrusor pressure. The stimulation could have been delayed only on three subjects, however this delay was less than 2.1s.

5.5.4 Discussion

Serial cystometries were conducted in patients with NDO to assess bladder capacity and to find out the level of processed EMG signal in order to determine threshold levels for conditional neuromodulation. The mean bladder capacity of each of these subjects is 221 ± 128 ml. This capacity is very low compared to a healthy volunteer. This means the number of catheterisation per day is high; therefore this capacity needs to be improved using the proposed device. The smallest bladder capacity was found on people who had required a high dose of antimuscarinic drugs. Also this

study proved that increase in bladder capacity due to repeated filling is not statistically significant ($p > 0.05$).

The patients with NDO had high level of detrusor pressure with the mean of 88 ± 27 cmH₂O. If these high transient pressure were left untreated; may result chronic renal failure and repeated bladder infections [12].

The mean value of the level of processed EMG signal during DSD is $13.7\mu\text{V}$. This value varies with each person. For the next part of the study this signal will be used as the trigger for the stimulation. It is important to obtain the best level of the processed signal as the trigger, because missing a contraction or being delayed to apply stimulation will result leakage of the urine. Therefore the minimum level of the processed signal during DSD will be used as the trigger level for conditional neuromodulation.

The level of processed signal is not very high on each of the patient, but this can be improved using amplifiers which will be discussed next chapter. Furthermore by increasing the size of the recording electrode the quality of the recorded EMG signal can also be improved. Finally if the recording electrodes can be pushed further into the sphincter muscle, by increasing the width of the device near the sphincters, better contact can be made with muscle resulting increase in amplitude of the EMG signals. However the limitation for this is; it can permanently stretch the tissues of the patient.

5.6 Suppressing the detrusor overactivity through the device

Once the suitable patients with NDO and the relationship between the external anal sphincter and detrusor contraction were identified, the next stage was to focus on suppressing these contractions through transrectal stimulation using the mechanism of conditional neuromodulation; as per semantics of operation of ACONTI.

5.6.1 Objective

In incontinence due to neurogenic detrusor overactivity at low volumes, the detrusor muscle contract even though it does not satisfy the situation to urinate. However in most of the patients the urethral sphincters remains closed during detrusor contraction in order to prevent the leakage, which is known as detrusor sphincter dyssynergia.

In order to treat NDO through conditional neuromodulation, whenever a detrusor is detected; the stimulation is applied to the Pudendal nerve. As a result of that continence is achieved in two ways, sphincter contraction to prevent the leakage as well as bladder suppression to increase its capacity.

Objective of this study is to evaluate the efficacy of the Pudendal nerve stimulation in increasing the bladder capacity as well as preventing the leakage using the external anal sphincter EMG as the trigger for the conditional neuromodulation.

5.6.2 Method

Experiment set up remains the same as explained in section 5.4. First part of the procedure is to obtain the intensity of the stimulating current.

Setting the stimulating parameters

It is important to set the stimulating current at the optimum level. Lowering the amplitude saves the battery life, but may not be enough to generate an action potential in the pudendal nerve. The stimulation was delivered through DS7 constant current stimulator by Digitimer.

The sensory threshold was defined as the intensity at which the subject could initially feel the electrical stimulation through the device.

For the incomplete SCI patients, the sensory threshold was determined by giving a 5s burst of stimulation and increased it from 5mA to 90mA, until the patient felt the stimulation.

For complete SCI patient had no sensation of the stimulating current. Therefore the sensory threshold was obtained by evaluating motor evoked potentials (MEP) by direct motor efferent. For this 30 stimulating pulses were delivered at a given current (varying from 10mA) and the response was averaged using SPIKE software in order to remove the noise. This procedure was repeated until the motor response (M-wave) can be seen, and at that intensity was established as the sensory threshold.

The amplitude of the stimulating current was set at twice the sensory threshold [31, 40, 95, 159, 160] to elicit the bulbocavernosus reflex [12, 108, 161].

The optimum stimulation parameters for conditional neuromodulation (frequency of 15 Hz and pulse width of 200 μ s with the maximum allowable voltage set to 200V) were used for this procedure [25, 78, 91, 108, 162]. The duration of the stimulation was also set to 60s (1min of continuous stimulation train has shown to increase MCC by 144% [32], where as 10s on and off stimulation increased the MCC by 53%-66% [31]) [95] and repeated after 5s, as long as the detrusor pressure is above 15cmH₂O [31].

The trigger level for the stimulation of each subject was set to the minimum level of the processed signal as explained in the previous section.

5.6.3 Experimental protocol

When all the stimulating parameters were set, the experiment begins by catheterising the bladder. First of all, the conditional neuromodulation principle was tested on each subject by performing standard CMG at 60 ml/min with stimulation through the device to investigate whether the electrical stimulation could suppress the detrusor contraction. In case of the patient cannot tolerate the stimulation, the intensity was lowered during any point of the study to a bearable level. If this experiment was successful the final part of the experiment begins by performing standard CMG at 15 ml/min (closer to the physiological rate). Filling was continued until there is leakage, patient discomfort or when the 500ml capacity was reached. [157] Signs or

symptoms of autonomic dysreflexia were monitored and if the patient complains any discomfort the experiment was terminated at that point.

5.6.4 Results and analysis

Stimulating current

Example motor evoked potential waveform, which was used to determine the threshold of the complete SCI subjects is shown in the Figure 5:11. Table 5-6 shows the sensory threshold and the stimulating current of each of the subject.

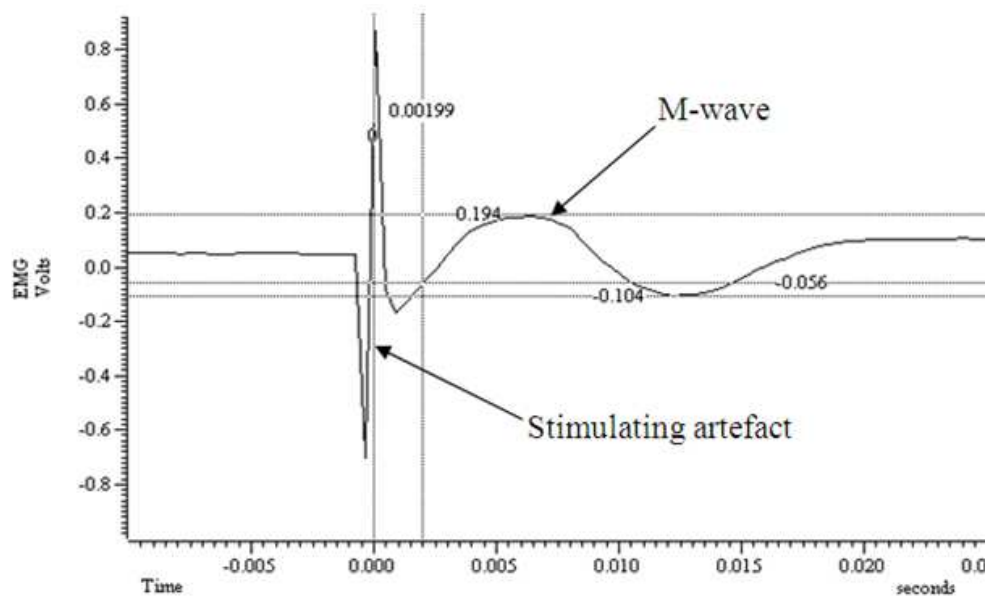


Figure 5:11 – Motor evoked potential

Shows the average of 20 samples of MEP recorded through the device electrodes, when stimulating with a current of 30mA in complete SCI patient.

Table 5-6 - Shows the sensory threshold and the stimulating current of each subject, which was utilised in delivering the stimulation.

	Subject	Sensory threshold (mA)	Stimulating current (mA)
Incomplete SCI	P1	30	57
	P3	30	60
	P5	3	40
	P9	20	25
Complete SCI	P2	30	60
	P4	30	60
	P11	50	90
	P12	40	80

Even though the subject P5 had sensory threshold of 3mA, the stimulating current was set to 40mA, this is because 6mA is too low and will not stimulate the nerve. Stimulating current of P9 was not doubled as 40mA was not tolerable for him.

According to the Table 5-6, the mean stimulating current across all subjects was 59mA with standard deviation of 20mA.

The distance between the stimulating electrodes of the device and the external sphincter is about 5cm and from the Figure 5:11 the latency between the stimulating pulse and the start of M-wave is 2ms, results the velocity of conduction as 25m/s. The motor fiber that conducts this information is A γ type in which the conduction velocity is between 15 - 30m/s [148, 163] showing that the stimulation resulted direct motor contraction.

Figure 5:12 illustrates the urodynamics traces with and without conditional neuromodulation using processed EMG signal as the threshold. Figure 5:13 shows the neuromodulation effect on the bladder condition of each individual.

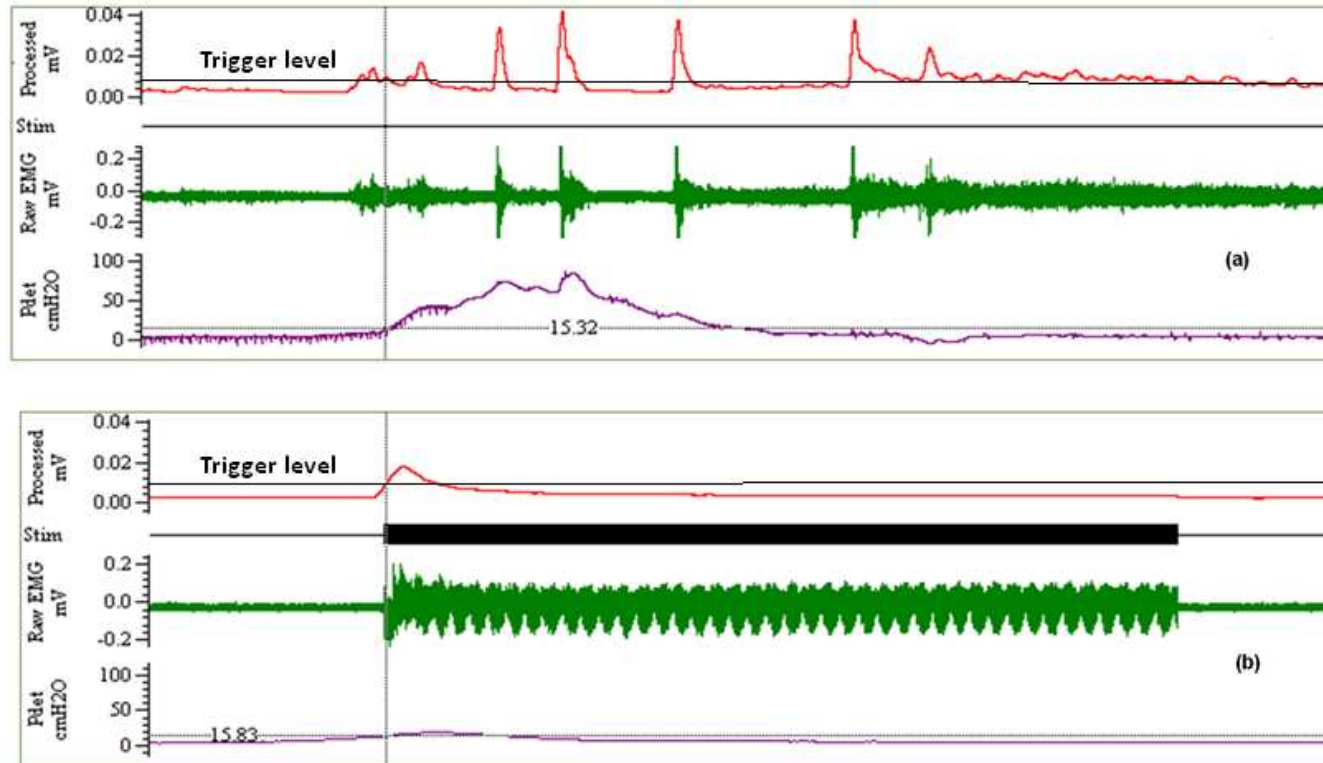
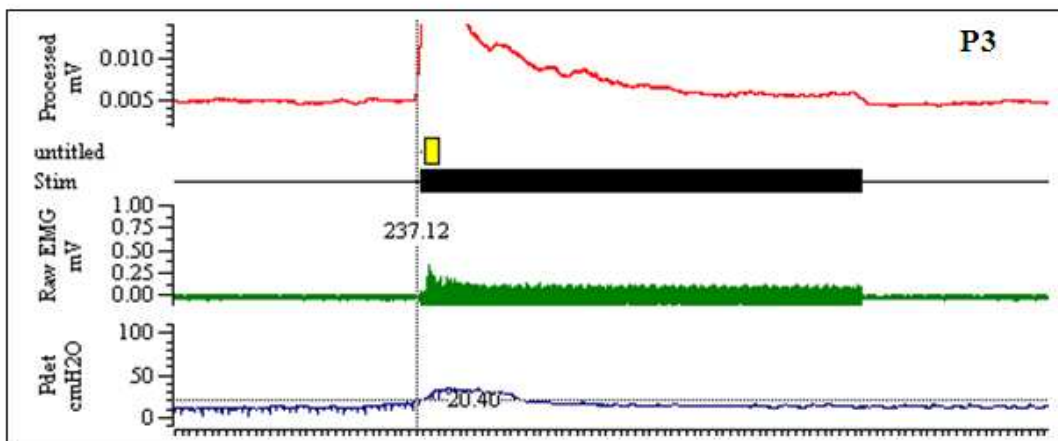
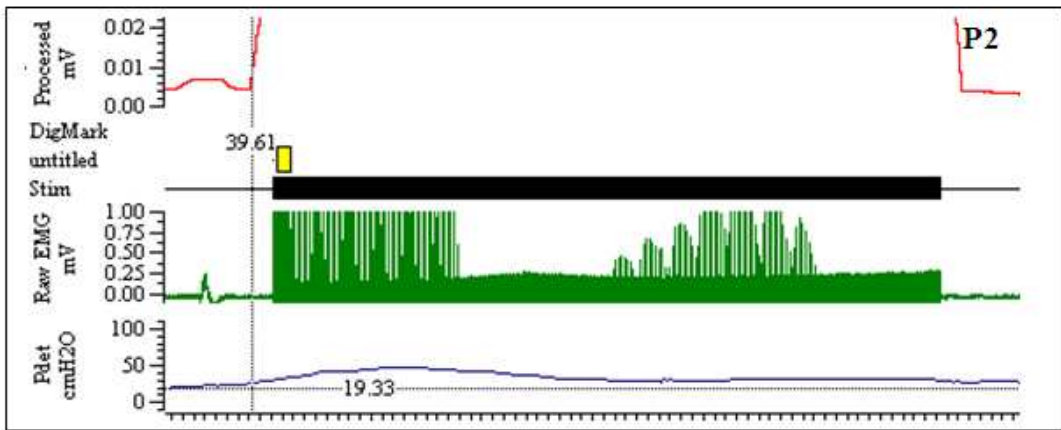
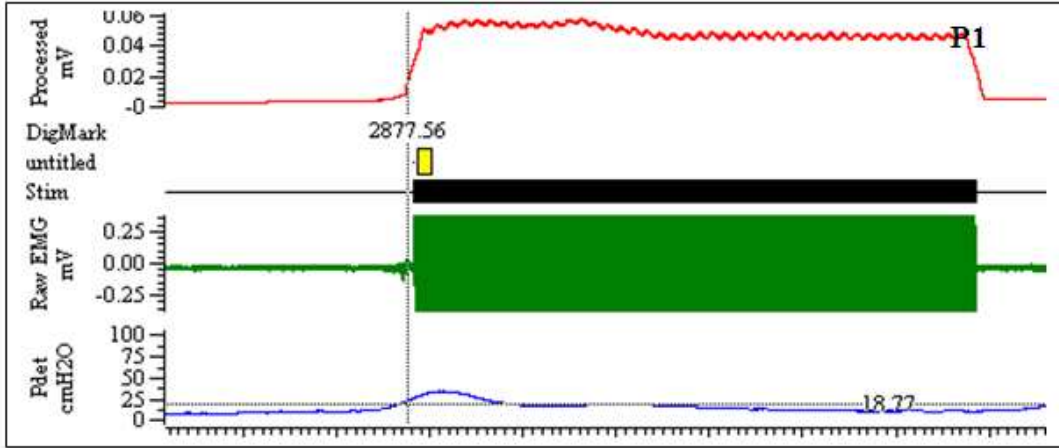
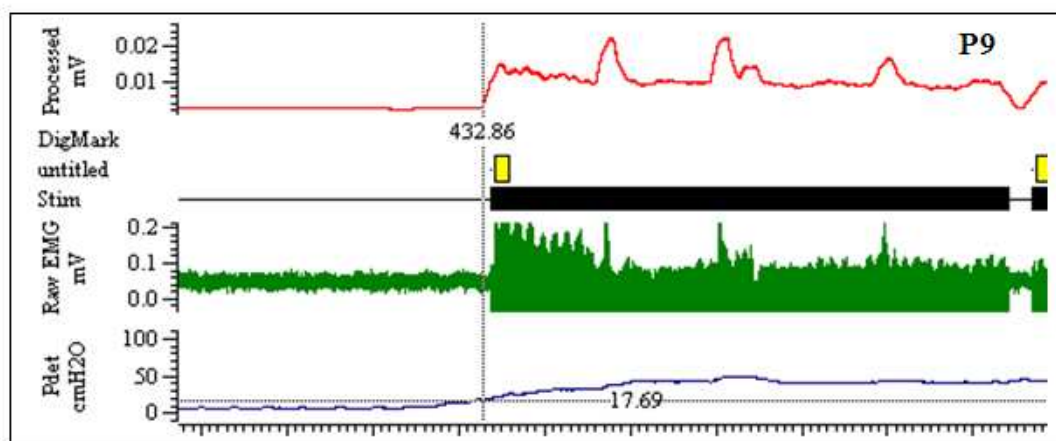
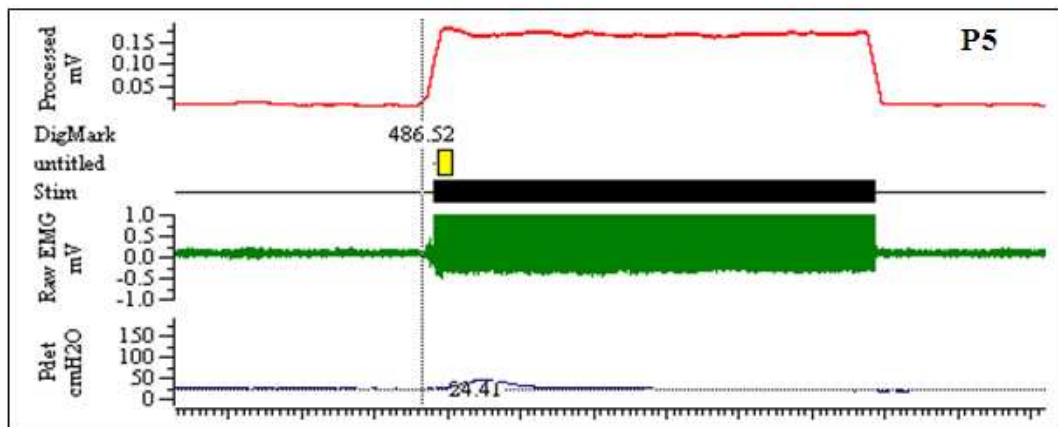
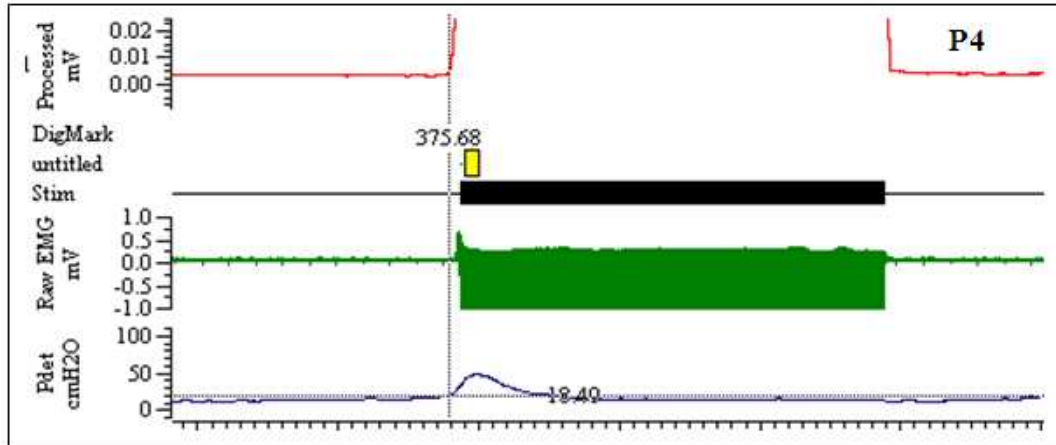


Figure 5:12- Shows the effect on detrusor contraction with and without stimulation.

(a) NDO contraction and DSD of P3; (b) neuromodulation through the device using EMG threshold set at the dotted line in the processed signal to trigger the stimulation while filling the bladder at 60ml/min. Thickening of EMG trace is due to stimulus artefact pulses. It can be clearly seen that detrusor contraction diminished with the stimulation.





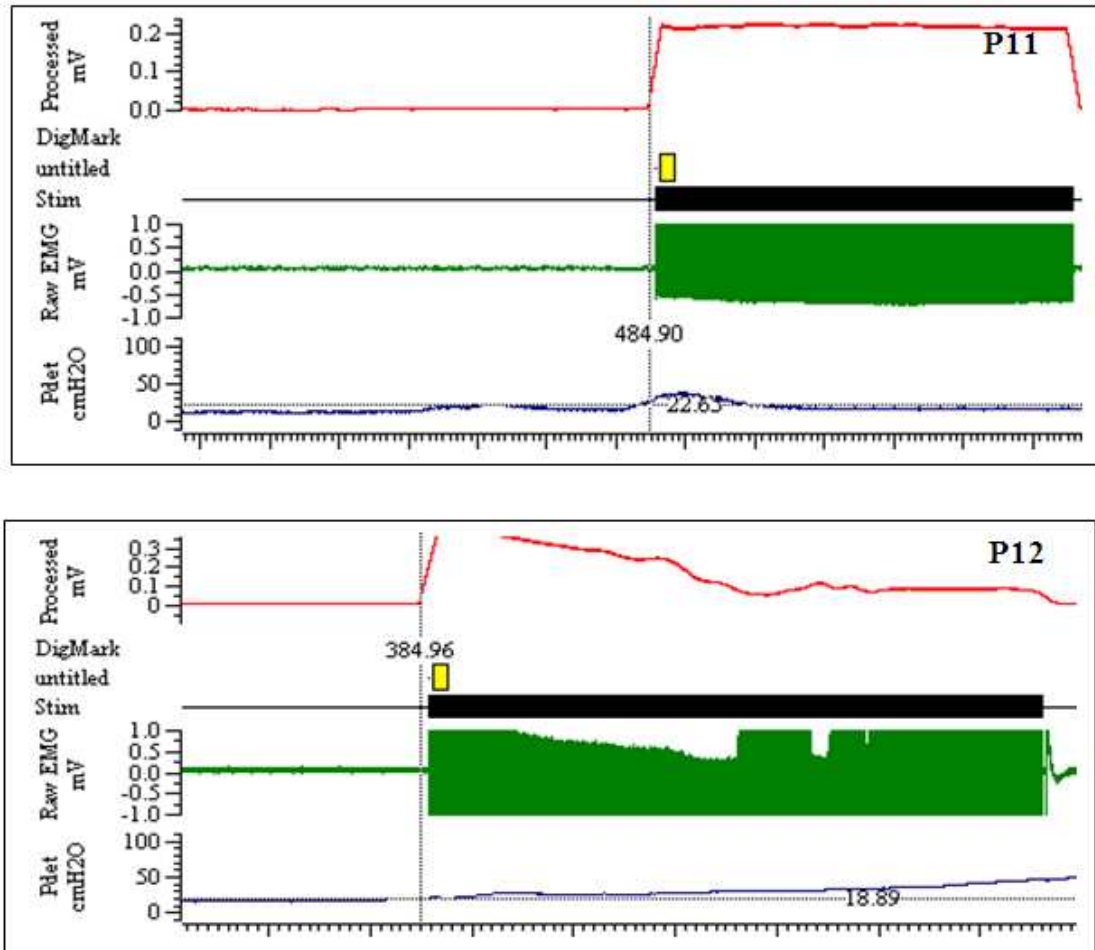


Figure 5:13 - Shows the effect of single burst (60s) stimulation on detrusor pressure in each participant.

The bladder was filling at 60ml/min, and the trigger level for activating stimulation was set on the processed signal. In some traces, only a part of the processed signal can be seen. This is due to the signal being saturated during the stimulation, but for triggering this saturation does not cause any problem.

According to the Figure 5:13, the conditional neuromodulation through the device has successfully suppressed the detrusor contraction on P1, P2, P3, P4, P5 and P11. For the patient P9, due to high sensitivity, the stimulating current used was 25mA (when his threshold was 20mA). Failure to produce enough current to generate action potential on the pudendal nerve resulted not being able to arrest the detrusor contraction [161]. For the subject P12, the symptoms of autonomic dysreflexia (sweating and headache) occurred during the experiment. Due to these reasons the experiment was terminated at this point for P9 and P11.

Time between each contraction

As the bladder being filled with saline, detrusor contractions become more frequent reducing the time between each suppressed contraction. At one point (when the bladder reached MCC), the stimulation can no longer inhibit the contraction resulting the discomfort to the patient or leak. This phenomenon is shown in the Figure 5:14 and the measurements are shown in the Table 5-7.

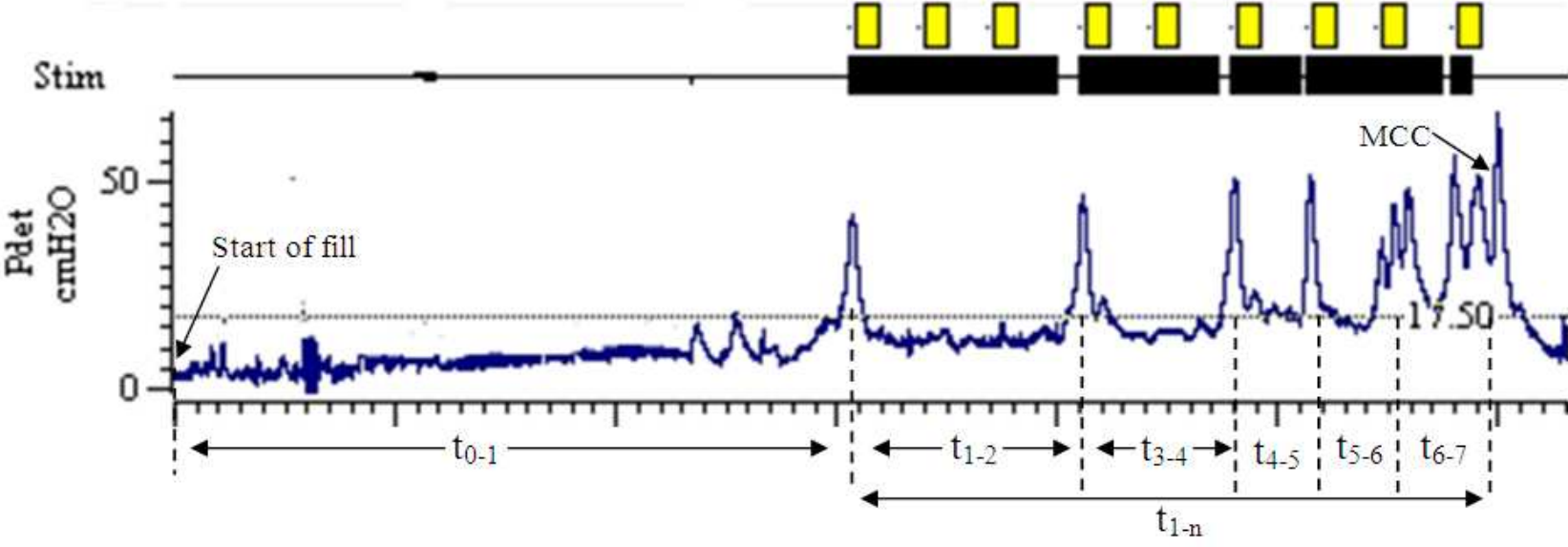


Figure 5:14 - Sample conditional stimulation fill, starting with an empty bladder. t_{1-n} represent the increase in catheterisation time as a result of neuromodulation.

Table 5-7 - Shows the time between each detrusor contraction of each individual.

Subject	Time between each contraction (s)							
	t ₀₋₁	t ₁₋₂	t ₂₋₃	t ₃₋₄	t ₄₋₅	t ₅₋₆	t ₆₋₇	t _{1-n}
P1	648	72	-	-	-	-	-	132
P2	240	210	300	-	-	-	-	1710
P3	928	385	292	221	78	27	-	1189
P4	370	90	128	120	92	254	70	1672
P5	507	136	112	98	67	52	41	570
P11	597	220	139	75	60	57	-	623

The graphical illustration of the data shown in the Table 5-7 is shown in the Figure 5:15.

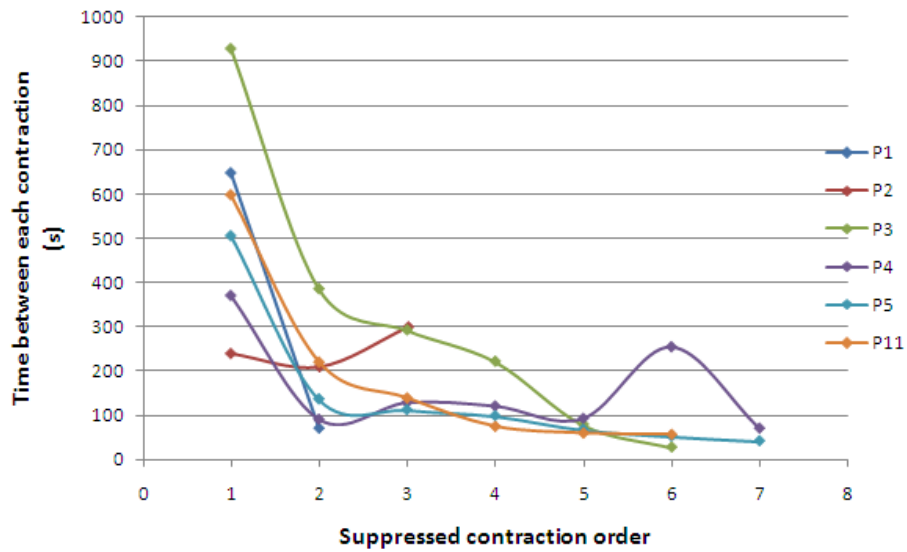


Figure 5:15 - Time between suppressed hyperreflexic contractions during the continuous filling at 15ml/min.

According to the figure the time between each contraction decreases with the increasing number of contraction. The decreasing line takes the shape of the exponential decay curve. However, for the subject P2, the time had increased between contractions 2 to 3, this because as his first contraction happened earlier compared to others and it required few blocks of stimulation bursts to inhibit. Therefore this effect of stimulation might have stretched his bladder.



Figure 5:16 - Average time between each contraction across all subjects. Error bars represent the standard deviation.

The average time between the contractions 1-2 is 9.13 ± 3.98 min and that of 2-3 is 3.09 ± 1.92 min.

As a result of conditional neuromodulation, the bladder compliance had increased resulting decrease in the number of catheterisation required.

$$\text{Increase in bladder compliance} = \frac{t_{1-n}}{t_{0-1}} \times 100\% \quad \text{Equation 5-1}$$

The mean increase in bladder compliance across all subjects is 179.21%. In other words, the catheterisation time of the patient had increased by an average of 2.8 times (from 548s to 1531s).

External anal sphincter EMG trigger level

As explained the earlier experiment, the trigger level was set as the minimum value of the processed signal resulted in the three controlled fills. The threshold algorithm successfully detected all true contractions resulting no negative (true negative or false negative) detections.

External anal sphincter EMG was not monitored during the stimulation, due to large stimulating artefacts and therefore 5s stimulation off period was left followed by 60s automatic stimulation.

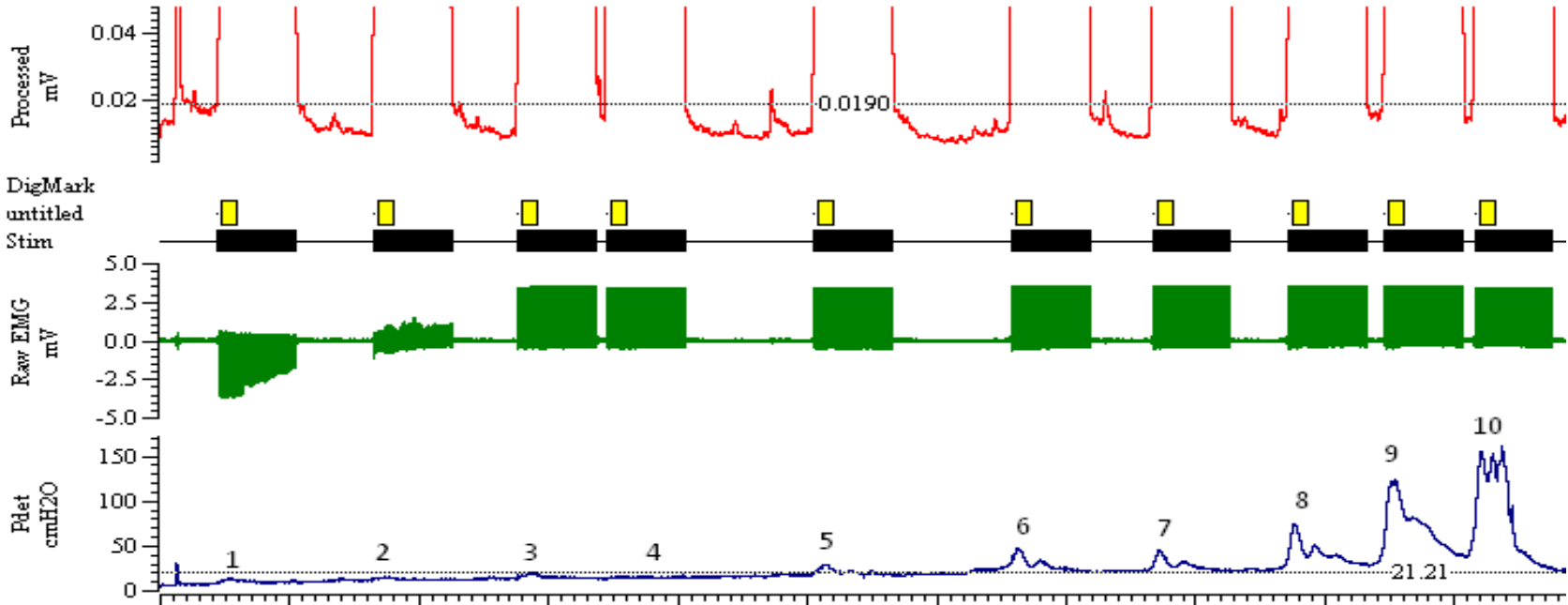


Figure 5:17 - Show the real time implementation of the conditional neuromodulation based on the level on processed signal to trigger the stimulation. With the bladder filling, contractions become more and more frequent and at one point (contraction number 10), the bladder can no longer be suppressed. Processed signal been amplified to shows the trigger level.

Four false positive (1, 2, 3, 4) and six true positive detection (5, 6, 7, 8, 9, 10) were triggered by the algorithm. In order to visualise the trigger level, only half of the processed signal is shown here. This is due to stimulating artefact being picked up, and it is high compared to the trigger level.

The positive predictive value (PPV) or precision rate of a test is the probability of true positive result [164].

$$\text{Positive predictive value} = \frac{\text{True positive}}{\text{True positive} + \text{False positive}} \quad \text{Equation 5-2}$$

The PPV was calculated for all six patients participated for this study and is shown in the Table 5-8.

Table 5-8 - Calculates the precision rate and the percentage of unwanted stimulation of a given threshold level for each patient.

Patient	Threshold level (µV)	Negative		Positive		% of unwanted stimulation	PPV
		True	False	True	False		
P1	5.15	-	-	2	-	-	1
P2	2.25	-	-	9	-	-	1
P3	8.31	-	-	13	5	14.17	0.72
P4	3.45	-	-	16	2	5.88	0.89
P5	32.4	-	-	6	4	22.28	0.6
P11	4.6	-	-	6	3	14.75	0.67

Across all these trials there were 52 true positive outcome and 14 false positive outcomes over 2hours and 55min trial period. On average there were 8.67 (\pm 5.12) true positive and 2.33 (\pm 2.06) false positive over a period of 26 min (\pm 9.5s), resulting the positive predictive value of 0.79.

False positive outcomes are due to the fluctuation of abdominal pressure and this resulted to 9.13% of stimulation.

Suppression of the detrusor contraction

It is important to stimulation to be switched automatically immediately after the start of contraction. The Figure 5:18 shows the delay between the start of the contraction and time taken to suppress the contraction, while the mean values of each subject is shown in the Table 5-9.

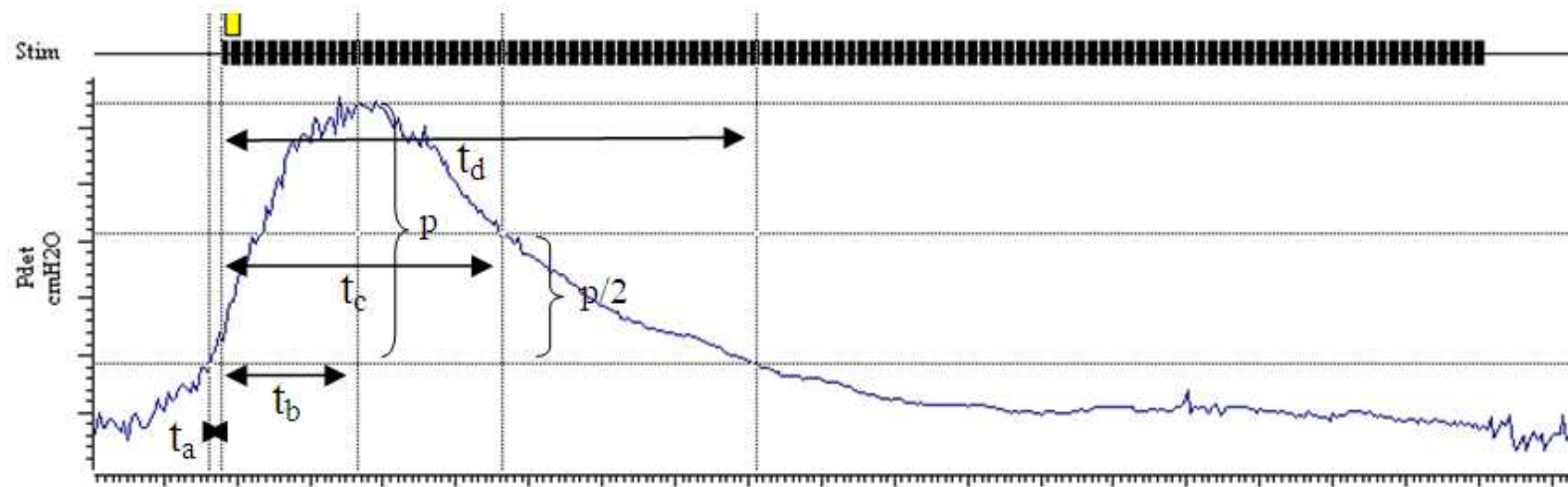


Figure 5:18 - Time taken to start the stimulation and the time taken to suppress the contraction.

t_a = delay in starting the stimulation, t_b = time taken for the detrusor pressure to reach its peak from the start of stimulation, t_c = time taken for the from the start of stimulation to 50% decay of the contraction, t_d = time taken for the detrusor pressure to reach 15cmH₂O (from the base line) from the start of stimulation.

Table 5-9 - The mean value of t_a , t_b , t_c and t_d (indicated in the Figure 5:18)

Patient	t_a (s)	t_b (s)	t_c (s)	t_d (s)
P1	1.795	3.17	6.77	9.31
P2	1.127	26.327	38.497	78.737
P3	1.187	110.285	167.892	233.305
P4	5.31	27.05	37.42	55.4
P5	2.18	6.81	12.45	48.2
P11	4.05	3.28	7.74	25.85

According to the table the stimulation starts after 2.6s ($\pm 1.7s$, range 1.13-5.31s). Since the start of stimulation it takes nearly 29.5s ($\pm 41s$, range 3.17-110.29) for the detrusor pressure to reach its peak. It takes 45s ($\pm 61.82s$, range 6.77-167.89s) for the contraction to decay to 50% of its peak and 75.13s ($\pm 81.13s$, range 9.31-233.3s) to reach the 15cmH₂O above the base line.

Table 5-10 - Shows the rise in detrusor pressure due to the delay in commencing the stimulation.

Patient	Stimulation delay (s)	Change in P_{det} (cmH ₂ O)
P1	1.795	8.12
P2	1.127	3.21
P3	1.187	1.0
P4	5.31	25.41
P5	2.18	6.05
P11	4.05	18.15

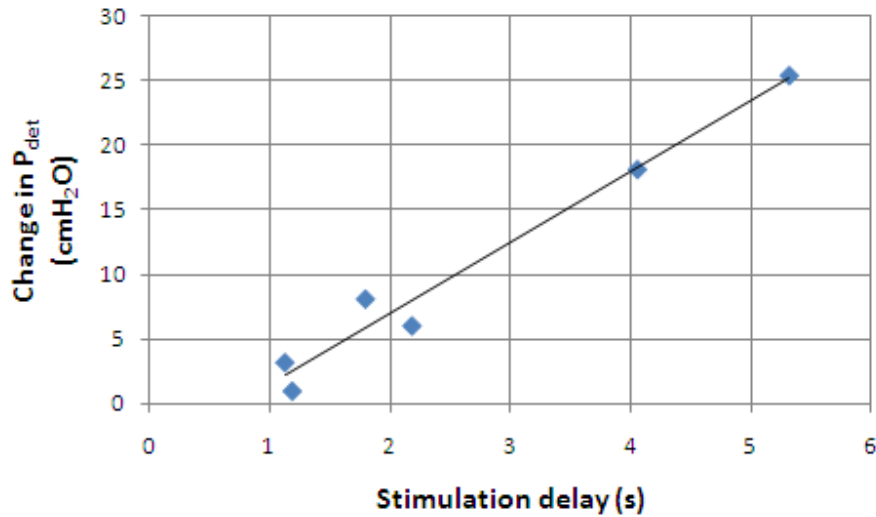


Figure 5:19 - Correlation between the mean delay in stimulation, since detecting the contraction and the rise in the detrusor pressure during that time.

The graphical representation in Figure 5:19 shows that the time delay is responsible for increase in detrusor pressure and follow linear regression. Statistical analysis on Pearson correlation resulted $r=0.99$ showing that the two parameters are highly related, while 2-tailed t test resulted $p=0.0003$ showing the values are highly significant.

Detrusor pressure analysis

The maximum detrusor pressure of each inhibited contraction was measure and shown in the Table 5-11.

Table 5-11 - The maximum detrusor pressure of each successfully inhibited contraction of each individual.

Subject	Maximum detrusor pressure (cmH ₂ O)						
	p ₁	p ₂	p ₃	p ₄	p ₅	p ₆	p ₇
P1	27.85	56.44	-	-	-	-	-
P2	40.74	48.89	72.96	-	-	-	-
P3	69.25	73.07	70.65	59.04	-	-	-
P4	46.22	55.2	69.18	21.37	61.39	53.13	52.25
P5	23.36	41.1	39.03	-	-	-	-
P11	39.64	43.89	48.14	48.84	-	-	-

According to the Table 5-11, the mean of peak detrusor pressure was 48.52cmH₂O (± 10.25 cmH₂O, range 34.5-63.93cmH₂O). The peak P_{det} of the 1st suppressed contraction was 41.18 ± 16.2 cmH₂O. The 2nd and 3rd contractions were 129% and 145.7% of the 1st contraction respectively. The Figure 5:20 highlights the mean peak detrusor pressure of each subject.

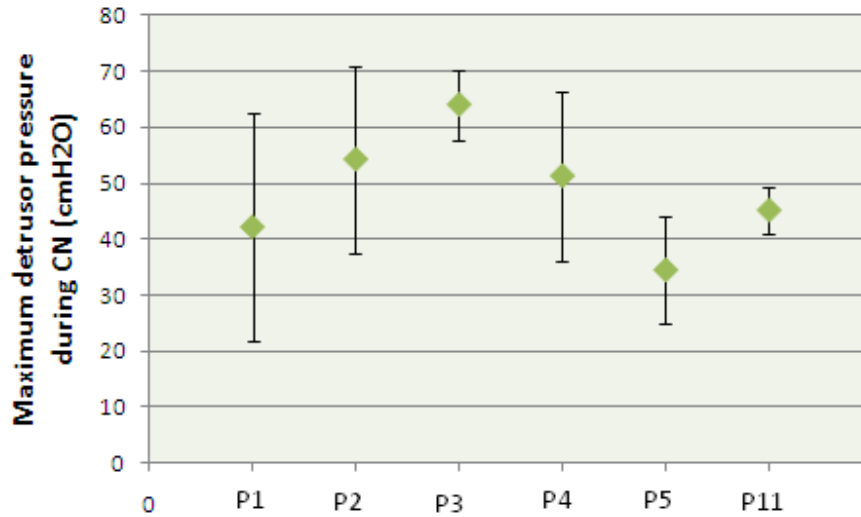


Figure 5:20 - Maximum detrusor pressure during conditional neuromodulation of each individual, the error bars represent the standard deviation.

One of the objectives of the experiment was to reduce the maximum detrusor pressure during bladder filling. Table 5-12 compares the mean peak detrusor pressure before and after stimulation.

Table 5-12 - Shows the mean of the maximum detrusor pressure across each fill during control study and with conditional stimulation.

Patient	Control P _{det} (max) (cmH ₂ O)	P _{det} (max) with CN (cmH ₂ O)
P1	57.27	42.14
P2	86	54.2
P3	100.67	63.93
P4	106	51.25
P5	138	34.5
P11	79.33	45.13

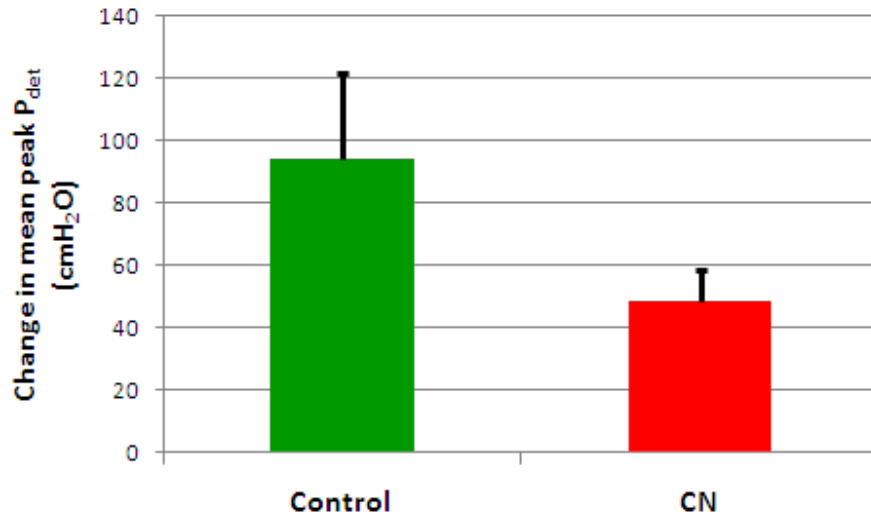


Figure 5:21- Change in mean peak detrusor pressure across all subjects with and without stimulation.

The mean P_{det} of the control study was 94.5 ± 27.4 cmH₂O and that of conditional neuromodulation study was 48.5 ± 10.2 cmH₂O. When the maximum P_{det} of the control study and the conditional neuromodulation was analysed using Wilcoxon's signed rank test resulted p value of 0.01. This shows the reduction in maximum detrusor pressure due to conditional stimulation was statistically significant.

Maximum cystometric capacity

One of the main criteria of this experiment is to measure the increase in bladder capacity due to conditional neuromodulation

Table 5-13 - Shows the maximum cystometric capacity across each fill during control study and with conditional stimulation.

Patient	Control MCC (ml)	MCC due to CN (ml)
P1	152	195
P2	97	488
P3	155	530
P4	81	510
P5	232	289
P11	386	405

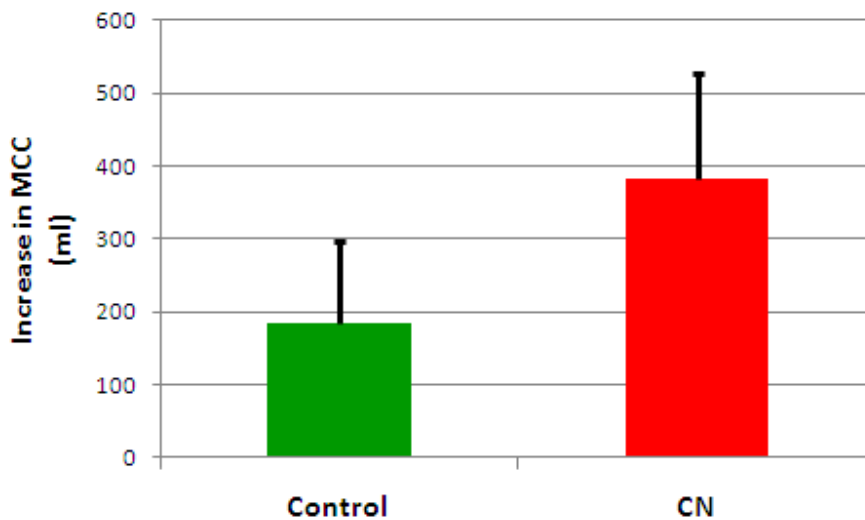


Figure 5:22- Change in maximum cystometric capacity across all subjects with and without stimulation.

The mean MCC of the control study was 183 ± 112 ml and that of conditional neuromodulation study was 402 ± 134 ml. When the maximum cystometric capacity of the control study and the conditional neuromodulation was analysed using

Wilcoxon's signed rank test resulted p value of 0.03. This shows the increase in maximum cystometric capacity due to conditional stimulation was statistically significant.

5.6.5 Discussion

In every patient examined, conditional neuromodulation through the device increased bladder capacity by 220% compared to the control study. The increase in maximum cystometric capacity was statistically significant. However, it is possible that conditional neuromodulation over week or months would gradually increase capacity beyond the modest acute rise seen here, in a similar way to the gradual increase in capacity seen after posterior rhizotomy [31, 165].

The later the stimulation starts during a detrusor contraction, the higher the detrusor pressure will become and therefore less chance there is to prevent incontinence. The average delay was 2.6s; hence having low EMG trigger level might benefit to suppress the contraction. Inhibitory stimulation must be delivered soon after hyper-reflexic contraction, conditional neuromodulation may not be effective at suppressing contractions that begin during the 5s "off" phase [92]. The average time takes to suppress the contraction back to 15cmH₂O was 75.13s.

The ability to switch on stimulation is essential for effective conditional neuromodulation. This relies on two key factors; the precision of the threshold level and the delay between the detection and switching on the stimulation. The adaptive threshold should detect all true contraction (sensitivity of 100%) in order to avoid the leakage until the MCC is reached. The chosen threshold level for each subject

resulted the precision rate of 79% and the false positive outcome contributed to 9.13% of stimulation. This can be improved at any stage by keeping track record of all the activities (bladder diary) and reprogramming the threshold level to the required. There is high significant correlation between the delay in stimulation to the rise of detrusor pressure during that time.

During the continuous filling with conditional neuromodulation switched on, the bladder contractions can inhibit, but with the filling contractions become more frequent. The average time between the 1st and 2nd contraction is 9.13%. Due to the continuous filling the bladder compliance increased by 179%, reducing the catheterisation by 2.8 times.

In conclusion the conditional neuromodulation through the device proved to be an effective treatment for neurogenic detrusor overactivity. The initial study showed that increase in bladder capacity and reduction of detrusor pressure is highly significant. It also showed that the external anal sphincter EMG recorded through the device can be used as a trigger level for the conditional neuromodulation, resulting this device as a closed loop control in treating detrusor overactivity.

Chapter 6 - Design and realisation of the electronic circuitry

6.1 Introduction

Although ACONTI was tested and used clinically, this does not allow patients to use this daily, as the device is not portable. Therefore the next stage in development is to include a self-standing system, which requires no external equipment while the device is being used. The electronic circuitry described in this chapter is a standard design and requires no special components.

This chapter begins by stating the objective of designing the electronic circuitry. Then the chapter divides into two main sections as the amplification and signal processing (section 6.3) and the stimulator design (section 0). Each of these sections, starts by giving a background about the nature of the signals and highlights the design challenges. Then it discusses the system that is currently being used and moves on to derive the specification for the required circuitry. Under the realisation of the circuit (section 6.3.4 and section 6.4.4), each of the individual circuit is discussed together with their performance followed by the overall system testing. Results and discussion of these two sections are highlighted in section 6.6. The following specification in table 6-1 was resulted due to this circuit.

Table 6-1 – The specification for the electronic circuitry

Power supply	Two 9V PP3 batteries
Connection to the device	Mini DIN connector

Gain of the recording circuit	20000 (in 3 stages)
Input coupling	AC coupled with time constant 0.03s
Input impedance	5.6M Ω (differential)
High pass filter cutoff	1Hz
Low pass filter cutoff	500Hz
Common mode rejection ratio	88dB
Notch filter	Tuned at 50Hz and 41dB attenuation
Comparator reference voltage	Variable between 0V to 5V
Stimulating current	Variable between 10mA to 80mA
Stimulation on time	60s
Stimulation off time	3s
Maximum stimulating supply voltage	200V
Stimulating frequency	15Hz
Stimulation pulse width	200 μ s
Charge balancing	RC circuit with 30ms time constant

6.2 Aim and objectives

It is very important that the device be simple as for the daily use. The aim is to increase the mobility of the device. At a first stage of this design, all the electronics will be mounted into a box, which can be worn on a belt. The connection to and from the device is made via a wire, which runs through the buttocks to the belt-worn box. Although this is a standard signal processing system, realising a circuit especially for ACONTI makes the circuitry simpler, which is important in miniaturisation and also allows future hardware and software modifications. This also provides some insight into the electronic circuitry.

Objectives of the design are listed below: -

- Design amplifier which is capable of detecting low amplitude signal and amplify to a processable level.
- Filter and process the signal so that the condition for stimulation can be determined accurately.
- Design a constant current stimulator which provides stimulation pulses, in which the amplitude and the pulse duration can be varied depending on patient requirements.
- Design a system, which consumes low power in order to maximise the battery life.

6.3 Amplification and signal processing

Often in biomedical engineering, current and voltage outputs must be amplified, attenuated or filtered safely in order to achieve the best possible electronic signal with minimal risk to the patient or the operator.

In order to decide whether to apply the stimulation or not, it is required to compare the amplitude of the EMG to a pre determined level. In order to do this, the signal needs to be processed and as this is a low amplitude signal, it requires amplification.

6.3.1 Background

In order to achieve good signal processing, it is required to know some basic characteristics of the biomedical signals of interest.

EMG signal characteristics

Electromyography (EMG) is one of the widely used bioelectric signals, it represents the electrical activity of the muscle [166]. On arrival of an action

potential, each motor unit contracts and causes an electrical signal that is the summation of the action potentials of all of its constituent cells [167]. The characteristics of the recorded EMG signal varies with the tissues through which it passes and the type of the electrode used to detect it. The tissues, electrode-electrolyte interface act as a low-pass filter and the rejects some high frequency components [168].

The SENIAM recommendation for filtering EMG signal are to use a high-pass filter of 10Hz and a low-pass filter with cut-off frequency of about 500Hz [168]. This is a generalised frequency spectrum, but the results of the clinical testing can be used to determine the frequency spectrum in relation to external anal sphincter EMG.

EMG signal processing

In EMG signals, the maximisation of the signal to noise ratio should be done with minimal distortion. Therefore it is important that any detecting and recording device to process the signal linearly. The following characteristics are important for achieving this requirement [169].

- Differential amplifier – Any signal common to both electrodes will be removed only the difference signal will be amplified. Therefore relatively distant noise signals, such as ECG, motion artefact etc. The accuracy of this differential signal depends on CMRR, it is recommended for EMG amplification at least 90dB of CMRR.
- Input impedance – In order to reduce the attenuation and the distortion of the EMG signal due to the effect of input loading, the input impedance of the differential amplifier should be large as possible. However in order to provide return path for the bias current, this amplifier's input impedance is limited by the value of the bias resistors. In addition to these, the

difference in electrode impedance should be minimised to provide a better signal processing.

- Filtering – The EMG signal contaminated with noise. The quality of the signal can be improved by filtering between 10-500Hz. It is advisable to use a filter such as Butterworth for this purpose, in order to preserve the linearity.

Considering the safety of the patient, it is advised to power the circuitry by low voltage (3-15)V battery. This will also reduce power line interference distorting the signal [169].

Noise and interference

It is difficult to obtain high quality bio-electric signal, because the signals have low amplitudes (in the range of μV to mV) and so are easily corrupted by electrical noise and interference. EMG signals can be recorded either from ‘surface’ electrodes on the skin above the muscle of interest, or ‘intramuscular’ electrodes inserted into the muscle [170]. Even though recording the surface EMG is more convenient, it also suffers from greater interference due to poor connection [171]. Interference comes from artificial sources, such as movement artefact, lights, electromagnetically coupled signals from power lines, radiated signals from mobile phones, radio/TV transmitters etc. Noise generated due to movement induced artefact can be removed using a high pass filter with a cut-off frequency between 2-20Hz, while the notch filter is used to remove power line interference [170, 172-174]. Furthermore by using an amplifier with high CMRR, can reduce the effect of common mode signal produced by the body.

These issues need to be considered in order to obtain good signal processing and achieve the true sensitivity of the system.

6.3.2 System that is being used in clinical setting

Currently for the clinical set up a commercially available amplifier system was used and is shown in the Figure 6:1. The amplifier system is a general purpose isolated preamplifier developed by Lectromed and mainly intended for bio potential signals. For the purpose of recording the EMG signals through the wearable device, certain settings of the front of the amplifier were adjusted and are shown in the table 6.1.



Figure 6:1 – Shows the Lectromed 5361 differential amplifier,

This amplifier is approved by the 89/336/EEC directive. The two pressure transducers and the EMG signals from the device are connected to the class II b electrically isolated bio-potential amplifier.

Table 6-2 – The settings of the front end of the Lectromed amplifier [175]

Gain	1 (This is due to a fault in the system) and gain accuracy of $\pm 2\%$
Coupling	AC coupled with time constant 0.03s
Input impedance	5.6M Ω (differential)
Low pass filter cutoff	500Hz
Common mode rejection ratio (CMRR)	90dB
Notch filter	Tuned at 50Hz and set to 20dB attenuation at the notch frequency

This amplified EMG analogue signal was then passed onto CED 1401 data acquisition system in order to convert to a digital signal, which can be further

processed through SPIKE software programme. This system was developed by Cambridge Electronic Devices. The analogue signal was sampled at a rate of 333kHz [176].



Figure 6:2 – CED 1401 plus data acquisition system, act as an interface to the real time analogue signal and SPIKE digital signal [176].

This digital signal was then displayed through SPIKE graphical user interface. An example waveform is shown in the Figure 6:3.

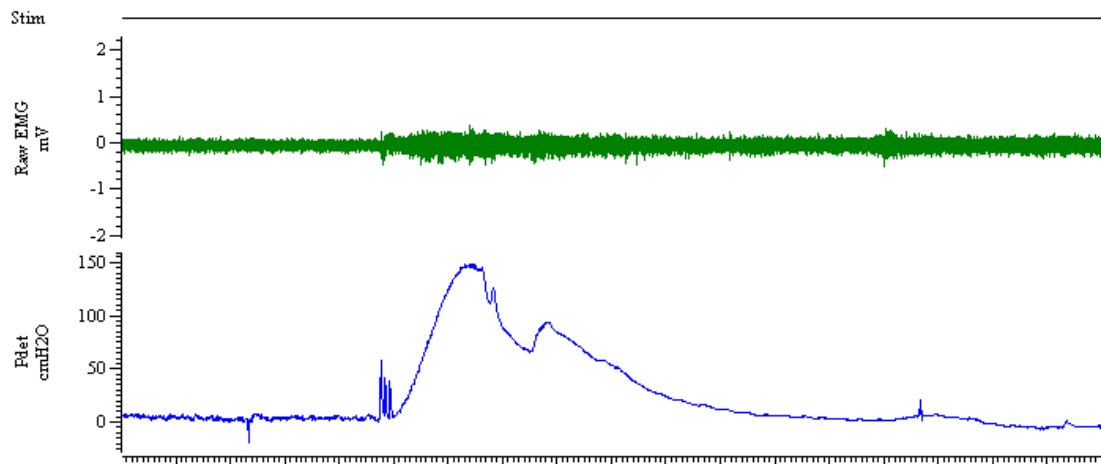


Figure 6:3 – Shows the EMG (green) and the detrusor pressure (blue) of a signal recorded through SPIKE programme.

At this point digital signal processing can be added to the recorded signal, through SPIKE software. In order to analyse the frequency components present in this signal Fast Fourier Transform (FFT) can be applied and is shown in Figure 6:4.

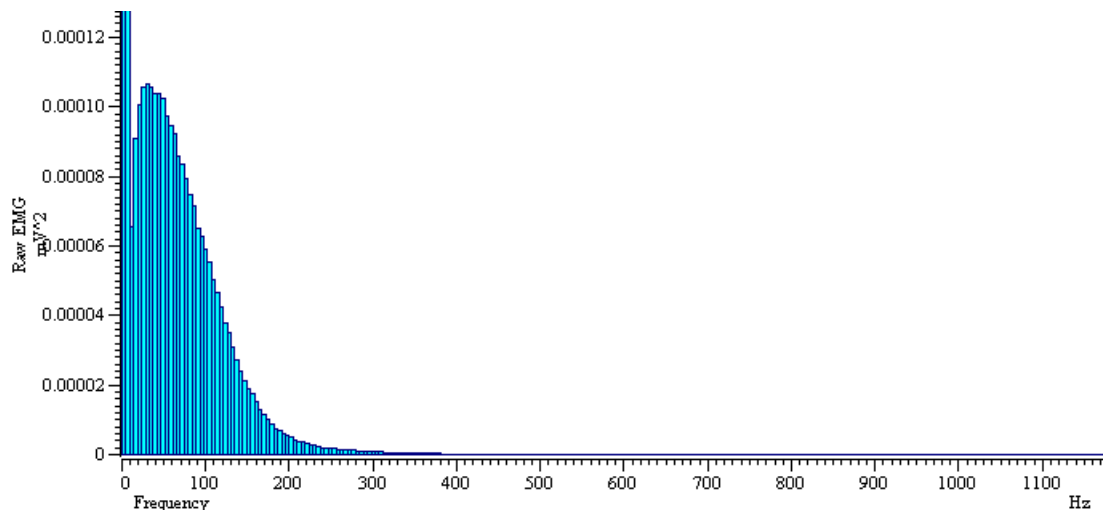


Figure 6:4 – The raw EMG waveform shown in the Figure 6:3 is transformed in to frequency domain by 512 Hanning window in order to assess its frequency components.

According to the Figure 6:4, there is a large DC (0Hz) component present and most of the signal is concentrated below 500Hz. Therefore online band-pass filter was added to the system.

The digitally programmed band-pass filter provided 70dB attenuation in the stop band. The reason for choosing 60Hz as the lower cut-off was to eliminate the 50Hz mains interference, but better attenuation of mains interference can be obtained by using a 50Hz notch filter.

The filtered signal was then rectified and smoothed in order to obtain the DC equivalent. These results are shown in Figure 6:5.

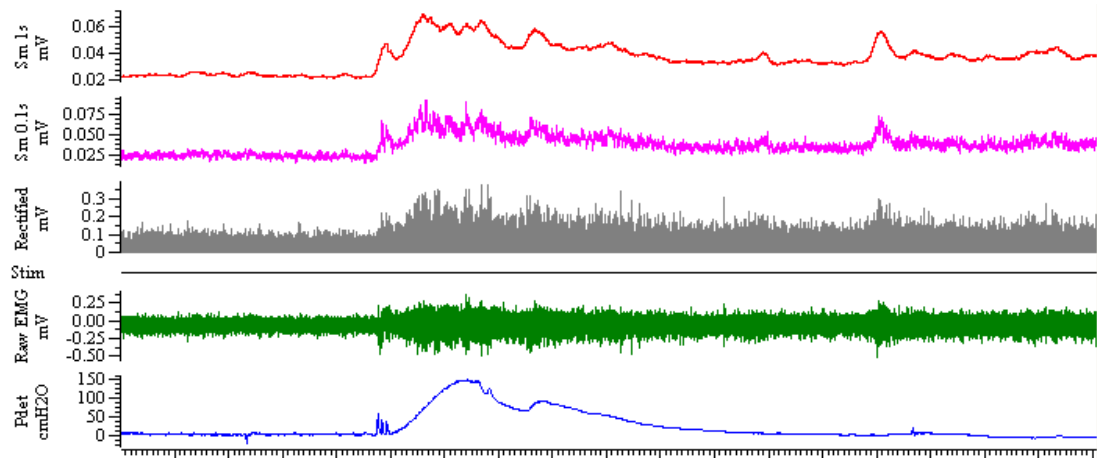


Figure 6:5 – Optimising the processing parameters.

The raw EMG signal (green) was digitally filtered with band pass 60Hz-500Hz, to remove the noise and interference. This filtered signal was then rectified (grey) and smoothed with different time constants. Pink wave shows the smoothing time constant of 0.1s, where as the red is 1s.

After testing with different values it was decided, that 1s is the best smoothing time constant to be used as the trigger signal for the stimulation. Even though this is comparatively slow time constant, in this application it did not cause any leakage of urine.

The threshold detector for triggering stimulation was set on the smoothed signal. When the signal exceeds this level, the stimulation was activated automatically.

All of the signal processing mentioned above is summarised in Figure 6:6.

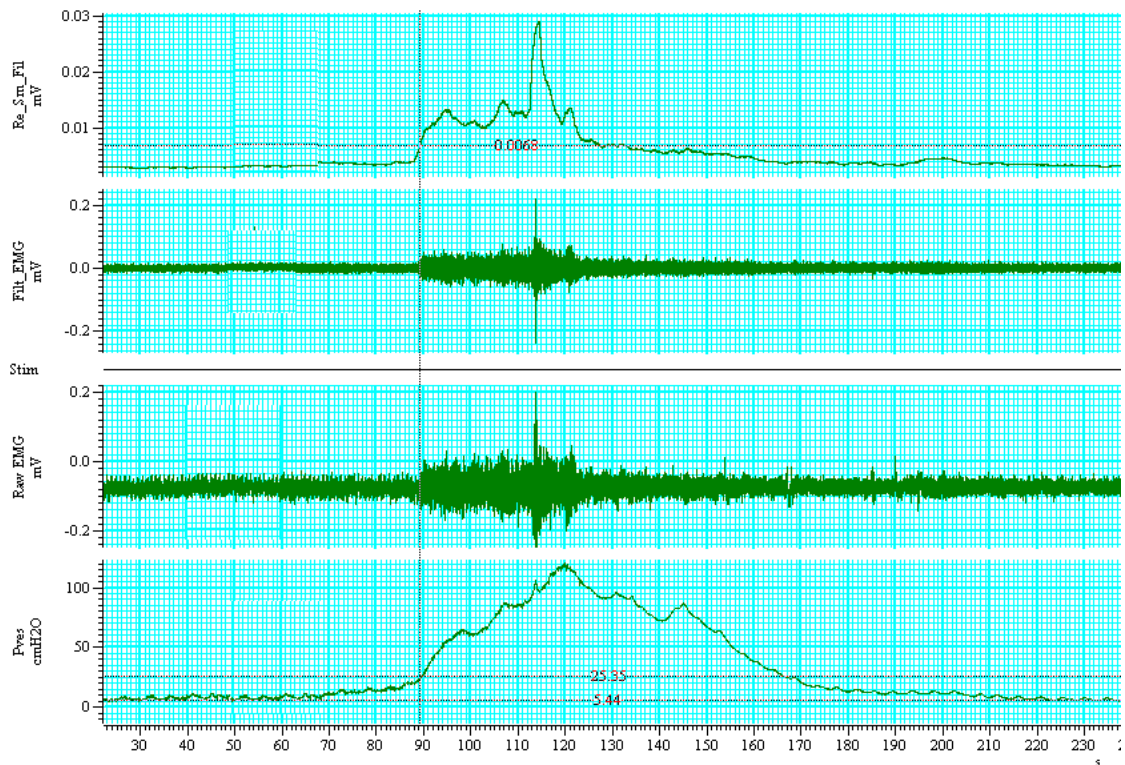


Figure 6:6 - The bladder pressure is shown in Pves and the EMG signal recorded through ACONTI is shown in “Raw EMG” channel.

This channel will then be band-pass filtered and shown as “Filt_EMG”. Finally this filtered signal will be rectified and smoothed and is shown as “Re_Sm_Filt”.

6.3.3 Derivation of the required system

Considering the system that is being used in the clinical study, the block diagram of the proposed circuitry can be derived as shown in the Figure 6:7.

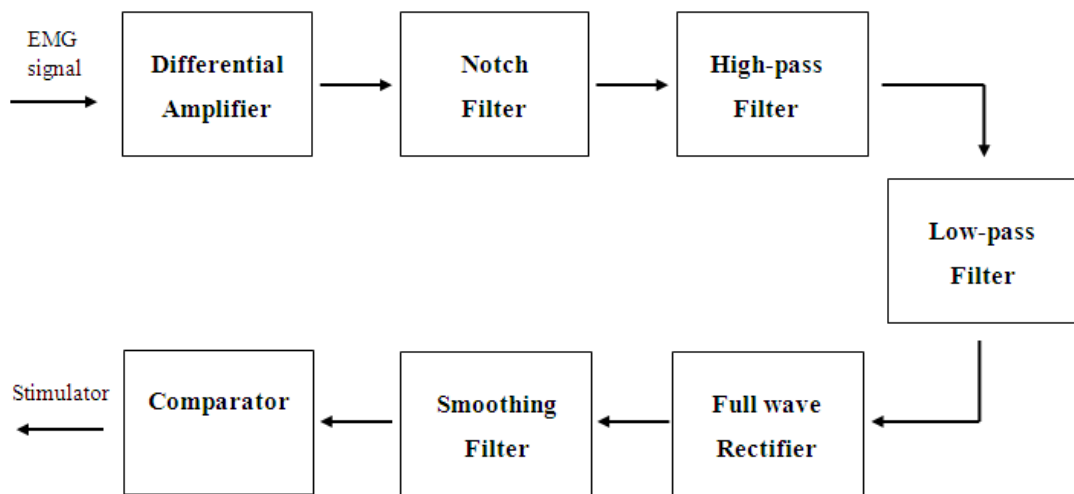


Figure 6:7 - The block diagram of the proposed circuit.

The EMG signal is amplified by the differential amplifier and then passed on to three stage filtering circuit to remove 50Hz interference, movement artefact, DC offset and high frequency components. This signal is further processed through a precise full wave rectifier, followed by the smoothing filter. This processed signal is compared with the pre determined threshold. If it crosses the threshold level, the stimulation will be activated.

Section 6.3.4 describes the design and the testing of each of these functional units.

6.3.4 Realisation of the circuit

Pre-amplifier

This is the heart of an EMG recording system. The basic requirement that biopotential amplifier has to satisfy are [177]:

- The physiological process to be monitored should not be influenced by the amplifier.
- The measured signal should not be distorted.
- The amplifier should provide the best separation of signal and interference.
- The amplifier should provide protection from any hazard.

Input impedance

EMG of the external anal sphincters is recorded through the recording electrodes of the device. In order to obtain a less attenuated signal, the electrode skin interface should be low impedance. This can be achieved by maintaining good electrode skin contact and by using electrodes with low impedance.

The electrodes' impedance were measured when ACONTI was in saline solution using the Wayne Kerr 6500B precision impedance analyser. Figure 6:10 shows the impedance of the left and the right recording electrode of the device over the range of frequencies from 20Hz to 10kHz. According to Figure 6:10, at 1kHz the electrode impedance is around 92Ω , however when the device is in the body impedance of the left recording electrode relative to the ground electrode of the device was $11.79k\Omega$, whereas that of the right electrode was $9.98k\Omega$.

This may be due to the electrodes not making good contacts with sphincter muscles. If the electrodes can be pushed toward the sphincters, by increasing the diameter of the recording part of the device, this impedance can be reduced. Also by applying KY-gel ensures good electrode conductivity.

Another method to minimise the effects of imbalance in electrode impedance is by using buffers at the amplifier input [178]. However as the signals are of low amplitude and by using an amplifier without a gain will reduce the signal to noise ratio.

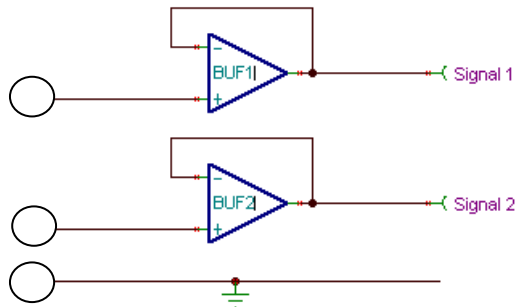


Figure 6:8 - Each electrode is connected to a buffer amplifier, so that the mismatch of the electrode impedance can be minimised.

An alternative approach to minimise the effect of high electrode impedance is by using an amplifier with high input impedance. This impedance should be at least 100 times the electrode impedance to avoid attenuation of the input signal [168]. However the sensor circuit must provide a path for the input bias current of both inputs [179-181]. A simple circuit to solve this problem is by placing a resistor from each input terminal to the ground as shown in the Figure 6:9 [179].

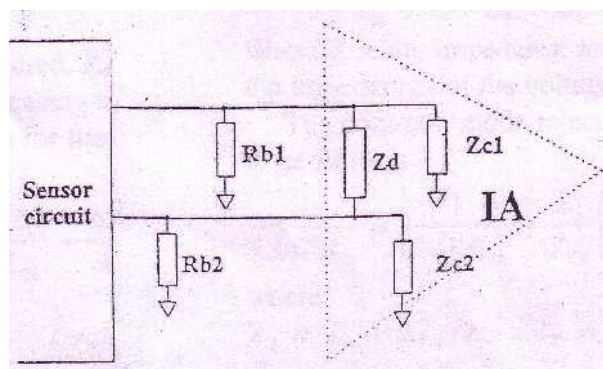


Figure 6:9 - A simple circuit to provide the path for the bias current.

Z_d , Z_{c1} and Z_{c2} are the amplifier differential input impedance, common mode impedance of the input 1 and the common mode impedance of the input 2 respectively. R_{b1} and R_{b2} are the two external resistors to the ground to provide the return bias current [179].

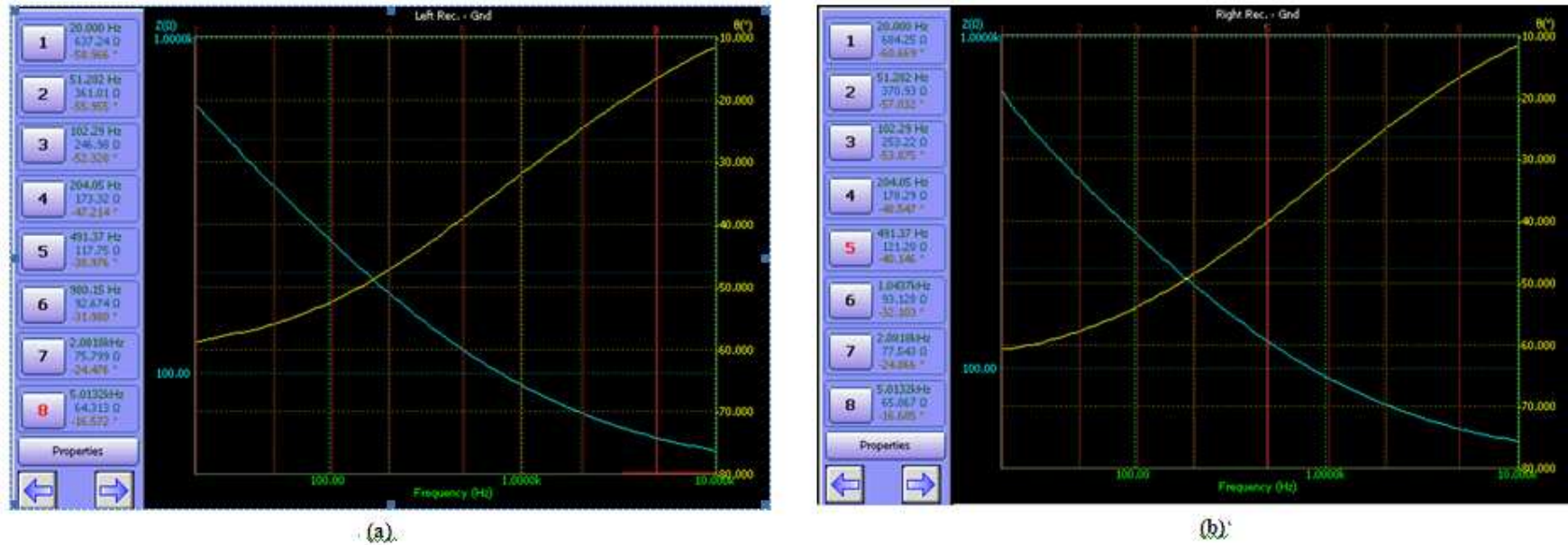


Figure 6:10- Shows the electrode impedance versus frequency, when the device is in a saline solution

(a) Impedance between the left recording electrode and ground (b) electrode impedance between the right recording electrode and the ground.

When the device in the body, the impedance of the left and right recording electrodes at 200Hz (mid-band EMG frequency), were $10.303\text{k}\Omega$ at -26.1° and $8.83\text{k}\Omega$ at -24.2° respectively. This can be represented using the model shown in Figure 6:11.

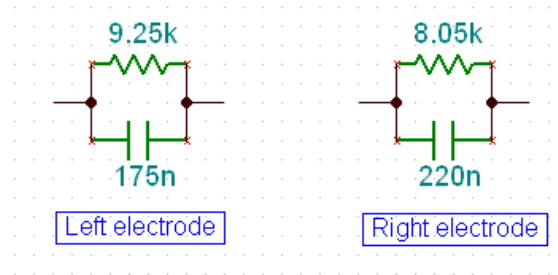


Figure 6:11 - Model of the recording electrode

Common mode rejection

Using a single electrode would result two-phase depolarisation signal, which contains mains at approximately 100mV. This is considerably large compared to the EMG signal, thus the amplifier may saturate. This is overcome by using bipolar configuration, which is recording using two electrodes and a reference and passes onto a differential amplifier [168]. Strong rejection of common mode signal is one of the most important characteristics of a good bio potential amplifiers [177].

The common mode rejection ratio (CMRR) is defined as the ratio of the differential mode gain (A_d) over the common mode gain (A_c). Ideally the common mode signal (V_{cm}) can be removed by using an amplifier with infinite CMRR and using electrodes with matched impedance ($Z_1 = Z_2$).

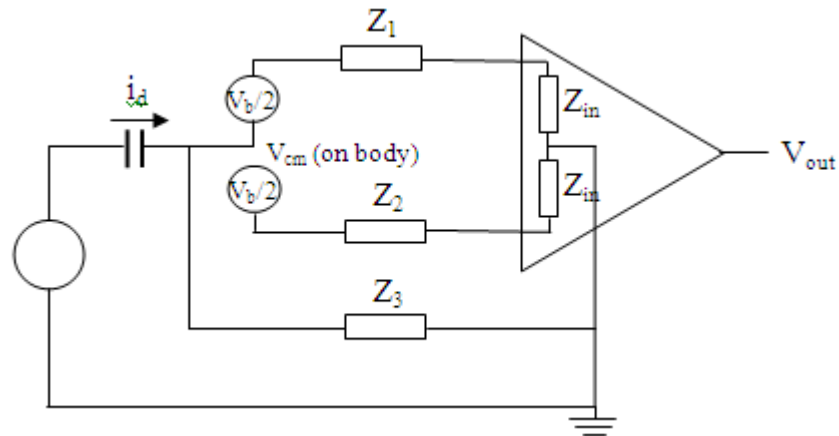


Figure 6:12 - Instrumentation amplifier with non-infinite CMRR and non-infinite input impedance.

The common mode signal V_{cm} causes currents to flow through Z_1 and Z_2 . Therefore the output of the amplifier is a combination of the common mode and the differential signal as shown in the Equation 6-1.

$$V_{out} = A_d \left(V_b + \frac{V_{cm}}{CMRR} + V_{cm} \left\{ \frac{Z_2 - Z_1}{Z_{in}} \right\} \right) \quad \text{Equation 6-1}$$

where A_d = differential gain; V_b = biological signal and Z_{in} = input impedance of the amplifier.

In order to increase the amplifier performance the second and the third term of the Equation 6-1, CMRR of the amplifier should be increased and also the difference between the electrode impedance should be reduced, while increasing the input impedance of the amplifier [177].

Imbalance of the electrodes impedance is not uncommon in biomedical signals. The bias resistors are required for the return pathway of the current. Input

impedance of the amplifier is limited by the values of the bias resistors. The star configuration shown in the Figure 6:13, propose optimal bias circuit, to maintain the high common-mode input impedance and not to reduce the CMRR [179].

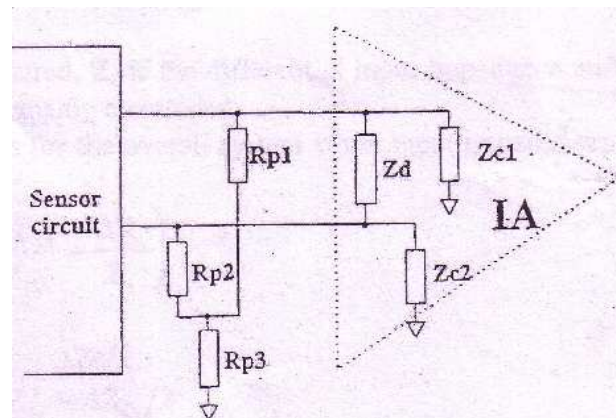


Figure 6:13- An optimal biasing circuit with three resistors in a star configuration.

Z_d , Z_{c1} and Z_{c2} are the amplifier differential input impedance, common mode impedance of the input 1 and the common mode impedance of the input 2 respectively. R_{p1} , R_{p2} and R_{p3} are the three external resistors to the ground [179].

In practice the perfect elimination of the mains hum is not possible, but it is recommended in biomedical applications to obtain CMRR of 10000 (80dB) or more [167].

AC coupling

Figure 6:4 shows that the EMG signal being distorted with large DC component. It would be desirable to block this by simply adding a capacitor working as a passive high pass filter as shown in the Figure 6:14.

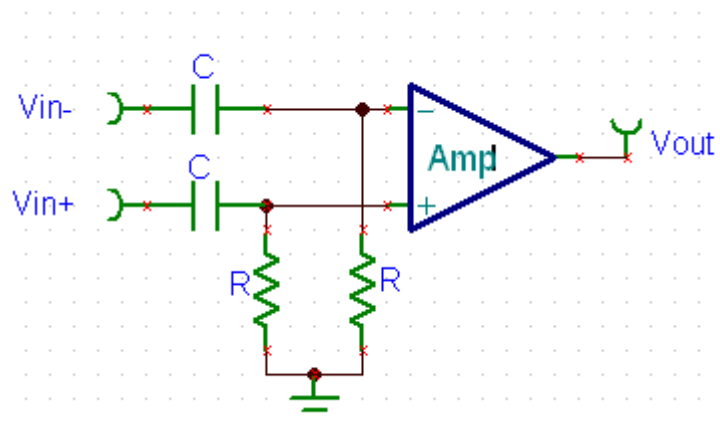


Figure 6:14 - AC coupled amplifier using simple RC filter.

A capacitor C results charging effect from the input bias current. Perfectly matched capacitors are required at both inputs, to maintain high CMRR. The resistor R reduces the mismatch of the input impedance as well as provides the return path for the input bias current.

This would eliminate the electrode offset potentials, which limits the gain of the amplifier due to saturation. Therefore this arrangement permits a higher gain resulting in high CMRR.

Gain

In order to provide optimum signal quality and adequate voltage level for further signal processing, the ratio of the input voltage to the output voltage should be large and in the range of 20,000. The presence of high level of interference signal restricts the gain of the pre-amplifier. The gain of the pre-amplifier is reduced and several amplification stages being added to the system [177].

The required frequency response depends upon the frequencies contained in the EMG signal. About 95% of the EMG signal is normally in the range up to 400Hz [168]. Gain bandwidth product of the amplifier limits the bandwidth of the recorded signal, but most of the EMG amplifiers can easily meet such bandwidth with high gain.

Considering all these factors, the following circuit (Figure 6:15) was derived for initial amplification of the EMG signal.

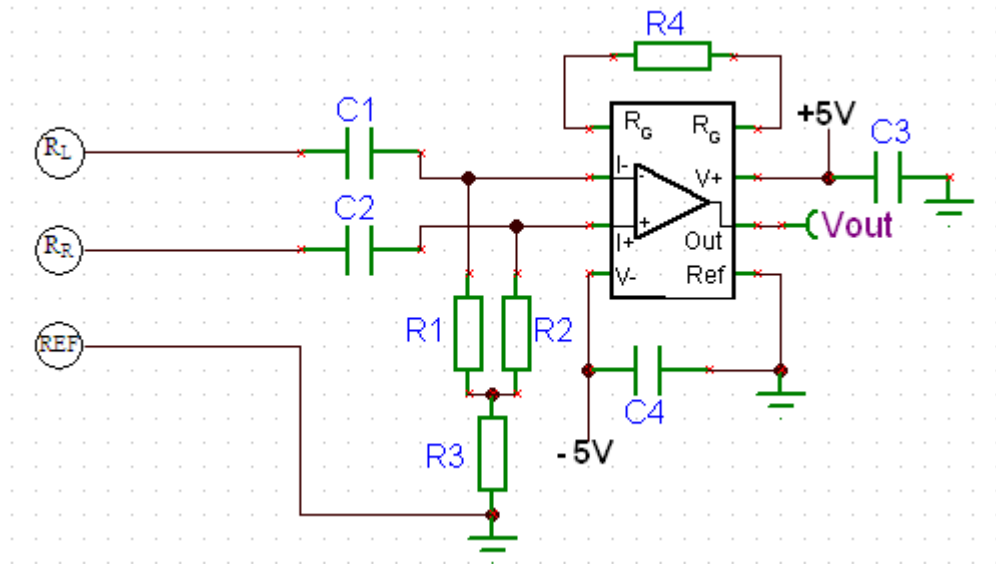


Figure 6:15 - Shows the circuit diagram of the pre-amplifier.

The amplifier shown is INA118 instrumentation amplifier and is powered by $\pm 5V$ battery supply. The ref electrode and the ref pin of the amplifier are connected to the ground.

The INA118 amplifier has a wider power supply range from ± 1.35 to $\pm 18V$, but for this application it is powered by $\pm 5V$. The power supply lines are de-coupled using 100nF capacitors (C_3 and C_4 .)

R_1 , R_2 and R_3 were chosen to be high enough to increase the CMRR of the amplifier and should be low enough to prevent the saturation of the amplifier due to offset voltages. The bias resistors R_1 , R_2 and R_3 are $4.71M\Omega$, $4.71M\Omega$ and $10M\Omega$ respectively. Furthermore C_1 , R_1 and C_2 , R_2 are passive high pass filters with cut-off frequency of 0.34Hz to block any DC signals. Therefore C_1 and C_2 were chosen as 100nF each. All these resistors and capacitors are matched to 0.01% tolerance using the impedance analyser. This capacitor resistor network, act as a high pass filter as well as a path for bias current.

The resistor R4 was used for setting the gain according to the Equation 6-2.

$$G = 1 + \frac{50k\Omega}{R_G} \quad \text{Equation 6-2}$$

The gain of the amplifier was set to 200, therefore $R_G = 251.3\Omega$. The gain bandwidth product of the amplifier is 800kHz, therefore with a gain of 200, the amplifier bandwidth limits to 4kHz. As most of the EMG frequencies are below 500Hz, INA118 amplifier satisfies the bandwidth requirements.

The frequency response of the amplifier (Figure 6:16) tested by injecting a sinusoidal wave using the TTI TGA1241 arbitrary waveform generator.

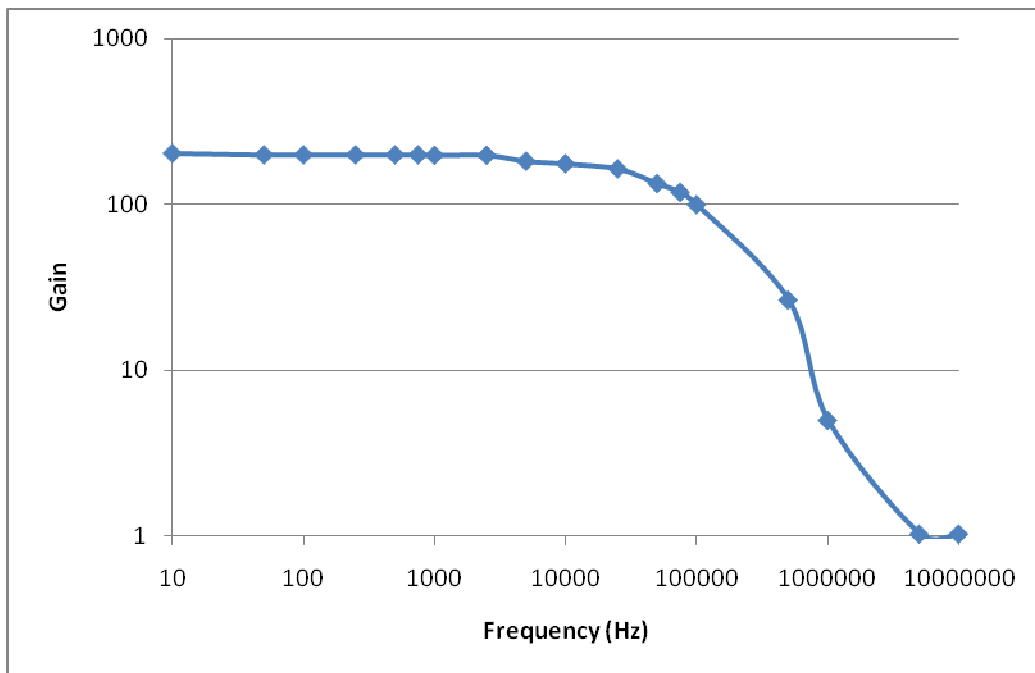


Figure 6:16 - The gain vs frequency of the INA118 amplifier.

The inputs of the INA118 are individually protected for voltages up to $\pm 40V$. If the input is overloaded, the protection circuitry limits the input current to a safe

value of approximately 1.5 to 5mA. These inputs are protected even if the power supplies are disconnected or turned off [180].

According to Equation 6-3 this high pass filter has a time constant of 1.471s; therefore the cut-off frequency is 0.1081Hz (Equation 6-4).

$$\tau = RC \quad \text{Equation 6-3}$$

$$f = \frac{1}{2\pi\tau} \quad \text{Equation 6-4}$$

The common mode gain (A_c) and the differential gain (A_d) of the amplifier were calculated.

$$A_d = \frac{6.24V}{31.2mV} = 200 \quad \text{Equation 6-5}$$

$$A_c = \frac{20mV}{12.2V} = 1.639 \times 10^{-3} \quad \text{Equation 6-6}$$

$$CMRR = \frac{A_d}{A_c} = \frac{200}{1.639 \times 10^{-3}} = 2.4405 \times 10^4 = 87.75dB \quad \text{Equation 6-7}$$

However this calculation does not take the imbalance in the electrode impedance into consideration.

Common mode analysis of the amplifier

Let Z_1 and Z_2 be the electrode impedances of R_L and R_R respectively.

$$\text{Im pedance of the - ve input } (Z_i^-) = \frac{1}{\left(\frac{1}{R_1 + R_3}\right) + \left(\frac{1}{R_2 + Z_2}\right)} \quad \text{Equation 6-8}$$

$$\text{Im pedance of the + ve input } (Z_i^+) = \frac{1}{\left(\frac{1}{R_2 + R_3}\right) + \left(\frac{1}{R_1 + Z_1}\right)} \quad \text{Equation 6-9}$$

$$\text{common mode voltage} = v_{in} \left[\frac{Z_i^+}{Z_2 + Z_i^+} - \frac{Z_i^-}{Z_1 + Z_i^-} \right] \quad \text{Equation 6-10}$$

Substituting the measured impedance values to equation 6-8 and equation 6-9 gives,

$$\text{Im pedance of the - ve input } (Z_i^-) = \frac{1}{\left(\frac{1}{4.71M + 10M}\right) + \left(\frac{1}{4.71M + 8.83k}\right)} = 3.572M\Omega$$

$$\text{Im pedance of the + ve input } (Z_i^+) = \frac{1}{\left(\frac{1}{4.71M + 10M}\right) + \left(\frac{1}{4.71M + 10.303k}\right)} = 3.574M\Omega$$

Therefore;

$$\text{Amplifier's common mode voltage} = v_{in} \left[\frac{3.574M}{8.83k + 3.574M} - \frac{3.572M}{10.303k + 3.572M} \right] = V_{in} \cdot 4.2 \times 10^{-4}$$

Therefore the CMRR of the amplifier = $200 / 4.2 \times 10^{-4} = 113.56\text{dB}$

Output offset voltage

The DC levels of inputs and the output of the amplifier were measured using ISO-Tech IDM93N digital multi-meter and the values obtained are shown in Figure 6:17. This DC offset value limits the gain of the amplifier, which might cause saturation.

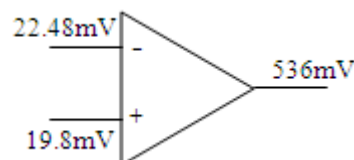


Figure 6:17 - DC offset values of the amplifier measured by the digital multi-meter.

The bias resistors of the differential amplifier in Figure 6:15 are 14.71MΩ each. The manufacturer’s data sheet of the INA 118 specifies that there can be bias current typically in the range of ±1nA upto ±5nA. With the bias resistor configuration this can generate offset voltage upto 73.55mV. Even though there are capacitors to block any DC from the electrodes, there is still offset voltage generated at the amplifier input due to bias current. This is what was shown in Figure 6:17. The difference of the input offset voltages (22.4-19.8) is amplified with the gain of the amplifier (x200) to produce output offset voltage of 536mV.

Noise calculation

In general, the noise introduced by the biasing resistors diminishes as their value increases, provided that they are large enough [179]. Therefore, for the purpose of noise calculation the circuit can be simplified as in Figure 6:18.

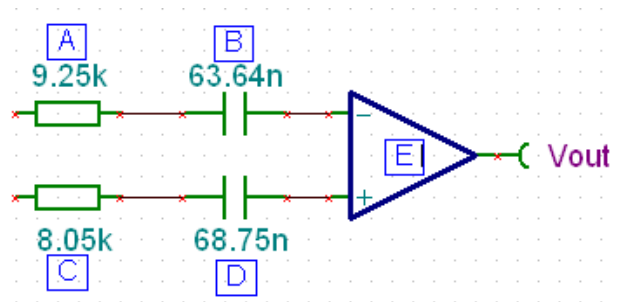


Figure 6:18 - Simplified recording electrodes and the amplifier.

Noise from resistor A;

$$\sqrt{4kTRB} = \sqrt{4 \times 1.38 \times 10^{-23} \times 300 \times 9.25 \times 10^3 \times 4000} = 782.76nV$$

Noise from capacitor B;

$$I_{Amp_Noi} \times \frac{1}{2\pi fC} \sqrt{B} = 2 \times 10^{-12} \times \frac{1}{2 \times 1.414 \times 200 \times 63.64 \times 10^{-9}} \sqrt{4000} = 1581.68nV$$

Noise from resistor C;

$$\sqrt{4kTRB} = \sqrt{4 \times 1.38 \times 10^{-23} \times 300 \times 8.05 \times 10^3 \times 4000} = 730.23nV$$

Noise from capacitor D;

$$I_{Amp_Noi} \times \frac{1}{2\pi fC} \sqrt{B} = 2 \times 10^{-12} \times \frac{1}{2 \times 1.414 \times 200 \times 68.75 \times 10^{-9}} \sqrt{4000} = 1464.12nV$$

$$\text{Noise from amplifier E} = 10^{-8} \times \sqrt{4000} = 632.46nV$$

Therefore the total noise in the amplifier front end;

$$n_{Total} = \sqrt{n_A^2 + n_B^2 + n_C^2 + n_D^2 + n_E^2} = 2.5\mu V$$

Notch filter

The most frequent common mode signal coupled into a bio-potential system is the 50Hz, sinusoidal interference from the mains power [182]. Minimizing this interference signal requires shielded cables between the patient and the apparatus and use of narrow band rejection filter (notch filter) [177].

A simple notch filter is shown in the Figure 6:19 using a single op-amp, provides high performance using both negative and positive feedback around the amplifier [183].

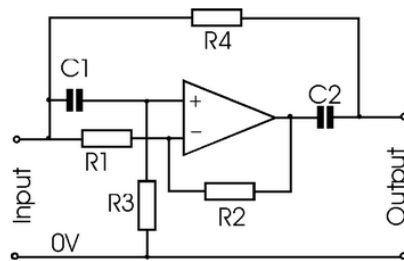


Figure 6:19 - Active operational amplifier notch filter circuit [183].

However the components should match at least 1% or better to obtain a notch depth 45dB. Also the quality factor (Q) cannot be varied in this arrangement. In order to ensure the optimum operation, the source impedance should be less than 100Ω and the load impedance 2MΩ [183].

Therefore in order to be able to vary the Q and also impedance matching problems, active twin T notch filter circuit was used in this application.

The variable Q function for the notch filter is provided by the 1kΩ potentiometer R4. The notch frequency is determined by Equation 6-11.

$$f_{notch} = \frac{1}{2\pi RC} \quad \text{Equation 6-11}$$

In order to provide the notch frequency of 50Hz, the following component values were used. C1 = C2 = 1.49nF; C3 = 3.05nF; R1 = R2 = 2.12MΩ; R3 = 1.06MΩ.

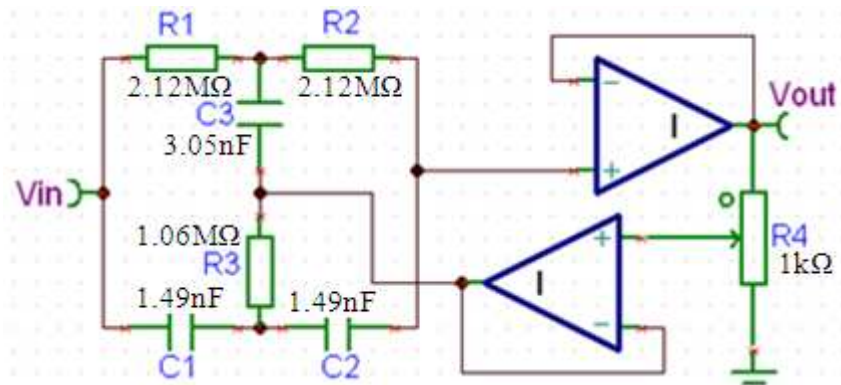


Figure 6:20 - Active twin T notch filter circuit with variable Q [183].

The two amplifiers are from a TS358 dual operational amplifier package which is powered by $\pm 5V$ supply. The power supply lines are decoupled using 100nF capacitors to reduce the power line interference.

The resultant circuit was tested on the Tektronix TDS 2004B four channel digital storage oscilloscope.

The potentiometer was adjusted until good rejection of the notch frequency is obtained. The frequency response of the notch filter is shown in the Figure 6:21.

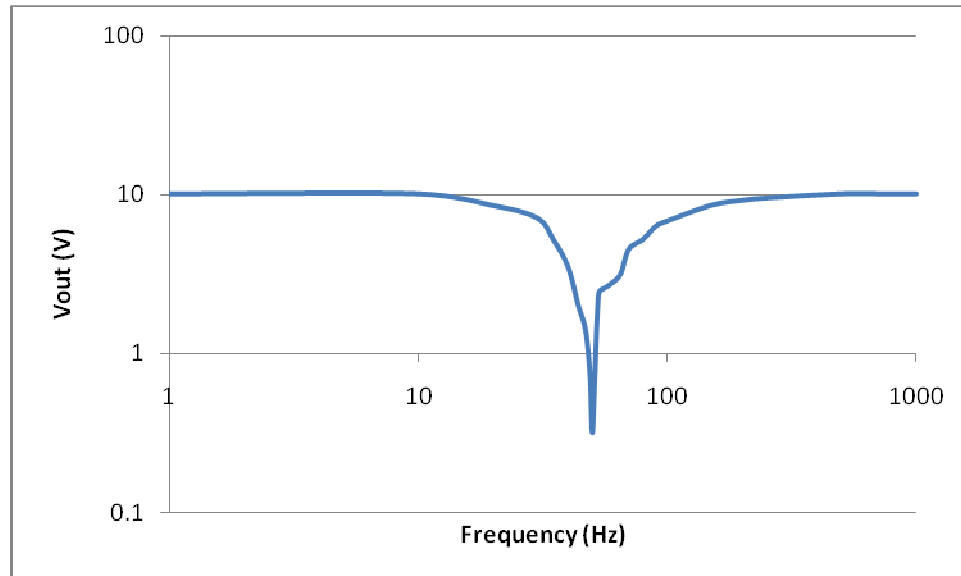


Figure 6:21 - Shows the frequency response of the notch filter. The input to the notch filter is a sinusoidal wave with amplitude 10.2V.

Analysing the above diagram, the notch frequency is at 50.026Hz and the attenuation at notch is 41.28dB.

It is advantageous to lower the Q to ensure some rejection over wider range of frequencies [184].

High-pass filtering

As shown in the Figure 6:17, the output of the pre-amplifier has a DC offset of 536mV, this signal needs to be filtered before further amplification, otherwise this may cause saturation of the signal. As the signal needs high pass filtering as well as further amplification, a multiple feedback high pass filter with gain was chosen.

The designed filter is a 2nd order Butterworth multiple feedback filter with cut-off at 10Hz and gain of 10. In order to determine the component values, the following design equations were used.

The transfer function is given by:

$$\frac{V_{out}}{V_{in}} = \frac{-As^2}{s^2 + \alpha\omega_c s + \omega_c^2} \quad \text{Equation 6-12}$$

Where, A = voltage gain; s = complex frequency (j ω); ω_c = cut-off frequency;

α = 1/quality factor (Q) = $\frac{1}{\sqrt{2}}$ for Butterworth

From Appendix 2, multiple feedback filter design: re-arranging the Equation 6-12 gives,

$$C_1 = AC_4 \quad \text{Equation 6-13}$$

$$R_5 = \frac{(C_1 + C_3 + C_4)}{\alpha\omega_c C_3 C_4} \quad \text{Equation 6-14}$$

$$R_2 = \frac{1}{\omega_c^2 C_3 C_4 R_5} \quad \text{Equation 6-15}$$

By solving the Equation 6-13, Equation 6-14 and Equation 6-15 the following components values were obtained. $C_1 = 100\text{nF}$, $R_2 = 53.59\text{k}\Omega$, $C_3 = 100\text{nF}$, $C_4 = 10\text{nF}$, $R_5 = 4.73\text{M}\Omega$

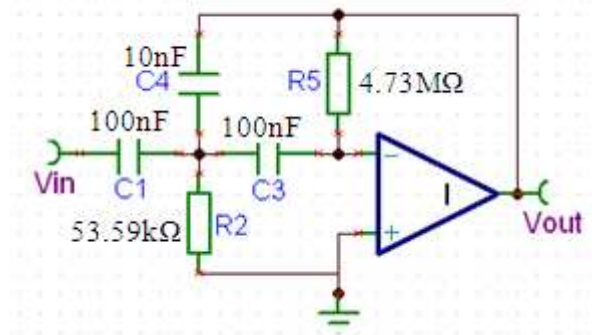


Figure 6:22 - Multiple feedback high pass filter

The amplifier used is from the TS358 dual operational amplifier package and powered by $\pm 5V$, where the power lines are decoupled using 100nF capacitors.

The filter was tested using the TTI TGA1241 arbitrary waveform generator and the Tektronix TDS 2004B four channel digital storage oscilloscope. The Figure 6:23 represents the frequency response of the high pass filter.

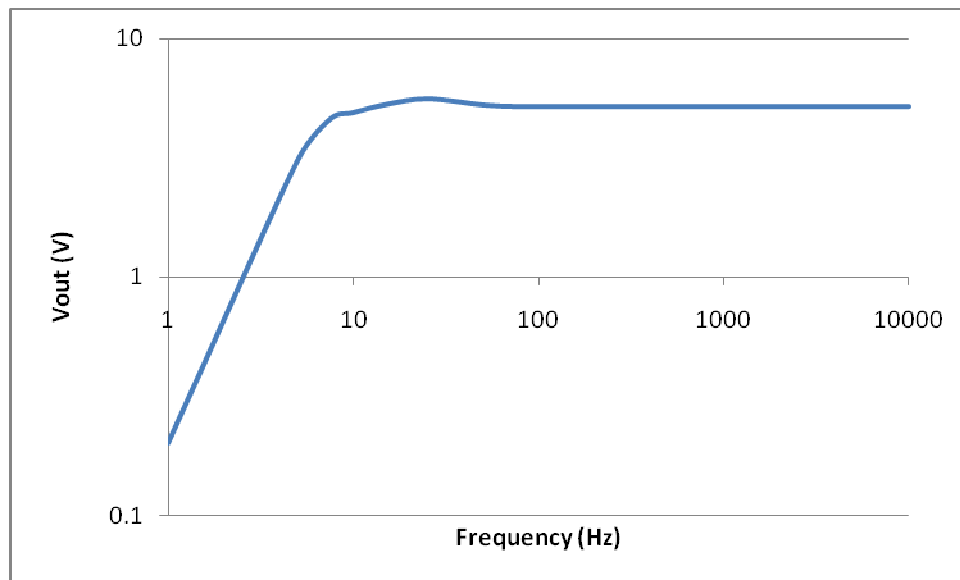


Figure 6:23 - Shows the frequency response of the high pass filter with gain of 10.

The input to the filter is a sinusoidal wave with amplitude 520mV.

According to the Figure 6:23 the attenuation at 1Hz is 8.3dB (including the gain of 10).

Low-pass filtering

One of the SENIAM recommendation for filtering EMG signal is to use a low-pass filter with cut-off frequency of about 500Hz to remove unwanted high frequency interference [168]. Further gain is also introduced at this stage using an active filter. The designed filter is a 2nd order Butterworth multiple feedback filter with cut-off at 500Hz and gain of 10. In order to determine the component values, the following design equations were used.

The transfer function is given by;

$$\frac{V_{out}}{V_{in}} = \frac{-A\omega_c^2}{s^2 + \alpha\omega_c s + \omega_c^2} \quad \text{Equation 6-16}$$

Where, A = voltage gain; s = complex frequency ($j\omega$); ω_c = cut-off frequency;

α = 1/quality factor (Q) = $1/\sqrt{2}$ for Butterworth

From Appendix 2, multiple feedback filter design: re-arranging the Equation 6-16 gives,

$$R_1 = \frac{R_4}{A} \quad \text{Equation 6-17}$$

$$R_3 = \frac{1}{\alpha\omega_c C_2 R_1 R_4 - R_4 - R_1} \quad \text{Equation 6-18}$$

$$C_5 = \frac{1}{\omega_c^2 C_2 R_3 R_4} \quad \text{Equation 6-19}$$

By solving the Equation 6-17, Equation 6-18 and Equation 6-19 the following components values were obtained. $R_1 = 10\text{k}\Omega$, $C_2 = 100\text{nF}$, $R_3 = 8.92\text{k}\Omega$, $R_4 = 100\text{k}\Omega$, $C_5 = 1.136\text{nF}$

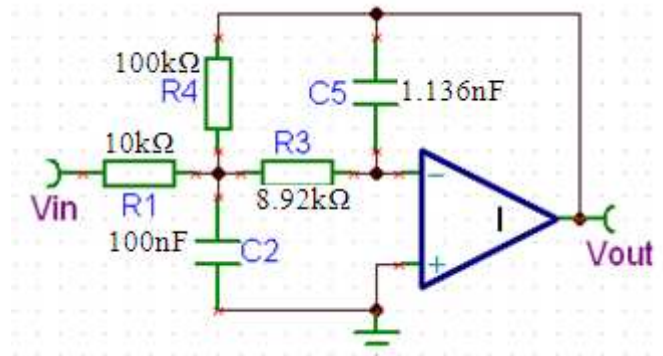


Figure 6:24 - Multiple feedback low pass filter

The amplifier used is from the TS358 dual operational amplifier package and powered by $\pm 5\text{V}$, where the power lines are decoupled using 100nF capacitors.

The filter was tested using the TTI TGA1241 arbitrary waveform generator and the Tektronix TDS 2004B four channel digital storage oscilloscope. The Figure 6:23 represents the frequency response of the low pass filter.

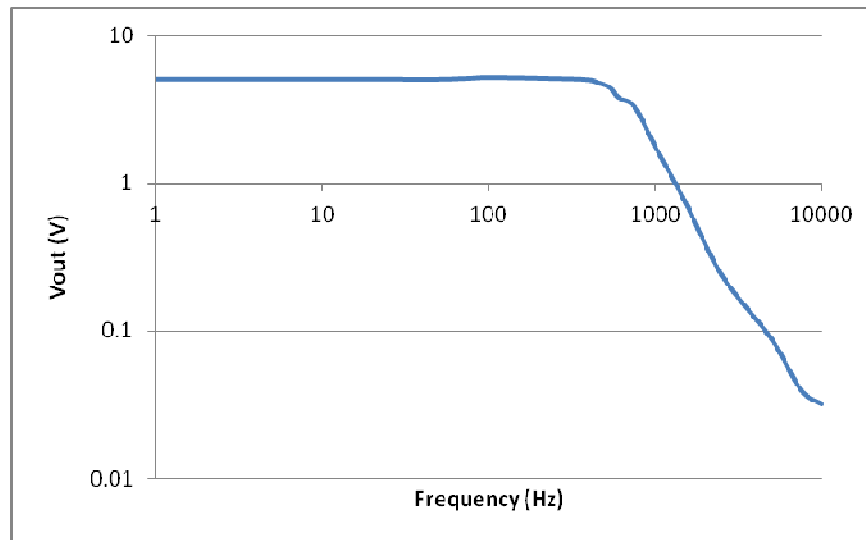


Figure 6:25 - Shows the frequency response of the low pass filter with gain of 10.

The input to the filter is a sinusoidal wave with amplitude 520mV.

According to the Figure 6:23, the filter has a cut-off slope of 34.8dB/decade.

Full wave rectification

Currently the filtered EMG signal has two polarities; however it is required to determine the amplitude therefore this signal needs to be rectified. The conventional full-wave diode rectifiers cannot rectify signals whose amplitudes are less than threshold voltage (approximately 0.7V) of the diode [185, 186]. Precision rectifier is implemented with an op-amp and includes diode in the feedback loop. This effectively cancels the forward voltage drop of the diode, so very low level signals can still be rectified with minimal error [187]. There are various precision rectifier circuits available, but due to the simplified design and the easiness of choosing the components, the following design recommended by Burr-Brown was used.

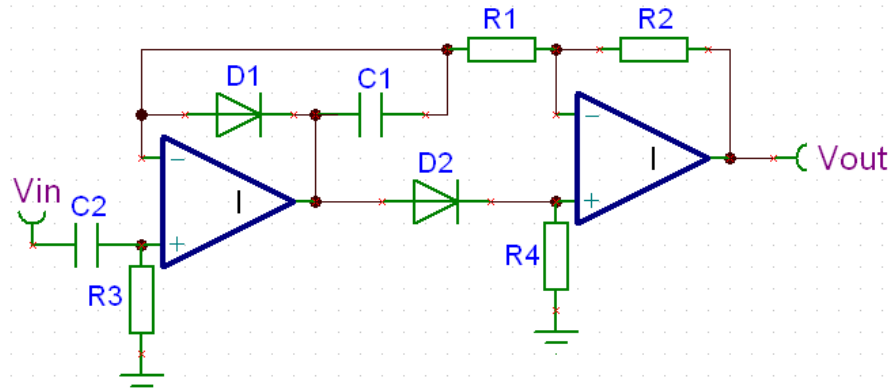


Figure 6:26 - This precision rectifier requires two amplifier and the two resistors R1 and R2.

The amplifiers used are TL082 low power dual FET operational amplifier. The main reasons for choosing this are low power, dual packaging and high gain bandwidth product (GBW) of 4MHz. An amplifier with high GBW is important for this application, as the rectified signal has high frequency component present. The amplifiers are powered by $\pm 5V$ and are decoupled using 100nF capacitors.

The input signal is high pass filtered with time constant 32ms (5Hz) to remove any further DC components present. $R_3 = 30k\Omega$ for input bias current compensation, while C_2 is 1.06 μF .

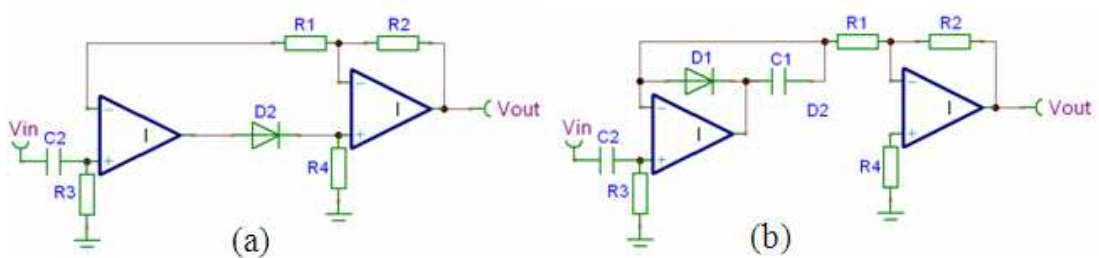


Figure 6:27 - (a) During the positive half of the cycle the circuit acts like a voltage follower. (b) During the negative half the circuit acts as a simple inverting amplifier.

During the positive input signal diode D1 become reverse biased. The current flows through the forward biased D2 to the non inverting input of the second amplifier. Since there is no feedback path, no current flows through R1 and R2. Therefore the second amplifier act as a voltage follower, resulting the $V_{out} = V_{in}$. During the negative half D2 becomes reverse biased and the output of the first amplifier drives the resistor R1 through forward biased diode D1. The second amplifier acts as a unity gain inverter, resulting $V_{out} = - V_{in}$. The capacitor C1 ensures the circuit is stable with the second amplifier in the feedback loop. According to the application bulletin [188] for good stability and best speed $R1.C1 = 1/4^{th}$ GBW of the second amplifier. Therefore calculation resulted $C1 = 15.9\text{pF}$. $R1 = R2 = 10\text{k}\Omega$ and matched to 0.001% using Wayne Kerr 6500B precision impedance analyser. R4 was chosen to be $20\text{k}\Omega$ to provide path for bias current of the second amplifier.

The full-wave rectification circuit was tested using the TTI TGA1241 arbitrary waveform generator by injecting sinusoidal waveform with different frequencies and the Tektronix TDS 2004B four channel digital storage oscilloscope for monitoring the output.

According to the Figure 6:28, there is slight distortion of the leading edge of the rectified output for the input frequencies 250Hz and 500Hz. This can be improved by using an amplifier with higher GBW. For the EMG signal processing in this application, this will not be a problem. Therefore the circuit remains unchanged.

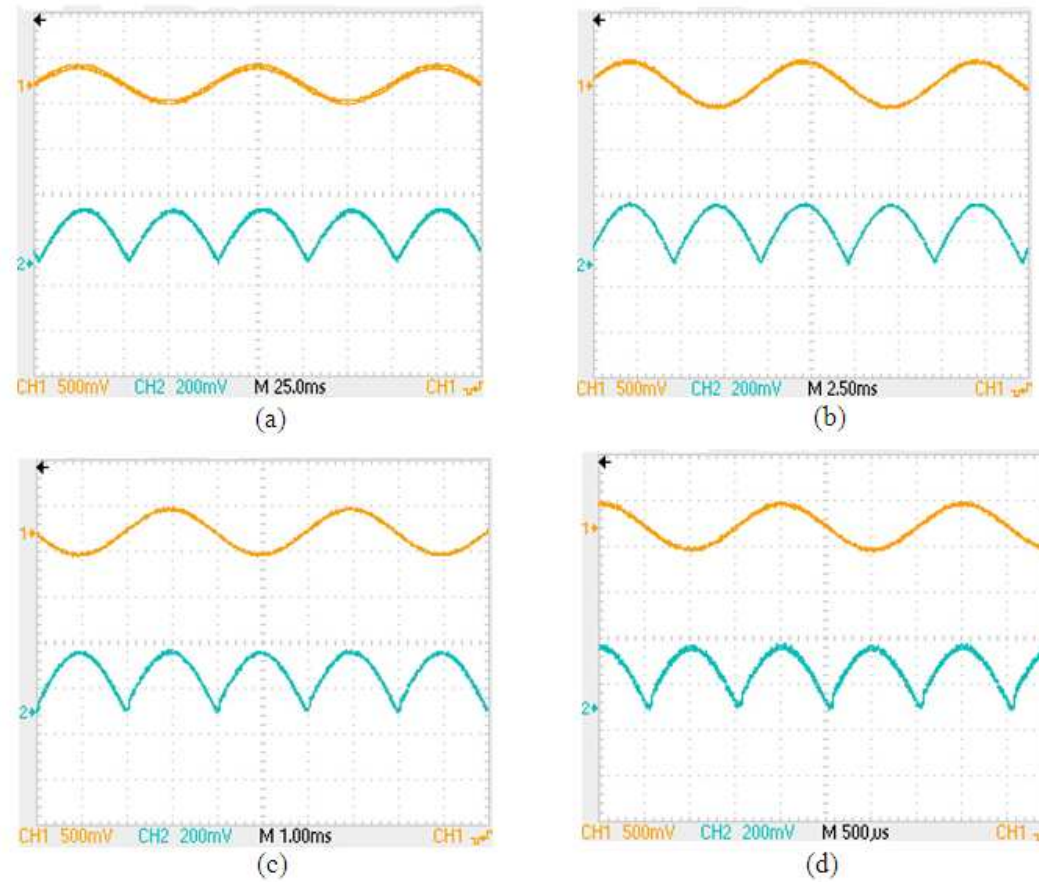


Figure 6:28 - Shows the input and the output to the full-wave rectification circuit at different frequencies. (a) 10Hz , (b) 100Hz, (c) 250Hz and (d) 500Hz.

Smoothing

Smoothing is an essential part followed by full-wave rectification. In order to compare the processed signal with the set threshold, this ripples needs to be smooth. The easiest and cost effective method to remove this is by using RC filter. However there will be small ripple drop across the series resistor [189], but as the signal will be used for comparison it would not be a problem. The effect of RC filter to the ripple voltage is shown in the Figure 6:29 and in the Equation 6-21.

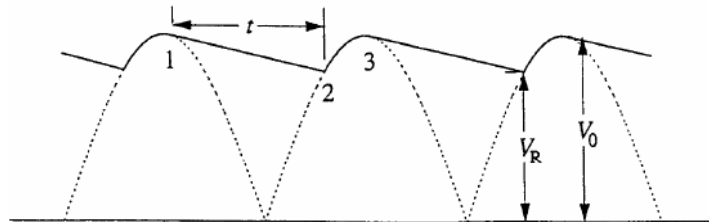


Figure 6:29 – In a RC filter, at position 1, the voltage across the capacitor is V_0 .

The capacitor discharges through the resistor for a time t until the voltage reaches position 2. From position 2 to 3, the capacitor recharges [190].

During the period from 1 to 2

$$V_R = V_o \exp\left(-\frac{t}{RC}\right) \quad \text{Equation 6-20}$$

Hence the ripple voltage = $V_o - V_R$ is given by

$$V_{ripple} = V_o \left(1 - \exp\left(-\frac{t}{RC}\right)\right) \quad \text{Equation 6-21}$$

In clinical studies to obtain required amount of smoothing digital filter with time constant is 1s was used. However this will slow down the response, therefore when building the electronic circuitry two stage of filtering being used. One is single pole passive low pass filter and the other is two pole active low pass filter.

The reason for choosing the passive filter is to get rid of the high frequency ripple before the active stage.

The designed passive filter has a cut-off frequency of 5Hz and is shown in Figure 6:30 . RC values were chosen according to the $\tau = RC$ Equation 6-3 and

$$f = \frac{1}{2\pi\tau} \quad \text{Equation 6-4.}$$

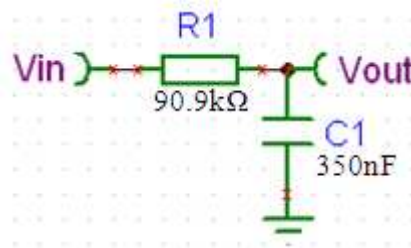


Figure 6:30 - 1st order passive low pass filter with cut-off frequency 5Hz.

The response of the passive filter is shown in the Figure 6:31.

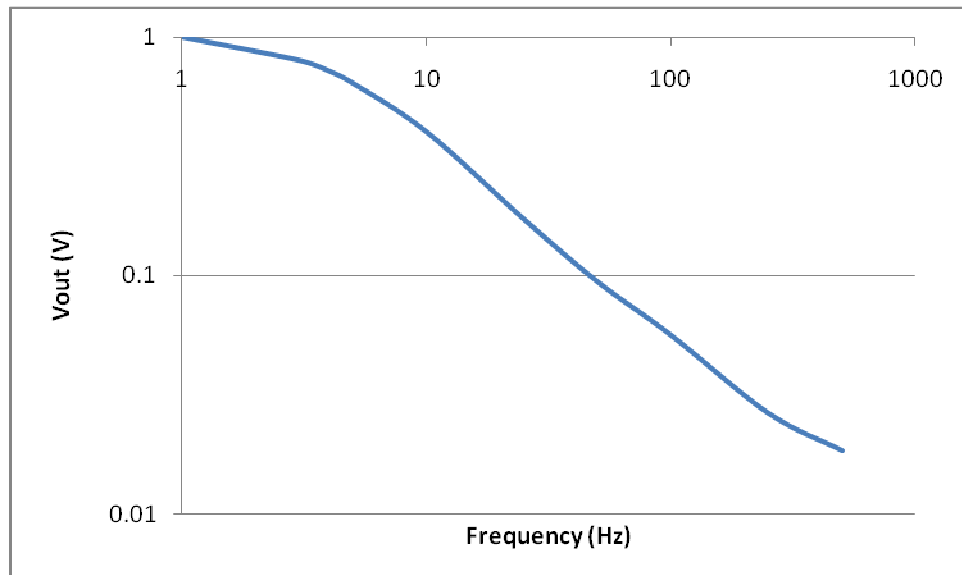


Figure 6:31 - Shows the frequency response of the 1st order passive low pass filter.

The input to the filter is a sinusoidal wave with amplitude 1V.

According to the Figure 6:31, the filter has the cut-off slope of 17.07dB/decade.

For the active filter stage Sallen-Key 2nd order low-pass filter was used. The reason for choosing the Sallen-Key is to obtain non-inverted signal at the output as well as to obtain faster response. The filter was designed using the calculations provided by Bronzite [191] and is shown in the Figure 6:32.

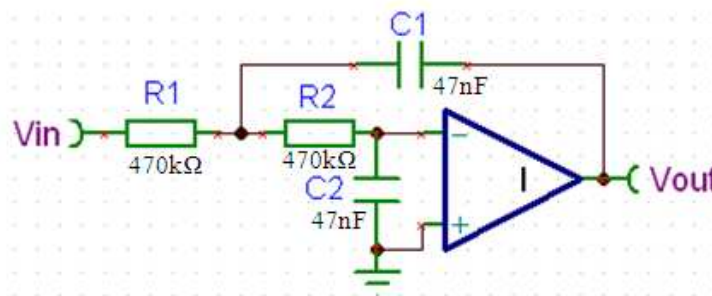


Figure 6:32 - 2nd order Sallen-key filter with cut-off frequency 7.2Hz.

The amplifier used is TL082 and the power lines are decoupled using 100nF capacitors.

The filter response is shown in the Figure 6:33.

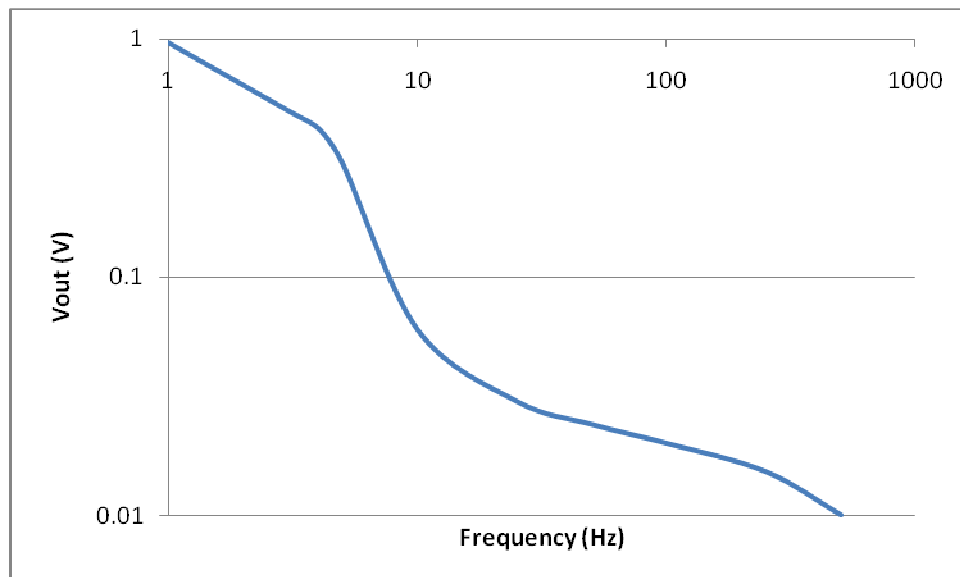


Figure 6:33 - Shows the frequency response of the 2nd order active low pass filter. The input to the filter is a sinusoidal wave with amplitude 1V.

According to the Figure 6:33, the filter has the cut-off slope of 24.08dB/decade.

Comparator

Comparator is a circuit that compares the input voltage with same reference voltage. The output voltage of the amplifier flips from one saturation limit to the other as the processed EMG signal reaches above the preset threshold. This threshold level can be varied by adjusting the potentiometer as shown in Figure 6:34.

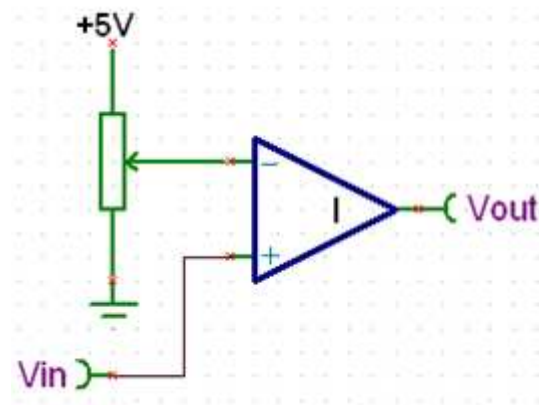


Figure 6:34 - Simple comparator circuit designed using TL082 amplifier and is powered by 5V.

The built circuit for the amplifier and the signal processing system is shown in Figure 6:35.

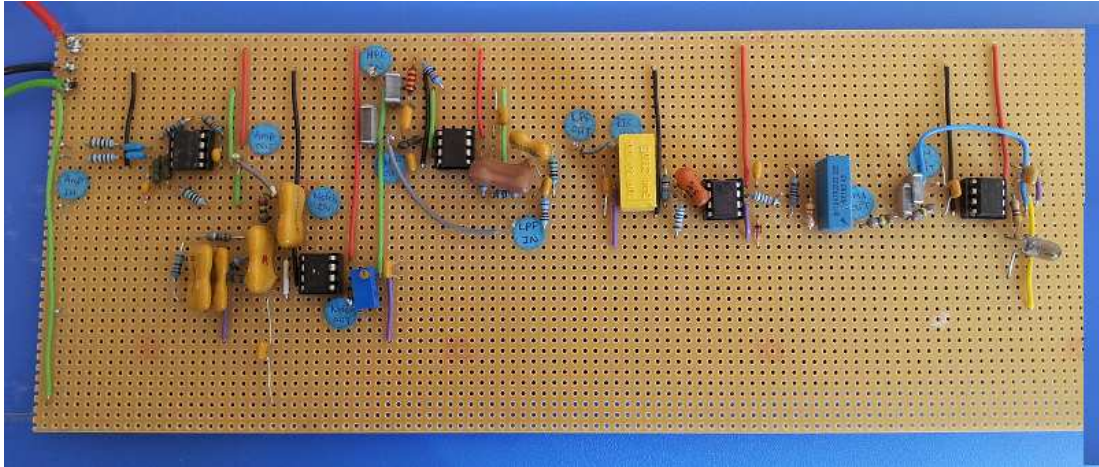


Figure 6:35 - Amplifier and signal processing circuit.

6.4 Stimulator design

When the processed EMG signal reaches above the predetermined threshold, a burst of stimulation should be delivered to the patient through the stimulating electrodes. Since the device is small and portable, the stimulator should be designed with few components. Section 6.4.1 describes some major considerations in designing a simple stimulator.

6.4.1 Background

Safety considerations

Electric shock may result in fatal burns and can cause muscle and even heart to malfunction. Often the degree of damage depends on the magnitude of the current applied, how long the current applied and which points through the current passes [192].

Type of stimulators

Stimuli parameters vary widely according to the type of muscle stimulation, the number of channel and the type of electrodes. Many commercially available stimulators are constant voltage stimulators, in which delivered current level varies with change in electrode-skin impedance. Even though it is easy to design an additional circuitry is required to monitor the current level [193]. However in this device focus has been made to designing a simple constant current stimulator.

6.4.2 System that is being used in clinical setting

For the experiments described in the chapter 5, a commercially available constant current stimulator (DS7A) was used. The stimulation parameters were set in Spike software (Figure 6:36) and passed over to the stimulator via the data acquisition card shown as in the Figure 6:2.

```
func set%();  
var ok%;  
DlgCreate("Continuous Stimulation Parameters");  
DlgInteger(1,"Stimulation Frequency - Hz",1,100);  
DlgReal(2, "Stimulation On Time - secs",1.0, 6000.0);  
ok%:=DlgShow(freq%,tim);  
text1%:=Printf("%s, %d, %s, %.1f, %s", "Stim: Freq = ",  
freq%, "Hz; Duration = ", tim, "secs");  
return;  
end;
```

Figure 6:36 – Spike software code for setting the stimulator parameters.

The software code shown opens up a dialog box to the user to enter the stimulation parameters. The stimulating frequency can be set between 1Hz to 100Hz and the stimulating period can be set between 1s to 6000s.

Even though the stimulating frequency and the period can be varied, in clinical experiments these parameters were set at fixed values of 15Hz and 60s respectively, which were said to be the optimum stimulating parameters from previous studies [162]. Reducing the variables simplifies the circuit design.

This stimulator was developed by Digitimer Ltd and is shown in the Figure 6:37. The specification of the DS7A stimulator is highlighted in Table 6-3.



Figure 6:37 - Shows the Digitimer DS7A constant current stimulator.

This is FDA and MDD compliant for clinical use. The trigger signal is connected to the stimulator through DAC. The output of the DS7A is connected to the stimulating electrodes of the device through 4mm shrouded sockets [194].

Table 6-3 - The specification of the DS7A constant current stimulator [194].

Current	0 to 99.9mA when the dial is in x10 position
Pulse duration (μs)	50, 100, 200, 500, 1000 and 2000
Compliance	Variable from 100V to 400V
Trigger level	+3V on the rising edge
Maximum trigger input	$\pm 15\text{V}$
Minimum pulse duration for the trigger	5 μs
Maximum trigger frequency	1000 pulses /s

The stimulating current, pulse of width of 200 μs and the compliance voltage of 200V were set using the adjustments on the front panel of the stimulator. The stimulation off period of 3s was set using the software in order for the signal processing and the physiological function to recover following the stimulation.

6.4.3 Derivation of the specification for the stimulator

Comparing the system that currently being used, the specification of the proposed stimulator circuit can be derived as shown in the Table 6-4.

Table 6-4 - The specification for the simple stimulator circuit.

Current	Variable between 10mA to 80mA
Stimulation on time	60s
Stimulation off time	3s
Stimulating voltage (maximum)	200V
Frequency	15Hz
Pulse width	200 μ s
Charge balancing	RC circuit

The above specification was realised in the design shown in the section 6.4.4, while isolating the signal processing and the patient interface from the stimulating circuitry.

6.4.4 Realisation of the stimulator

The stimulator circuit is made up with four functional units. Those are circuits for adjusting the stimulation on and off time, the width of the stimulating pulse, isolation barrier and the delivering constant current pulse per each trigger signal.

Stimulation duration adjustor

When the output of the comparator goes high, 60s of stimulation needs to be delivered. At the end of this period, there is 3s stimulation off period whatever the output of the comparator. This stimulation off period allows the EMG amplifier

to recover after stimulating artefacts and also the bladder and sphincter muscles to recover following stimulation.

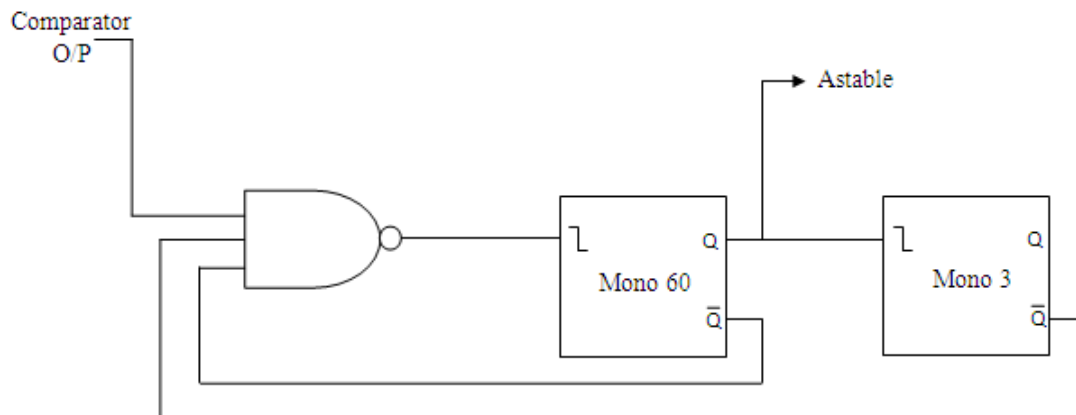


Figure 6:38 – Logic circuit to adjust the stimulator duration.

Output of the comparator, \bar{Q} of the Mono 60 and \bar{Q} of the Mono 3 connected to the three input NAND gate to generate 60s pulse for each time when the comparator output is high, while holding Q of Mono 60 low

The above circuit was implemented using HEF4023BP Phillips triple 3-input NAND gate and 74HC4538N Phillips dual retriggerable precision monostable multivibrator. Detailed circuit diagram with all the sub components is presented in Figure 6:39.

74HC4538N and HEF4023BP both are powered by 5V power supply and the supply lines are decoupled using 100nF capacitors (C1 and C3). $1\bar{R}_D$ and $2\bar{R}_D$ are held high to prevent them resetting the output pulse immediately. In order for the circuit to act as a non-retriggerable monostable in which triggering will be at falling edge the following arrangement (Figure 6:40) was used as specified in the manufactures data sheet [195].

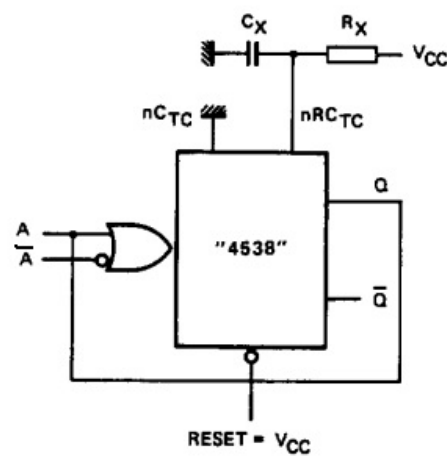


Figure 6:40 - Shows the arrangement of falling-edge triggered non-retriggerable monostable circuitry.

The input is connected to the $n\bar{A}$ and the nQ is connected to the nA .

Diode D1 and D2 are 1N4148 diodes were used as a safety precaution. In an instance of sudden power drop the charge stored in capacitors C2 and C3 will discharge through the monostable and may damage the input protection diodes.

The output pulse width was determined by the RC time constant and based on Equation 6-22 specified by the data sheet.

$$T = 0.7 \times R_t \times C_t \quad \text{Equation 6-22}$$

Based on the calculations 3s pulse width require $C2 = 1\mu\text{F}$ and $R1 + R2 = 4.105\text{M}\Omega$, whereas 60s pulse require $C4 = 10\mu\text{F}$ and $R3 + R4 = 8.205\text{M}\Omega$.

$$O3 = \overline{1Q} \cdot \overline{2Q} \cdot I9 \quad \text{Equation 6-23}$$

O3 is the trigger input of the 60s pulse, and 2Q is the trigger input of the 3s pulse.

The Figure 6:41 and Figure 6:42 show the verification of the above circuitry.

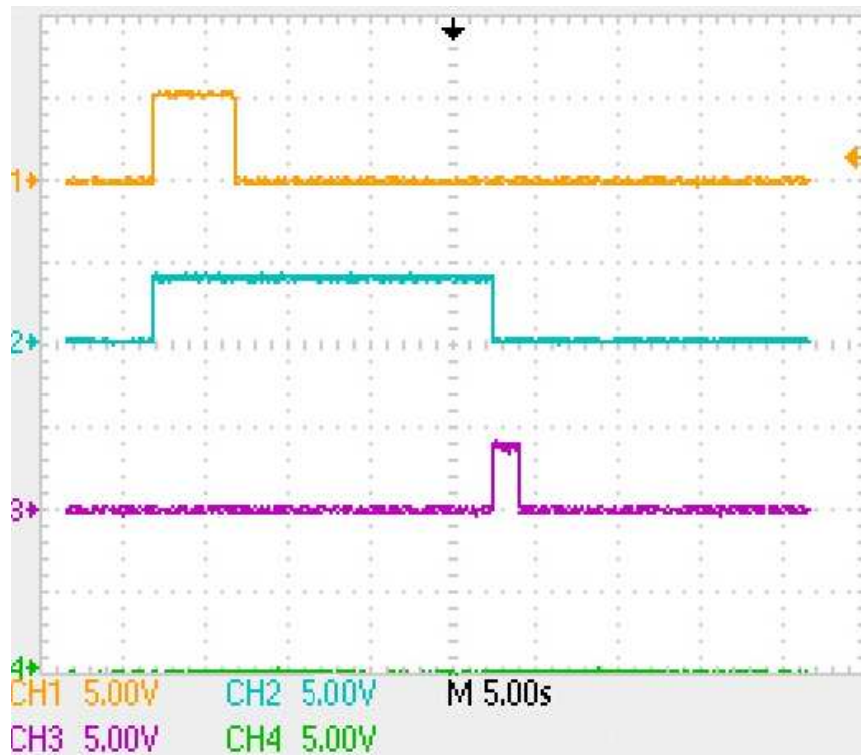


Figure 6:41 – Monostable output - 1.

The orange wave shows the output of the comparator goes high. At the active high edge of the comparator, the 60s pulse (blue waveform) goes high for 60s followed by 3s pulse (purple waveform) goes high. At the end of the 3s pulse, since the output of the comparator is low, the 60s pulse remains low.

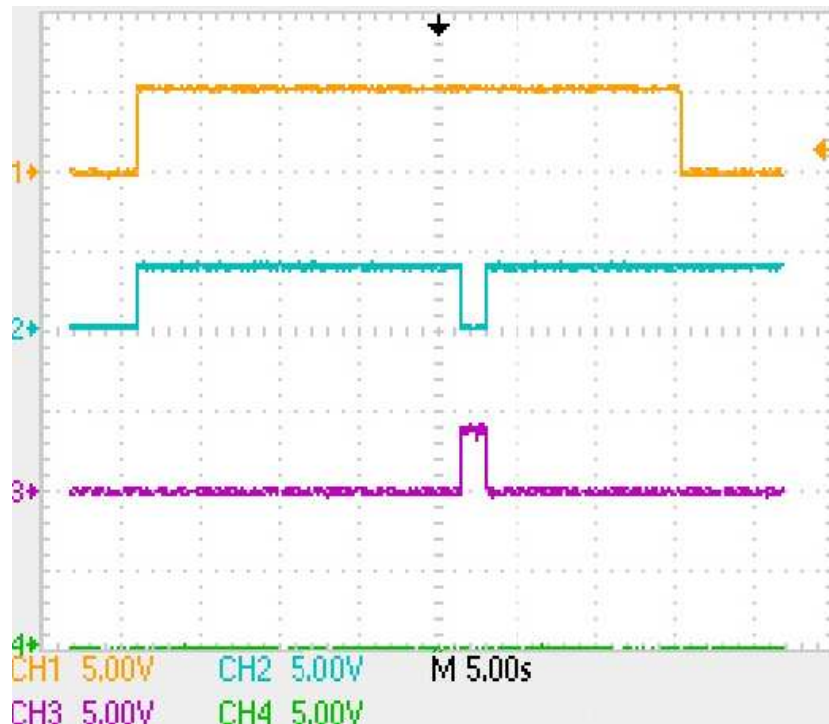


Figure 6:42 – Monostable output – 2.

At the active high edge of the comparator (orange) the 60s pulse goes high followed by 3s pulse. At the end of the 3s pulse, as the comparator still remains high another 60s pulse is triggered and this will repeat as long as the comparator output is high.

The 60s pulse (2Q) is then connected to the astable in order to adjust the stimulation pulse width.

Stimulation pulse width adjustor

When the stimulation duration is determined, the next step is to adjust the stimulation pulses. According to the specification derived in section 6.4.3, the stimulation frequency should be 15Hz and each should be 200 μ s wide and should be as shown in the Figure 6:43.

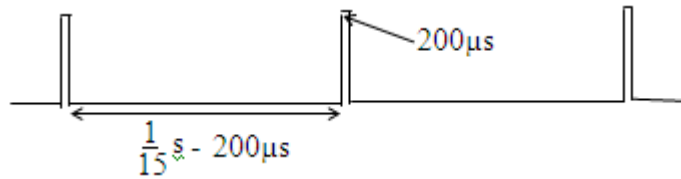


Figure 6:43 - 200µs stimulation pulses.

Duty cycle of an astable circuit is given in the Equation 6-24.

$$Duty\ cycle = \frac{T_m}{T_s + T_s} = \frac{200\mu}{1/15} = 0.3\% \quad \text{Equation 6-24}$$

For the circuit operation the duty cycle should be close to 50% or higher [196]. Therefore the astable was designed to produce opposite of what was required and then was inverted with the spare NAND gates on the circuit and multiply with the 60s pulse.

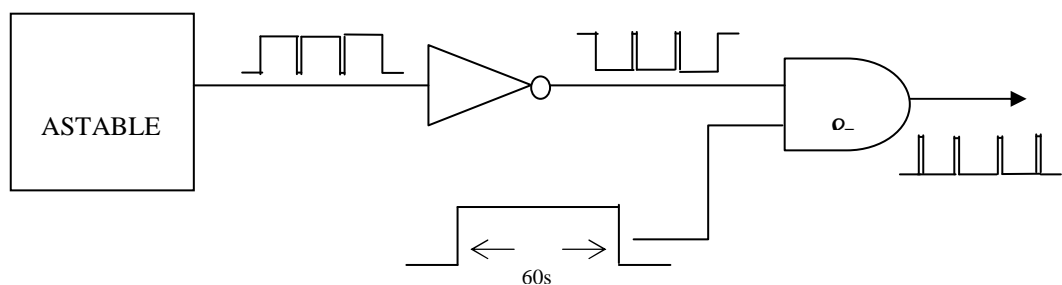


Figure 6:44 - Output of the astable was inverted and multiplied with the 60s pulse in order to produce stimulation pulses with duty cycle of 0.3%.

The above circuit was implemented using NE555P Texas Instruments precision timer and spare NAND gates were used to implement NOT and the AND gate and the circuit diagram is shown in the Figure 6:45.

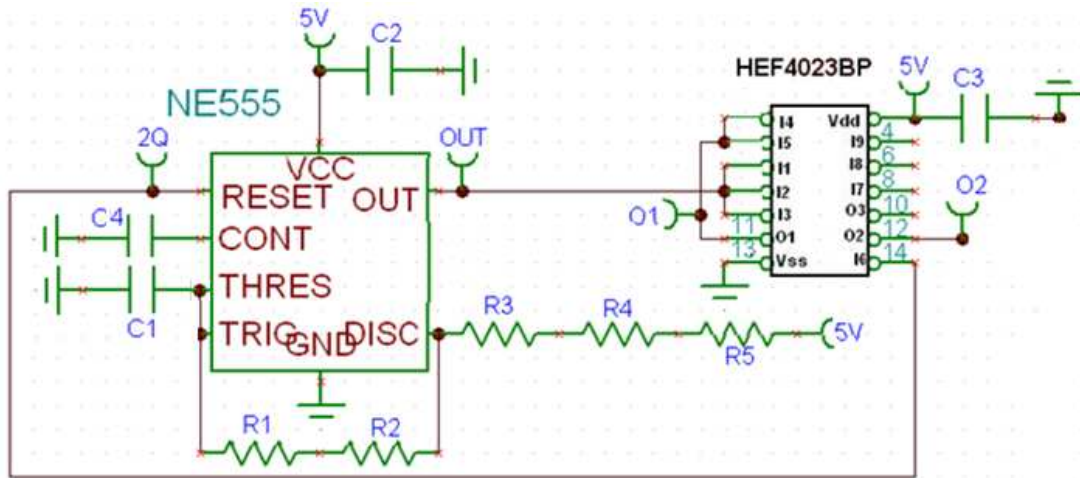


Figure 6:45 - The stimulator pulse width adjustor circuit consists of NE555 astable and NAND gates.

The astable was powered using 5V supply and the supply line was decoupled using 100nF capacitor (C2). The reset pin was connected to 2Q (60s pulse), which switches on the operation of astable circuit.

Capacitor C1 and resistor values were determined using the following formula, with the duty cycle set to 99.7%.

$$t_H = 0.693(R_A + R_B)C1 \quad \text{Equation 6-25}$$

$$t_L = 0.693(R_B)C1 \quad \text{Equation 6-26}$$

where $R_A = R3 + R4 + R5$ and $R_B = R1 + R2$.

Using Equation 6-25 and Equation 6-26 the following component values were obtained $R_A = 9.54k\Omega$, $R_B = 28.8\Omega$ and $C1 = 10\mu F$.

The output of the astable (OUT) was then connected to the 3-input NAND gate, where all the inputs are connected together to act as an inverter. The output of the inverter (O1) and the 2Q (60s pulse) were NAND to produce the inverted stimulation pulses, which was connected to the optocoupler input.

The Figure 6:46 shows the output of the stimulation pulse width adjustor circuit.

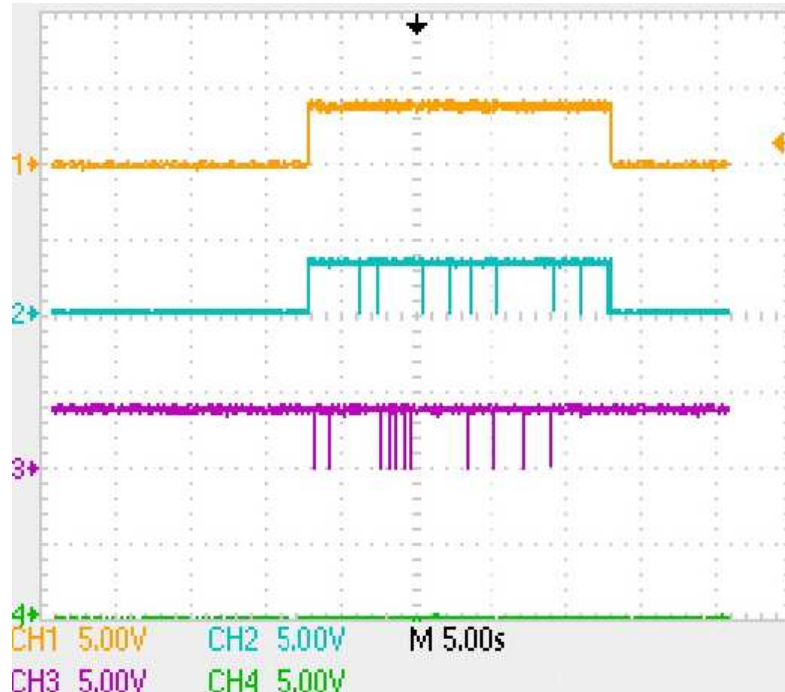


Figure 6:46 – The output of the stimulation pulse width adjustor circuit.

The orange wave shows the 60s pulse (2Q) and the blue shows the output of the astable (OUT). These two signals were then connected the NAND gate and the output of the NAND gate (O2) is shown in the purple waveform. The spacing between the stimulation impulses showed as non-linear, however when this signal is expanded, the stimulation pulses are linear.

In Figure 6:46 some of the stimulation pulses are missing from the actual displayed image, this is due to the effect known as aliasing and in common in digital images. This can be occurred either sampling stage or the reconstruction stage. According to the oscilloscope user manual the sampling rate on each channel is 1GS/s, this is well above the Nyquist frequency; however at a certain recorded time, this oscilloscope can only display 2500 points across all channels and as the display is nearly 120s long, the number of pixels is not sufficient to display all the stimulation pulses.

The output of NAND gate (O2) was then passed on to stimulator circuit through the isolation barrier.

Isolation barrier

When the 200 μ s pulse reached the final stage, these pulses need to be passed through a constant current stimulator. As the high voltages are used in delivering the stimulation pulses, this section needs to be isolated with the rest of the circuit and the recording site of the patient. The reason for this isolation barrier is to avoid the artefact of the stimulation flowing into the reference electrode.

The stimulator requires two supply voltages of 200V and 5V, which are isolated as well as the stimulation pulse adjustor signal. And the following components were used to provide this.

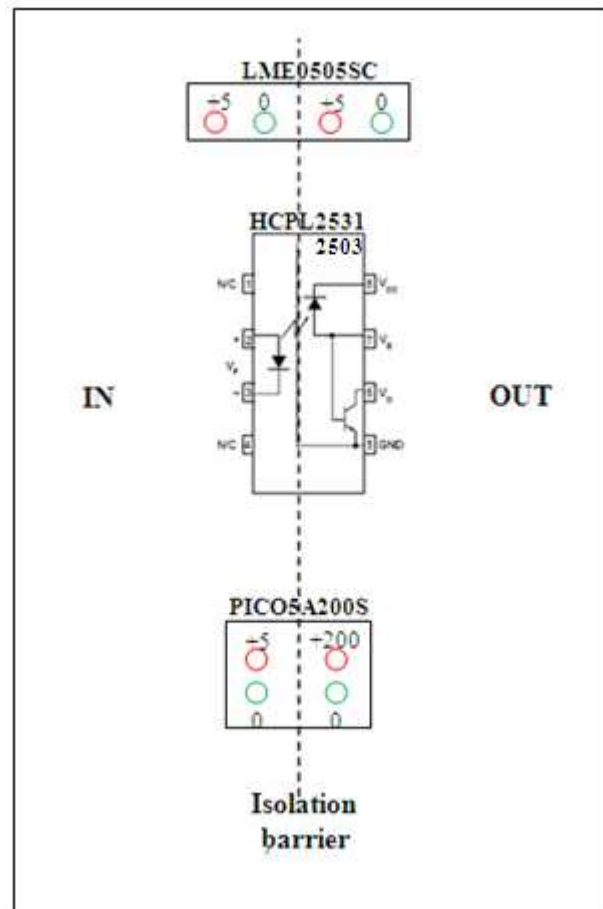


Figure 6:47 - Isolation power supply circuit for the stimulation consist of two DC-DC converters and an optocoupler.

LME0505SC is a DC-DC converter by Murata Power Solution (Figure 6:48) which provides isolated 5V output for input of 5V and has an isolation voltage of 1kV.

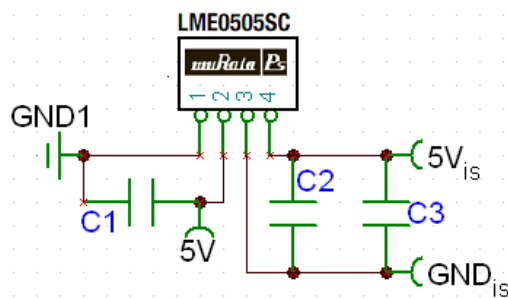


Figure 6:48 - LME0505SC 5V DC-DC converter. $5V_{is}$ is the isolated 5V output and GND_{is} is the isolated ground.

C1 and C2 are 100nF decoupling polyester capacitors to remove high frequency interference; whereas C3 is 35V 33 μ F electrolytic capacitor to remove low frequency noise.

PICO5A200S is an unregulated DC-DC converter by PICO Electronics (Figure 6:49) which produces isolated 200V from 5V input and has an isolation voltage of 500V.

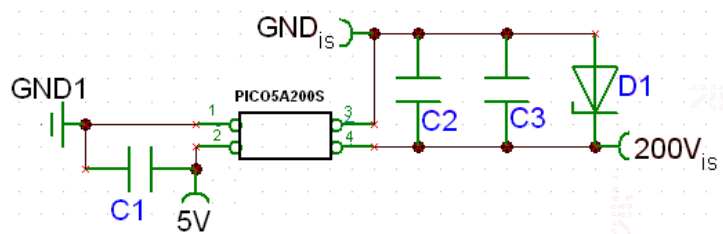


Figure 6:49 - PICO5A200S 5V to 200V DC-DC converter. $200V_{is}$ is the isolated 200V output and GND_{is} is the isolated ground.

C1 is low voltage 100nF decoupling capacitor and C2 is 10nF is 1000V decoupling capacitors to remove high frequency interference; whereas C3 is 450V 10 μ F electrolytic capacitor to remove low frequency noise. Diode D1 is a 220V zener diode to regulate the output of the DC-DC converter.

HCPL2503 is an optocoupler by Fairchild Semiconductor, which produces isolated output stimulating pulses for the input pulses and has an isolation voltage of 480V.

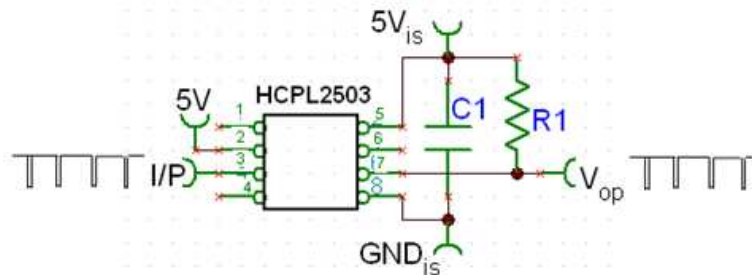


Figure 6:50 - HCPL2503 is an optocoupler consist of LED optically coupled to a high speed photo detector transistor.

The optocoupler is powered by isolated 5V supply and has a decoupling capacitor (C1) of 100nF. R1 is 10kΩ pull-up resistor. I/P to the optocoupler is from the output of the pulse width adjustor circuit and the output of this is passed to PMOS, which will be described later. Once the circuit is connected as shown in the Figure 6:50, there was a drop in input current to the optocoupler and this is shown in the Figure 6:51.

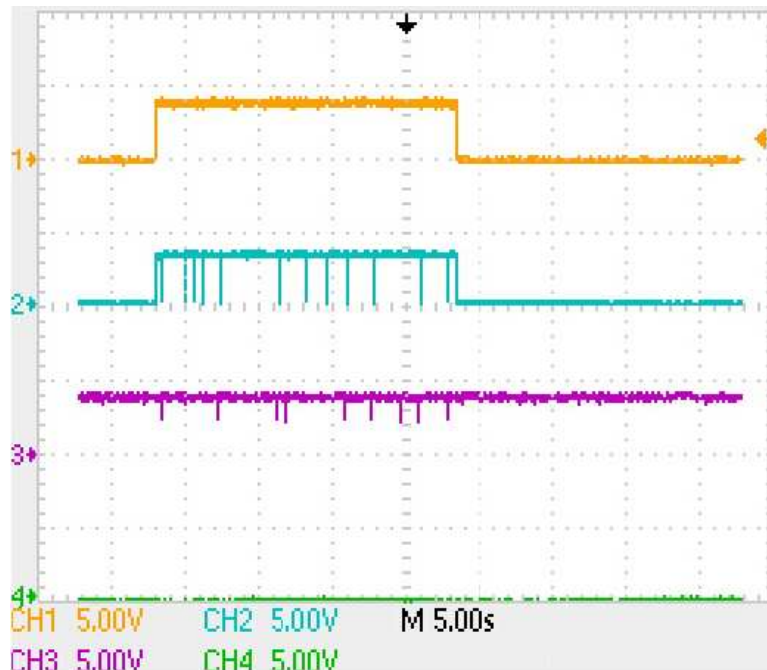


Figure 6:51 - Blue waveform is the output of the astable and the purple waveform is the input to the optocoupler when the HCPL2503 is in place.

Therefore the current level needs to be boosted and for this purpose an emitter follower circuit was built and is shown in the Figure 6:52.

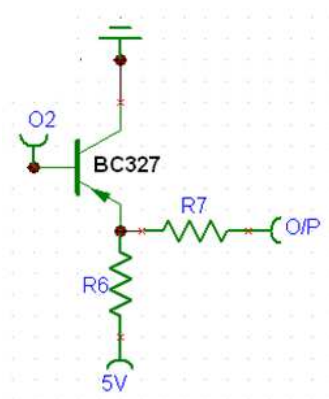


Figure 6:52 - An emitter follower circuit to boost the current entering the optocoupler.

In order to provide the required current boost, R6 and R7 were chosen to be 430Ω and 100Ω. The output of this emitter follower was then connected to the input of the optocoupler.

These isolated power lines and the isolated stimulating pulse will be used in constant current stimulator circuit to deliver the stimulating pulses.

Constant current stimulator

The final part of the circuitry is the constant current stimulator, which will be switched on and off for the input trigger pulse and also has an arrangement to vary the output current level. Figure 6:53 illustrates this arrangement.

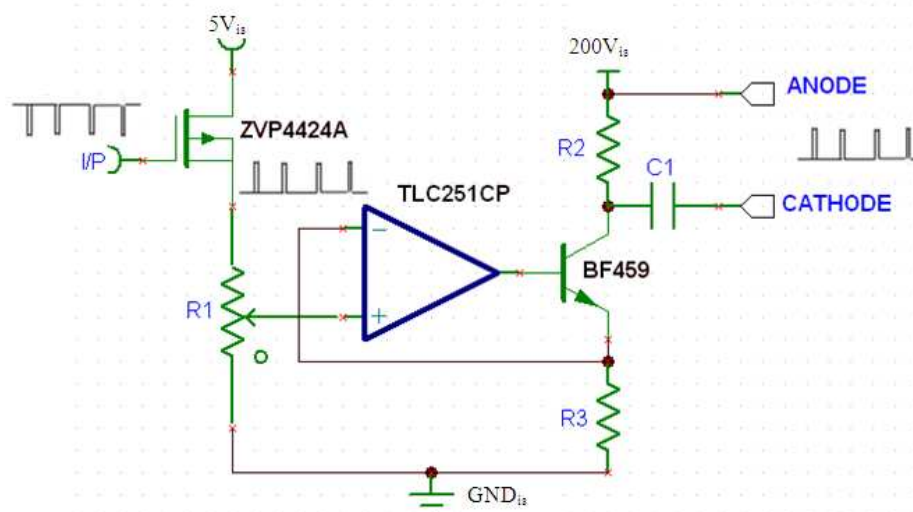


Figure 6:53 - Constant current stimulator circuit.

The anode is connected to the 200V line and when the pulse reached the PMOS and passed over to the amplifier and the transistor setup the potentiometer R1 controls the amount of current to be passed through.

The isolated trigger pulse connected to the gate of the p-channel MOSFET, which acts as a switch. The logic 0, switches on this MOSFET connecting the source to

the drain. The drain of the PMOS connected to the potentiometer R1 (100Ω), which varies the amplitude of the stimulating trigger pulse.

TLC251CP is powered by $5V_{is}$ and decoupled using 100nF capacitor. R3 was set to 10Ω and bias select pin of the op amp is connected to the GND_{is} to increase the amplifier performance [197].

The difference in voltages of the inverting and non-inverting is fed to the base of the BF459. As the collector current increases due to increase in load voltage, the voltage at the inverting input also increases. This decreases the voltage difference, so does the base-emitter voltage, counteracting the increase in output current.

R2 and C1 combination is charge balancing circuit. According to the Figure 6:53, the stimulation off time is about 66ms and if the stimulating charge to be discharges within half this time the values of R2 and C1 can be derived as shown below.

$$\tau_{disc} = R2.C1 \quad \text{Equation 6-27}$$

If $R2 = 10k\Omega$ and $\tau_{disc} = 30ms$, results $C1 = 3\mu F$. Therefore a 250V 3.3μF capacitor was chosen as C1.

The above design was tested on the oscilloscope with a load resistor of 1kΩ between the anode and cathode and the results are shown in Figure 6:54 and Figure 6:55

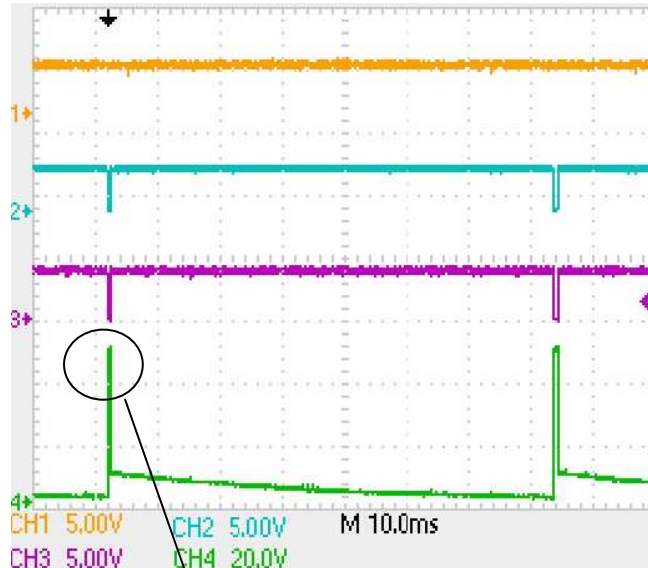


Figure 6:54 – Stimulation pulses The orange wave shows the 60s pulse (2Q) and the blue shows the output of the astable (OUT). Purple waveform shows the output of the optocoupler and stimulator pulses with a frequency of 15Hz shown in the green waveform.

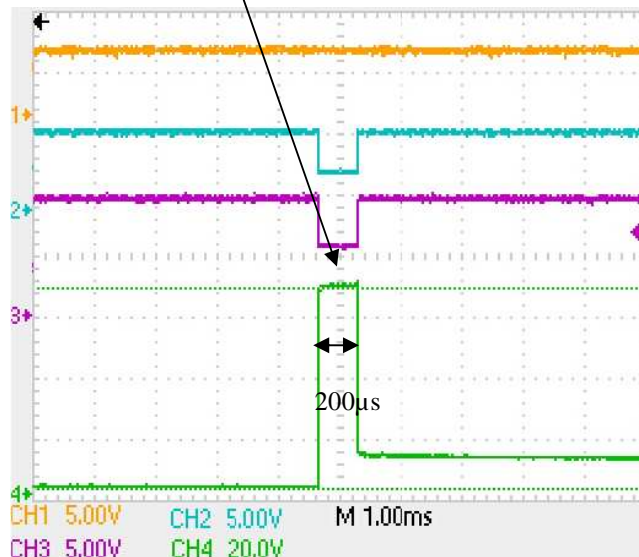


Figure 6:55 – Shows the stimulating pulse of pulse width of 200μs.

The stimulating electrode impedance (726Ω at 26.35°) was measured when the device in the body by measuring from the impedance analyser. The load was

represented by using a resistor (680Ω) and a capacitor (20nF) by calculating the impedance at 1kHz .

In order to determine the effect of supply voltage level, the transfer characteristics of the stimulator was measured. The DC to DC converter was disconnected from the circuit and replaced with a variable power supply. Differential probe of the oscilloscope was connected across the 680Ω resistor in order to measure the load current. When the supply voltage is at 200V the load current was set to 10mA , by adjusting the R1 potentiometer. The supply voltage was reduced from 200V to 0V in steps of 10V , while measuring the load current from the oscilloscope. This experiment was repeated for the load currents of 40mA and 80mA , and the results are displayed in Figure 6:56.

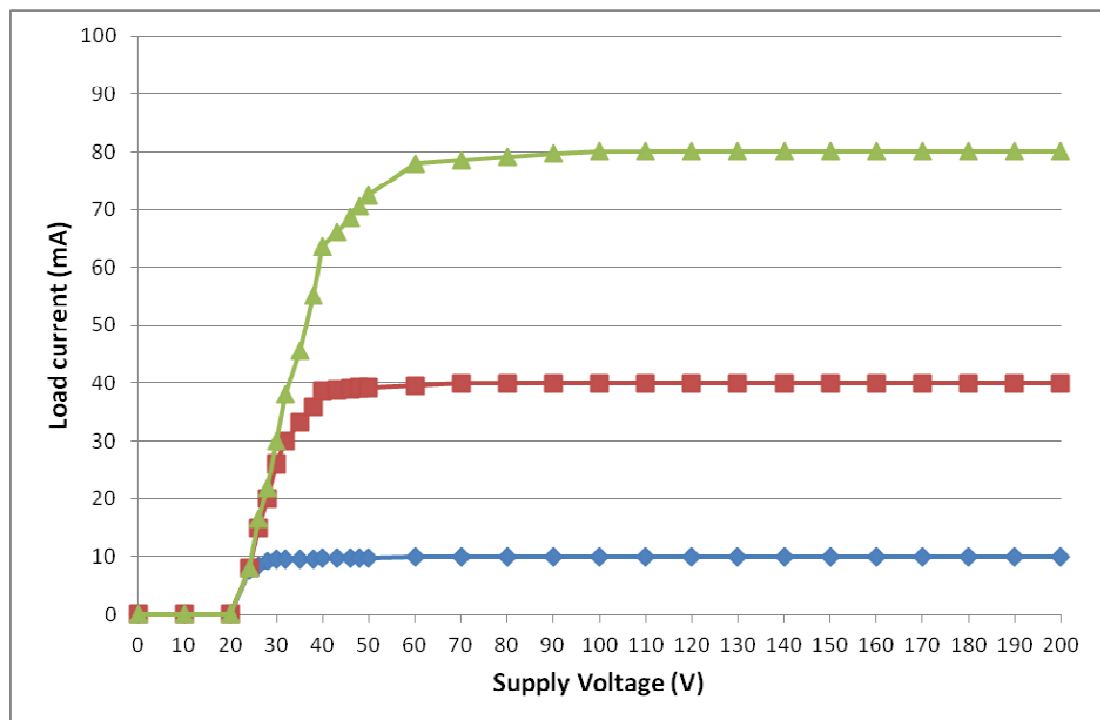


Figure 6:56 - Transfer characteristics of the stimulator

The stimulator circuit that was built is shown in Figure 6:57.

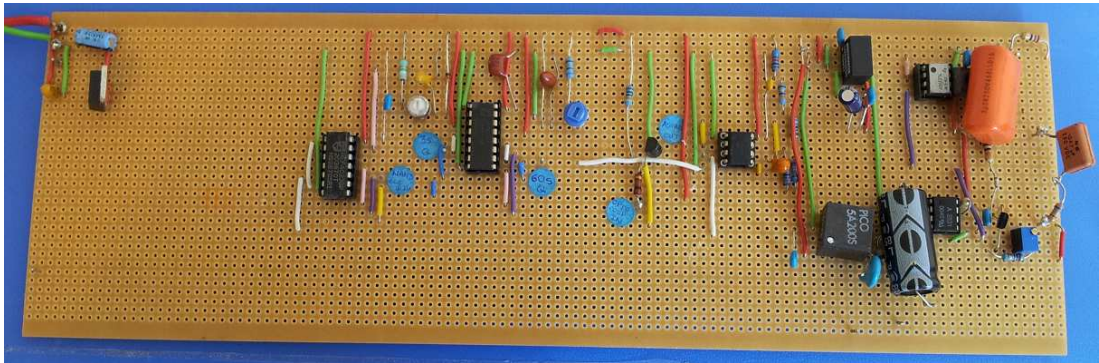


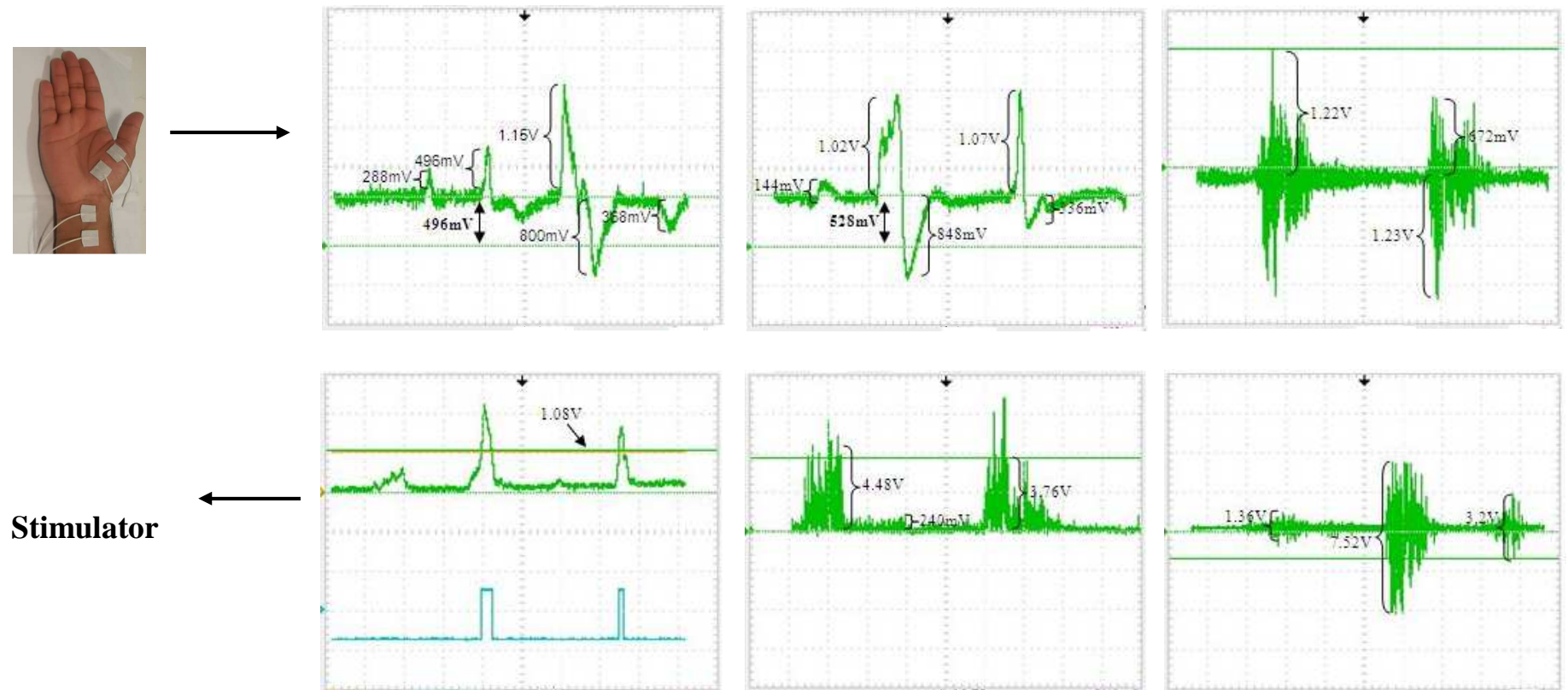
Figure 6:57 - The stimulator circuit.

6.5 Overall system testing

All of the design and testing of the each individual unit were done using the bench apparatus. However the real situation cannot be demonstrated in this manner. Therefore it is essential to test the device with biological signals.

In order to test the system using biological signals, the system was powered by two 9V PP3 batteries and monitored using the oscilloscope through a differential probe due to the safety considerations. EMG signals were recorded from the thenar muscle whereas the stimulating electrodes attached to the wrist using self-adhesive surface electrodes. The skin was cleaned using alcohol wipes and conducting gel was applied to maintain good conductivity. The muscle was voluntarily contracted to investigate whether the output of the comparator goes high and the stimulator was set up to switch on automatically. Section 6.6 highlights the output of each stage with biological signals.

6.6 Results and discussion



- 206 -

Figure 6:58 – Testing the processing circuit on thenar muscle EMG

EMG signals are recorded from the thenar muscle using three electrodes. (a) output of the pre-amplifier (b) output at the notch filter stage (d) output of the high pass filter (e) output after the low pass filtration (e) filtered rectified signal output just before smoothing (f) the smoothed signal (green) and threshold of the comparator was set at 1.08V.

At the output of the pre-amplifier, the EMG contraction and noise can be clearly distinguished. The noise level is further minimised at the output of the notch filter. This signal was then passed onto band-pass filtration to remove DC offset, movement artefact and high frequency noise. The full-wave rectification produces reliable output with low offset level. The three pole smoothing resulted a signal that can be used as a triggering signal for stimulation. The threshold level of the comparator can be varied and when an EMG contraction is detected, the signal is sent to the stimulator to deliver the pulses.

6.6.1 Power management

If the device is switched on throughout the day, the amplifier and the processing circuit will always be switched on. By measurement the recording part of the circuit consumes 25mA. Therefore the charge required to leave the device on for 24 hours = $25\text{mA} \times 24\text{h} = 600\text{mAh}$.

During the stimulation the current consumption in the stimulating circuit is about 125mA, when stimulated with an average current of 60mA. For stimulation, 15 pulses per second each of width 200 μs , therefore the time that the device is on for 60s stimulus duration is $200 \mu\text{s} \times 15 \times 60 = 180\text{ms}$ per stimulation

Clinical studies showed that each fill, around 15-20 stimulation is required to increase the bladder capacity to 500ml, therefore during one day, the stimulation will be required about 60 times. Therefore the total duration of the stimulation required per day = $180\text{ms} \times 60 = 10.8\text{s}$

If the maximum current used during stimulation is 125mA, the total charge required is $125\text{mA} \times 10.8\text{s} = 0.375\text{mAh}$.

Therefore the total charge requires per day is about 600mAh. If 1Ah battery was used, it can be used nearly 2 days without recharging.

6.6.2 Other considerations

Enclosure for the electronic circuit must be waterproof (IP67) and should be easy to hold and control using single hand. The battery changing compartment should be easily accessible by the user, and the enclosure must have a belt clip for the user to be worn it easily. The maximum allowable size of the box is 10cm x 7cm x 3cm. Furthermore the box should also be able to worn on the thigh.

The box should have on/off switch and a button to override the stimulation. Furthermore an indicator for battery low sign and another indicator to show any fault in the system.

The cable from the device should have a mini DIN plug and equivalent socket on the box too.

6.7 Conclusion

The overall system noise was not an issue in signal processing or picking up the EMG contractions. However the noise can be further reduced by the following methods.

- When the system is integrated, the pick up from mains interference will be low (because picking up through cables).
- The attachment of the pre-amplifier to the skin near the electrode site reduces noise pick up and minimise any degradation of the CMRR arising from the differences between the cable resistances [168].

Introducing a notch filter does reduce the mains interference, but it cannot discriminate between hum and the component of the EMG signal at 50Hz, so that the filter distorts the signal [171] [170].

The input signal processing and the stimulation system is isolated using DC to DC converters and optocoupler, which provides an isolation barrier of 480V.

The stimulator supply voltage was set to 200V, however if the maximum voltage required during stimulation can be measured and the system should be modified accordingly, this might result in less current consumption.

By using 1Ah battery, the system can run for 2 days, without needing to be recharged. However if the system can be modified with low power components, this time may increase.

The system mentioned in this chapter was a prototype design, which can be modified with surface mount components in order to obtain the miniaturised and low power circuit.

Chapter 7 - Conclusions and future work

7.1 Summary

Urinary incontinence affects one in three of the population at some stage in their adult lives. This leads to a poor quality of life for sufferers and their families and has significant impact on society. Neurogenic detrusor overactivity is a common observation (16%) in patients with urinary incontinence and is characterised by involuntary detrusor contractions at low bladder volumes. The conventional method of treating NDO is antimuscarinic drugs to relax the detrusor muscle, which are not well tolerated by about 50% of patients mainly due to side effects. Electrical stimulation systems currently available for bladder dysfunction have disadvantages such as risk of implantation and stimulation becomes ineffective due to habituation. Therefore these systems are not widely acceptable among the patients. A novel device was developed in order to overcome the above stated problems. The background leading to this development is explained in detail in chapter 1 together with the aim of the project “to develop a novel wearable anal device designed to deliver conditional neuromodulation and ultimately prove its principle in small scale clinical study.”

Chapter 2 describes the basic anatomy and physiology knowledge required in order to understand the working concept of the device. A review of electrical stimulation for treating bladder dysfunction, since its first use by a pioneering Danish surgeon in 1878 was described in this chapter.

Chapter 3 focuses on the semantics of the operation of the device. The design requirements were derived based on the disadvantages of currently available treatment options. Considering the design requirements, the best method for detecting NDO was by recoding external anal sphincter EMG, which acts as a surrogate to the urethral sphincters during dyssynergia. Similarly trans-rectal stimulation was decided as the best option for intra-anal device. Using these two techniques a closed loop electrical control system was realised and incorporated as the project concept. Furthermore the proposed device was named as “ACONTI” (Anal Conditional Neuromodulator for Treating Incontinence), based on its principle of operation.

After deriving the principle of ACONTI operation, the next step was to come up with a patient acceptable model. The actual shape of the device was designed based on the anatomy of the anal canal as well as literature of anal and vaginal devices. Medical grade liquid silicone rubber was used as the device body material, while medical grade stainless steel was used for the electrodes. The ACONTI was made in clean room environment and the procedure was explained in the chapter 4.

The next step was to determine the efficacy of the ACONTI within the clinical environment, which is described in chapter 5. There are two stages for detecting the conditional signal and treating NDO through neuromodulation. The clinical trials were carried out on spinal cord injured people with NDO in Royal National Orthopaedic Hospital, while giving special attention to good clinical practice. This study concluded that the external anal sphincter EMG recorded through the device provides a reliable signal with 100% sensitivity, for early detection of bladder contractions. Most importantly conditional stimulation through the device successfully suppressed the detrusor contractions in six out of eight patients,

resulting significant increase in their bladder capacity by 220% compared to the control study as well as significant reduction in maximum detrusor pressure by 48%.

In order for the device to be practical for daily use, it should act as a self-standing system. The design of the electronic circuitry required for this operation is described in chapter 6. The system consists of two main circuits for amplification and signal processing as well as for stimulation. The specification for these circuits was derived by evaluating the parameters that were used in the clinical study. The gain of the recording circuit was set to 20000, which can be modified easily and the amplifier has common mode rejection ratio of 88dB. The constant current stimulator can deliver stimulating currents between 10mA to 80mA with maximum stimulating voltage of 200V.

7.2 Achievements

Achievements of this research can be summarised as follows.

- Derived a practical principle for the operation of the ACONTI.
- Designed and implemented a patient acceptable model of ACONTI based on the anatomy of the anal canal.
- The conditional neuromodulation through the device significantly increased the bladder capacity by 220%.
- Designed an electronic circuit, which is capable of providing conditional neuromodulation through the ACONTI device.
- Realised a system, which can be used to optimise the stimulating parameters of the device and verified that with the current configuration of electrodes do stimulate the afferent and efferent branches of the pudendal nerve.

7.3 Future work

As the ultimate goal of this project is to increase the quality of life of people with NDO, there is further work that needs to be carried out to reach this goal.

7.3.1 Clinical testing

This was a proof of principle clinical study to test the operation of the device and demonstrated on spinal cord injured men. However, to determine the efficacy of the ACONTI on wider community, testing should be carried out on both men and women with NDO due to other causes such as multiple sclerosis, Parkinson's disease.

By modifying the device with pressure transducers may lead to use of the device for treating other types of incontinence such as stress and mixed incontinence. These transducers can be added to the superior position of the device. By measuring the abdominal pressure through these transducers, a trigger level can be set to activate the stimulation. As this is a simple modification, it would be an advantage of proceeding further with this concept.

7.3.2 Optimising the device

The current version of the ACONTI device is the first prototype model developed. In order to optimise the recording and stimulating parameters the ACONTI should be modified further.

Shape

Due to a manufacturing limitation, the recording electrodes are situated about 160° apart. The literature has shown if the two recording electrodes can be made

180⁰ degrees apart, will lead to an increase in the signal to noise ratio of the external sphincter EMG. A similar increase can also be expected by pushing the recording electrodes further into the external anal sphincter by widening the recording end of the ACONTI.

The field experiment study should be conducted on different shapes, sizes of the electrodes as well as for the stimulating parameters to decide the best possible arrangement to achieve effective stimulation with a lowest possible current. The findings should be incorporated in to the design of the ACONTI.

With the available anatomical literature it was assumed that when the ACONTI is in the anal canal, the stimulating head sits on the ano-rectal junction. Therefore, it is important to determine the exact positioning of the electrodes using MRI, when the ACONTI is in the anal canal. Results of this will demonstrate the variation of the ACONTI dimensions on different people and if required devices of different sizes should be constructed.

Warning indicator

Chapter 3 shows a requirement of a warning indicator for patients who are unaware about their bladder contractions. It would be ideal to introduce this feature into the ACONTI via a body area network or through a wireless communication link such as Zarlink ZL70100.

Electronic circuitry

The electronic circuit was designed on a matrix-board. It would be better to develop a printed circuit board (PCB) for this design and put this into a box, which will be attached to a belt for the person to wear.

Ultimately this electronic circuitry can be miniaturised and embedded inside the ACONTI with a rechargeable battery on the anchor handle. The Zarlink wireless communication system can be added for programming the system.

7.3.3 Regulatory approval

In order to carry out clinical testing on different types of incontinence, it is required to obtain the approval from Medicine and Healthcare products Regulatory Agency's (MHRA).

References

- [1] Abrams P, Cardozo L, Fall M, Griffiths D, Rosier P, Ulmsten U, vanKerrebroeck P, Victor A and Wein A. The standardisation of terminology of lower urinary tract function: Report from the standardisation sub-committee of the international continence society. *American journal of obstetrics and gynecology* 187[1], 116-126. 1-7-2002.
Ref Type: Report
- [2] Bladder and bowel foundation. How common are bladder and bowel problems. Website . 2007. 9-4-2011.
Ref Type: Electronic Citation

- [3] Vulker R, *International Group Seeks to Dispel Incontinence "Taboo"*. Journal Of the American Medical Association 280, 951-953 (1998).
- [4] NHS. Urinary Incontinence. 30-4-2008. 17-5-2010.
Ref Type: Report
- [5] The Royal College of Physicians. Incontinence - Causes, management and provision of services. 1995.
Ref Type: Report
- [6] Norton PA, MacDonal LD, Sedgwick PM and Stanton SL, *Distress and delay associated with urinary incontinence, frequency and urgency in women*. British Medical Journal 297, 1187-1189 (1988).
- [7] Hu T, Moore K, Subak L, Versi E, Wagner T, Zinner N and Ouslander J. Economics of incontinence. 14, 965-983. 2002. International continence society.
Ref Type: Report
- [8] McDonagh D and Reid A. Living with Urinary Incontinence: Placing the individual at the heart of design research and product development. 2010. Department of Design and Technology, Loughborough University, Leicestershire. 1-6-2010.
Ref Type: Report
- [9] Porth CM and Matfin G, *Disorders of the bladder and lower urinary tract*. In *Essentials of pathophysiology: Concepts of altered health states*. (Ed. Surrena H) pp. 659-678, Lippincott Williams & Wilkins, 2010.
- [10] Milsom I, Abrams P, Cardozo L, Roberts RG, Thüroff J and Wein AJ, *How widespread are the symptoms of an overactive bladder and how are they managed? A population-based prevalence study*. BJU international 87, 760-766 (2001).
- [11] Koelbl H, Mostwin J, Boiteux JP, Macarak E, Petri E, Schafer W and Yamaguchi O. Pathophysiology. 4, 203-241. 2002. International continence society.
Ref Type: Report
- [12] Opisso E, Borau A, Rodriguez A, Hansen J and Rijkhoff NJ, *Patient controlled versus automatic stimulation of pudendal nerve afferents to treat neurogenic detrusor overactivity*. Journal of Urology 180, 1403-1408 (2008).
- [13] de Groat WC, Booth AM and Yoshimura N, *Neurophysiology of micturition and its modification in animal models of human disease, in the*.

In *Nervous control of the urogenital system: Autonomic nervous system*. (Ed. Maggi CA) pp. 227-290, Taylor & Francis, 1993.

- [14] Yoshimura N, *Bladder afferent pathway and spinal cord injury: A possible mechanisms inducing hyperreflexia of the urinary bladder*. *Progress in Neurobiology* 57, 583-606 (1999).
- [15] Bates CP, Bradley WE, Glen ES, Melchior H, Rowan D, Sterling AM, Sundin T, Thomas D, Torrens M, Turner-Warwick R, Zinner NR and Hald T, *Fourth report on the standardisation of terminology of lower urinary tract function. Terminology related to neuromuscular dysfunction of the lower urinary tract*. *British journal of urology* 53, 333-335 (1981).
- [16] Andersson KE, *Antimuscarinics for treatment of overactive bladder*. *Lancet Neurology* 3, 46-53 (2004).
- [17] Lai HH, Boone TB and Appell RA, *Pharmacologic treatment for detrusor overactivity*. *Current urology reports* 3, 365-372 (2002).
- [18] Freeman R and Malvern J, *Drug treatment for detrusor instability*. In *The unstable bladder*. pp. 45-54, Butterworth & Co, 1989.
- [19] The Royal Pharmaceutical Society of Great Britain, *Drugs for urinary frequency, enuresis and incontinence*. In *BNF*. pp. 445-448, RPS, London 2008.
- [20] Yarker YE, Goa KL and Fitton A, *Oxybutynin. A review of its pharmacodynamic and pharmacokinetic properties, and its therapeutic use in detrusor instability*. *Drugs & aging* 6, 243-262 (1995).
- [21] Hopkinson BR and Lightwood R, *Electrical treatment of incontinence*. *The British journal of surgery* 54, 802-805 (1967).
- [22] Alexander S and Rowan D, *Electrical control of urinary incontinence by radio implant. A report of 14 patients*. *The British journal of surgery* 55, 358-364 (1968).
- [23] Hopkinson BR, *Electrical treatment of incontinence using an external stimulator with intra-anal electrodes*. *Annals of the Royal College of Surgeons of England* 50, 92-111 (1972).
- [24] Janez J, Pelvnik S and Suhel P, *Urethral and bladder responses to anal electrical stimulation*. *Journal of Urology* 122, 192-194 (1979).
- [25] Pelvnik S, Vodusek DB and Janez J, *Electrical stimulation treatment of bladder instability*. In *The unstable bladder*. (Ed. Freeman R and Malvern J) pp. 81-92, Butterworth & Co., 1989.

- [26] Brindley GS, Polkey CE, Rushton DN and Cardozo L, *Sacral anterior root stimulators for bladder control in paraplegia: the first 50 cases*. Journal of Neurology, Neurosurgery and Psychiatry 49, 1104-1114 (1986).
- [27] Brindley GS, *The first 500 patients with sacral anterior root stimulator implants: general description*. Paraplegia 32, 795-805 (1994).
- [28] Craggs MD. Neuromodulation device for pelvic dysfunction. [WO/2007/101861]. 6-3-2006.
Ref Type: Patent
- [29] Ciancio SJ, Mutchnik SE, Rivera VM and Boone TB, *Urodynamic pattern changes in multiple sclerosis*. Journal of Urology 57, 239-245 (2001).
- [30] Hansen J, Media S, Nøhr M, Biering-Sørensen F, Sinkjaer T and Rijkhoff NJ, *Treatment of neurogenic detrusor overactivity in spinal cord injured patients by conditional electrical stimulation*. Journal of Urology 173, 2035-2039 (2005).
- [31] Kirkham AP, Shah NC, Knight SL, Shah PJR and Craggs MD, *The acute effects of continuous and conditional neuromodulation on the bladder in spinal cord injury*. Spinal Cord 39, 420-428 (2001).
- [32] Dalmose AL, Rijkhoff NJ, Kirkeby HJ, Nohr M, Sinkjaer T and Djurhuus JC, *Conditional stimulation of the dorsal penile/clitoral nerve may increase cystometric capacity in patients with spinal cord injury*. Neurology and Urodynamics 22, 130-137 (2003).
- [33] Craggs MD and McFarlane J, *Neuromodulation of the lower urinary tract*. Experimental physiology 84, 149-160 (1999).
- [34] Craggs M, Edirisinghe N, Leaker B, Susser J, Al-mukhtar M and Donaldson N, *Conditional neuromodulation using trans-rectal stimulation in spinal cord injury*. Neurology and Urodynamics 28, 836-837 (2009).
- [35] Chaurasia BD, *The urinary bladder and the urethra*. In *Human Anatomy* vol. 2. pp. 345-351, CBS, New Delhi 2006.
- [36] Ganong WF, *Renal function and micturition*. In *Review of Medical Physiology*. pp. 675-703, McGraw-Hill, San Francisco 2002.
- [37] Moore KL and Agur AMR, *Urinary Organs - Pelvis and Perineum*. In *Essential Clinical Anatomy*. pp. 203-270, Lippincott Williams & Wilkins, Toronto 2007.
- [38] Mathers LH, *The autonomic nervous system*. In *The peripheral nervous system*. pp. 123-157, Addison-Wesley, California 1985.

- [39] Hansen JT, *Pelvis and perineum*. In *Netter's Anatomy: companion workbook*. pp. 1-22, Elsevier, New York 2007.
- [40] Balasubramaniam AV. A neurophysiological assessment of the bladder guarding response in spinal cord injury. 2007. London, Institute of Urology and Nephrology, University College London.
Ref Type: Thesis/Dissertation
- [41] Fjorback MV. Electrical stimulation for management of the overactive bladder in patients with multiple sclerosis. 2006. Denmark, Centre for Sensory-Motor Interaction, Department of Health Science and Technology, Aalborg University.
Ref Type: Thesis/Dissertation
- [42] de Groat, *Integrative control of the lower urinary tract - preclinical perspective*. *British Journal of Pharmacology 147 Suppl 2*, S25-S40 (2006).
- [43] Craggs MD, Balasubramaniam AV, Chung EAL and Emmanuel AV, *Aberrant reflexes and function of the pelvic organs following spinal cord injury in man*. *Autonomic neuroscience 126-127*, 355-370 (2006).
- [44] Chapple CR and MacDiarmid SA, *Structure and function of the urinary tract*. In *Urodynamics made easy*. pp. 5-17, Harcourt, Toronto 2000.
- [45] Park LM, Bloom DA and McGuire EJ, *The guarding reflex revisited*. *British journal of urology 80*, 940-945 (1997).
- [46] Fowler C, *Integrated control of lower urinary tract--clinical perspective*. *British Journal of Pharmacology 147*, 14-24 (2006).
- [47] Midland Technical College. The urinary system. 2011. 25.
Ref Type: Slide
- [48] Hald T and Bradley WE, *Neuropathology*. In *The urinary bladder - Neurology and dynamics*. pp. 48-57, Williams and Wilkins, Baltimore 1982.
- [49] Anderson KD, *Targeting recovery: Priorities of the spinal cord-injured population*. *Journal of Neurotrauma 21*, 1371-1383 (2004).
- [50] Spinal cord. The Internet Encyclopedia of Science . 2010. 17-6-2010.
Ref Type: Electronic Citation
- [51] Daneshgari F, Liu G, Birder L, Ann T, Hanna M and Chacko S, *Diabetic bladder dysfunction: current translational knowledge*. *The Journal of urology 182*, 18-26 (2009).

- [52] Julia JJ and Cholham HJ, *Herpes zoster-associated acute urinary retention: a case report*. International urogynecology journal and pelvic floor dysfunction 18, 103-104 (2007).
- [53] Verpoorten C and Buyse GM, *The neurogenic bladder: medical treatment*. Pediatric Nephrology 23, 717-725 (2008).
- [54] Creasey GH, Grill JH, Korsten M, U HS, Betz R, Anderson R and Walter J, *An implantable neuroprosthesis for restoring bladder and bowel control to patients with spinal cord injuries: a multicenter trial*. Archives of Physical Medicine and Rehabilitation 82, 1512-1519 (2001).
- [55] Gomes CM, de Castro FJE, Rejowski RF, Trigo-Rocha FE, Bruschini H, de Barros FTE and Srougi M, *Experience with different botulinum toxins for the treatment of refractory neurogenic detrusor overactivity*. International Journal of Brazilian Society of Urology 36, 66-74 (2010).
- [56] Grosse J, Kramer G and Jakse G, *Comparing two types of botulinum-A toxin detrusor injections in patients with severe neurogenic detrusor overactivity: a case-control study*. BJU international 104, 651-656 (2009).
- [57] Hambrecht FT, *Neural Prostheses*. Annu Rev Biophys Bioeng 8, 239-267 (1979).
- [58] Creasey GH. and Dahlberg JE, *Economic consequences of an implanted neuroprosthesis for bladder and bowel management*. Archives of Physical Medicine and Rehabilitation 82, 1520-1525 (2001).
- [59] Yoo PB and Grill WM, *Minimally invasive electrical stimulation of the Pudendal nerve: A pre-clinical study for neural control of the lower urinary tract*. Neurology and Urodynamics 26, 562-569 (2007).
- [60] van Balken MR, Vergunst H and Bemelmans BL, *The use of electrical devices for the treatment of bladder dysfunction: a review of methods*. The Journal of urology 172, 846-851 (2004).
- [61] Jezernik S, Craggs MD, Grill WM, Creasey G and Rijkhoff NJM, *Electrical stimulation for the treatment of bladder dysfunction: Current status and future possibilities*. Neurological Research 24, 413-430 (2002).
- [62] Griffiths J, *Observations upon the urinary bladder and urethra - Part 3*. Journal of Anatomy of Physiology 29, 254-275 (1895).
- [63] Langworthy OR and Hesser FH, *Reflex vesical contraction in the cat after transection of the spinal cord in the lower lumbar region*. Bulletins of the Johns Hopkins Hospital 60, 204-214 (1937).

- [64] Boyce WH, Lathem JE and Hunt LD, *Research related to the development of an artificial electrical stimulator for the paralysed human bladder*. The Journal of urology 91, 41-51 (1964).
- [65] Ingersoll EH, Jones LL and Hegre ES. Urinary bladder response to unilateral stimulation of pelvic nerves. Proceedings of the society for experimental biology and medicine. 88[1], 46-9. 1955.
Ref Type: Conference Proceeding
- [66] Caldwell KP, *The electrical control of sphincter incompetence*. The Lancet 2, 174-175 (1963).
- [67] Kock NG and Pompeius R, *Inhibition of vesical motor activity induced by anal stimulation*. Acta chirurgica Scandinavica 126, 244-250 (1963).
- [68] Habib HN. Neural trigger points for evacuation of neurogenic bladder by electro stimulation. Surgical forum 14, 489-491. 1963.
Ref Type: Electronic Citation
- [69] Rossier A and Bors E, *Detrusor responses to perianal and rectal stimulation in patients with spinal cord injuries*. Urologia internationalis 18, 181-190 (1964).
- [70] de Groat WC and Ryall RW, *Reflexes to sacral parasympathetic neurones concerned with micturition in the cat*. The Journal of physiology 200, 87-108 (1969).
- [71] Sundin T and Carlsson CA, *Reconstruction of severed dorsal roots innervating the urinary bladder. An experimental study in cats. I. Studies on the normal afferent pathways in the pelvic and pudendal nerves*. Scandinavian journal of urology and nephrology 6, 176-184 (1972).
- [72] Sundin T, Carlsson CA and Kock NG, *Detrusor inhibition induced from mechanical stimulation of the anal region and from electrical stimulation of pudendal nerve afferents. An experimental study in cats*. Investigative urology 11, 374-378 (1974).
- [73] Godec C, Cass AS and Ayala GF, *Bladder inhibition with functional electrical stimulation*. Urology 6, 663-666 (1975).
- [74] Fall M, *Reflex mechanism for bladder inhibition*. Acta Pharmacol Toxicol 43, 13-18 (1978).
- [75] Kondo A, Otani T and Takita T, *Suppression of bladder instability by penile squeeze*. British journal of urology 54, 360-362 (1982).

- [76] McGuire EJ, Morrissey S, Zhang S and Horwinski E, *Control of reflex detrusor activity in normal and spinal injured non-human primates*. Journal of Urology 129, 197-199 (1983).
- [77] Lindström S, Fall M, Carlsson CA and Erlandson BE, *The neurophysiological basis of bladder inhibition in response to intravaginal electrical stimulation*. Journal of Urology 129, 405-410 (1983).
- [78] Nakamura M and Sakurai T, *Bladder inhibition by penile electrical stimulation*. British journal of urology 56, 413-415 (1984).
- [79] Vodusek DB, Light JK and Libby JM, *Detrusor inhibition induced by stimulation of pudendal nerve afferents*. Neurourology and urodynamics 5, 381-389 (1986).
- [80] Fall M and Lindström S, *Electrical stimulation. A physiological approach to the treatment of urinary incontinence*. The Urologic clinics of North America 18, 393-407 (1991).
- [81] Sheriff MK, Shah PJR, Fowler C, Mundy AR and Craggs MD, *Neuromodulation of detrusor hyper-reflexia by functional magnetic stimulation of the sacral roots*. British journal of urology 78, 39-46 (1996).
- [82] Hasan ST, Robson WA and Pridie AK, *Transcutaneous electrical nerve stimulation and temporary S3 neuromodulation in idiopathic detrusor instability*. The Journal of urology 155, 2005-2011 (1996).
- [83] Grill WM, Craggs MD, Foreman RD, Ludlow CL and Buller JL, *Emerging clinical applications of electrical stimulation: opportunities for restoration of function*. Journal of Rehabilitation Research and Development 38, 641-653 (2001).
- [84] Rijkhoff NJM, *Neuroprostheses to treat neurogenic bladder dysfunction: current status and future perspectives*. Child's nervous system 20, 75-86 (2004).
- [85] Fall M, *Advantages and pitfalls of functional electrical stimulation*. Acta obstetricia et gynecologica Scandinavica Supplement 168, 16-21 (1998).
- [86] Hansen J, Borau A, Rodriguez A, Vidal J, Sinkjaer T and Rijkhoff N, *Urethral sphincter EMG as event detector for Neurogenic detrusor overactivity*. IEEE transactions on bio-medical engineering 54, 1212-1219 (2007).
- [87] Pathak AS and Aboseif SR, *Overactive bladder: drug therapy versus nerve stimulation*. Nature clinical practice Urology 2, 310-311 (2005).

- [88] Siegel SW, *Management of voiding dysfunction with an implantable neuroprosthesis*. The Urologic clinics of North America 19, 163-170 (1992).
- [89] Gillenwater JY, Grayhack JT, Howards SS and Mitchell ME, *Voiding Dysfunction: Diagnosis, Classification and Management*. In *Adult and paediatric urology* vol. 2. pp. 1115-1217, Lippincott Williams & Wilkins, Philadelphia 2002.
- [90] Edirisinghe DT. Electrical stimulation for bladder dysfunction may increase fertility rate in women. 2010.
Ref Type: Hearing
- [91] Wheeler JS Jr, Walter JS and Zaszczurynski PJ, *Bladder inhibition by penile nerve stimulation in spinal cord injury patient*. Journal of Urology 147, 100-103 (1992).
- [92] Wenzel BJ, Boggs JW, Gustafson KJ and Grill WM, *Closed Loop Electrical Control of Urinary Continence*. The Journal of urology 175, 1559-1563 (2006).
- [93] Floeter MK, Gerloff C, Kouri J and Hallet M, *Cutaneous withdrawal reflexes of the upper extremity*. Muscle & nerve 21, 591-598 (1998).
- [94] Wenzel BJ, Boggs JW, Gustafson KJ and Grill WM, *Detecting the onset of hyper-reflexive bladder contractions from the electrical activity of the pudendal nerve*. IEEE transactions on neural systems and rehabilitation engineering 13, 428-435 (2005).
- [95] Horvath EE, Yoo PB, Amundsen CL, Webster GD and Grill WM, *Conditional and continuous electrical stimulation increase cystometric capacity in persons with spinal cord injury*. Neurourology and urodynamics 29, 401-407 (2010).
- [96] Lee YH and Creasey GH, *Self-controlled dorsal penile nerve stimulation to inhibit bladder hyperreflexia in incomplete spinal cord injury: a case report*. Archives of Physical Medicine and Rehabilitation 83, 273-277 (2002).
- [97] Kirkham AP, Knight SL, Craggs MD, Casey AT and Shah PJ, *Neuromodulation through sacral nerve roots 2 to 4 with a Finetech-Brindley sacral posterior and anterior root stimulator*. Spinal Cord 40, 272-281 (2002).
- [98] McCreery DB, Agnew WF, Yuen TG and Bullara LA, *Damage in peripheral nerve from continuous electrical stimulation: comparison of two*

stimulus waveforms. Medical & biological engineering & computing 30, 109-114 (1992).

- [99] The Urology Group. Conditions. Website . 2010. 23-7-2010.
Ref Type: Electronic Citation
- [100] Fjorback MV, Rijkhoff N, Petersen T, Nohr M and Sinkjaer T, *Event driven electrical stimulation of the dorsal penile/clitoral nerve for management of neurogenic detrusor overactivity in multiple sclerosis*. Neurology and Urodynamics 25, 349-355 (2006).
- [101] Martens FMJ, van Kuppevelt HJ, Beekman JA, Rijkhoff NJ and Heesakkers J, *Limited value of bladder sensation as a trigger for conditional neurostimulation in spinal cord injury patients*. Neurourology and urodynamics 29, 395-400 (2010).
- [102] Kurstjens GA, Borau A, Rodríguez A, Rijkhoff NJ and Sinkjaer T, *Intraoperative recording of electroneurographic signals from cuff electrodes on extradural sacral roots in spinal cord injured patients*. The Journal of urology 174, 1482-1487 (2005).
- [103] Jezernik S, Grill WM and Sinkjaer T, *Detection and inhibition of hyperreflexia-like bladder contractions in the cat by sacral nerve root recording and electrical stimulation*. Neurology and Urodynamics 20, 215-230 (2001).
- [104] Wenzel BJ, Boggs JW, Gustafson KJ, Creasey GH and Grill WM, *Detection of neurogenic detrusor contractions from the activity of the external anal sphincter in cat and human*. Neurourology and urodynamics 25, 140-147 (2006).
- [105] Fedirchuk B and Shefchyk SJ, *Membrane potential changes in sphincter motoneurons during micturition in the decerebrate cat*. J Neurosci 13, 3090-3094 (1993).
- [106] Thor KB and Muhlhauser MA, *Vesicoanal, urethroanal, and urethrovesical reflexes initiated by lower urinary tract irritation in the rat*. Am J Physiol Regul Integr Comp Physiol 277, R1002-R1012 (1999).
- [107] Blaivas JG, Sinha HP, Zayed AA and Labib KB, *Detrusor-external sphincter dyssynergia: a detailed electromyographic study*. Journal of Urology 125, 545-548 (1981).
- [108] Vodusek DB, Light JK and Libby JM, *Detrusor inhibition induced by stimulation of pudendal nerve afferents*. Neurology and Urodynamics 5, 381-389 (1986).

- [109] Vodusek DB, Pelvnik S, Vrtacnik P and Janez J, *Detrusor inhibition on selective pudendal nerve stimulation in the perineum*. *Neurology and Urodynamics* 6, 389-393 (1988).
- [110] Yang CC and Bradley WE, *Peripheral distribution of the human dorsal nerve of the penis*. *The Journal of urology* 159, 1912-1916 (1998).
- [111] O'Connell HE, Sanjeevan KV and Hutson JM, *Anatomy of the clitoris*. *The Journal of urology* 174, 1189-1195 (2005).
- [112] MacDiarmid SA, Peters KM, Shobeiri SA, Wooldridge LS, Rovner ES, Leong FC, Siegel SW, Tate SB and Feagins BA, *Long-term durability of percutaneous tibial nerve stimulation for the treatment of overactive bladder*. *The Journal of urology* 183, 234-240 (2010).
- [113] Kabay S, Kabay SC, Yucel M, Ozden H, Yilmaz Z, Aras O and Aras B, *The clinical and urodynamic results of a 3-month percutaneous posterior tibial nerve stimulation treatment in patients with multiple sclerosis-related neurogenic bladder dysfunction*. *Neurourology and urodynamics* 28, 964-968 (2009).
- [114] Amarenco G, Even-Schneider A, Ismael SS, Raibaut P, Demaille-Wlodyka S, Parratte B and Kerdraon J, *Urodynamic effect of acute transcutaneous posterior tibial nerve stimulation in overactive bladder*. *The Journal of urology* 169, 2210-2215 (2003).
- [115] Ohlsson BL, Fall M and Frankenberg-Sommar S, *Effects of external and direct pudendal nerve maximal electrical stimulation in the treatment of the uninhibited overactive bladder*. *British journal of urology* 64, 374-380 (1989).
- [116] Eriksen BC, Bergmann S and Mjølnerod OK, *Effect of anal electrostimulation with the 'Incontan' device in women with urinary incontinence*. *British Journal of Obstetrics and Gynaecology* 94, 147-156 (1987).
- [117] Suhel P, *Adjustable non implantable electrical stimulators for correction of urinary incontinence*. *Urologia internationalis* 31, 115-123 (1976).
- [118] Glen ES, *Effective and safe control of incontinence by the intra-anal plug electrode*. *The British journal of surgery* 58, 249-252 (1971).
- [119] Rectum and Anus. Website . 2010. 2-8-2010.
Ref Type: Electronic Citation

- [120] Risk Hansen Spinal Cord Injury Registry. Spinal cord injury - Facts and statistics. 2005. 4-8-2010.
Ref Type: Report
- [121] Gall A and Turner-Stokes L, *Chronic spinal cord injury: management of patients in acute hospital settings*. Journal of the Royal College of Physicians 8, 70-74 (2008).
- [122] Hansen RB, Biering-Sørensen F and Kristensen JK, *Urinary incontinence in spinal cord injured individuals 10-45 years after injury*. Spinal Cord 48, 27-33 (2010).
- [123] Balasubramaniam AV. A neurophysiological assessment of the bladder guarding response in spinal cord injury. 2007. Institute of Urology and Nephrology, University College London.
Ref Type: Thesis/Dissertation
- [124] Geisler WO, Jousse AT, Wynne-Jones M and Breithaupt D, *Survival in traumatic spinal cord injury*. Paraplegia 21, 364-373 (1983).
- [125] Foundation for spinal cord injury prevention care & cure. Spinal cord injury statistics. 2009. National Spinal Cord Injury Statistical Center, Birmingham, Alabama. 4-8-2010.
Ref Type: Report
- [126] Lemack GE, *Clinical evaluation: history and physical examination*. In *Neurogenic Bladder*. (Ed. Corcos J and Schick E) pp. 413-417, Informa Healthcare, Canada 2008.
- [127] Rackley R, Vasavada SP, Firoozi F and Ingber MS. Neurogenic Bladder. Emedicine, Medscape . 2009. 4-8-2010.
Ref Type: Magazine Article
- [128] Brindley GS, Rushton DN and Craggs MD, *The pressure exerted by the external sphincter of the urethra when its motor nerve fibres are stimulated electrically*. British journal of urology 46, 453-462 (1974).
- [129] Alexander S and Rowan D, *An electric pessary for stress incontinence*. The Lancet 1, 728 (1968).
- [130] Edwards L and Malvern J, *Electronic control of incontinence: A critical review of the present situation*. British journal of urology 44, 467-472 (1972).
- [131] DeSoldenhoff R and McDonnell H, *New device for control of female urinary incontinence*. British Medical Journal 230 (1969).

- [132] Merrill DC, Conway C and deWolf W, *Urinary incontinence: Treatment with electrical stimulation of the pelvic floor*. *Urology* 5, 67-72 (1975).
- [133] Sotiropoulos A, *Urinary incontinence management with electronic stimulation of muscles of pelvic floor*. *Urology* 6, 312-318 (1975).
- [134] Alexander S, Rowan D, Millar W and Scott R, *Treatment of urinary incontinence by electric pessary - A report of 18 patients*. *British journal of urology* 42, 184-190 (1970).
- [135] TensCare. Continence products. Website . 2011. 14-2-2011.
Ref Type: Electronic Citation
- [136] Netter FH and Colacino S, *Atlas of human anatomy*, CIBA-GEIGY Corp, 1989.
- [137] Olsen IP, Wilsgaard T and Kiserud T, *Transvaginal three-dimensional ultrasound: a method of studying anal anatomy and function*. *Ultrasound Obstet Gynecol* 37, 353-360 (2011).
- [138] Glen ES, *Intra-anal electrode: A stimulus to bowel and bladder control*. *Journal of Pediatric Surgery* 6, 138-142 (1971).
- [139] Snell R, *The perineum*. In *Clinical anatomy by regions*. pp. 387-425, Lippincott Williams & Wikins, 2007.
- [140] Dauber W, *Alimentary system*. In *Pocket atlas of human anatomy*. pp. 134-163, New York 2000.
- [141] Binnie NR, Kawimbe BM, Papachrysostomou M, Clare N and Smith AN, *The importance of the orientation of the electrode plates in recording the external anal sphincter EMG by non-invasive anal plug electrodes*. *International Journal of Colorectal Disease* 6, 5-8 (1991).
- [142] Ellis H, Logan B and Dixon A, *Pelvis*. In *Human sectional anatomy - Atlas of body sections, CT and MRI images*. pp. 149-192, Butterworth-Heinemann, 1999.
- [143] Curtis J and Colas A, *Medical applications of silicones*. In *Biomaterial science - An introduction to materials in medicine*. (Ed. Dow Corning Corporation) pp. 697-706, Elsevier Inc, 2011.
- [144] Courtney J and Gilchrist T, *Silicone rubber and natural rubber as biomaterials*. *Medical and Biological Engineering and Computing* 18, 538-540 (1980).

- [145] NuSil Technology. MED-4940 Liquid Silicone Rubber Product Profile. 2007.
Ref Type: Data File
- [146] Donaldson N. Electrodes 2. 2008. 15.
Ref Type: Slide
- [147] Newson T. Stainless steel - A family of medical device materials. 1, 1-3. 2002.
Ref Type: Report
- [148] Prutchi D and Norris M, *Stimulation of excitable tissues*. In *Design and development of medical electronic instrumentation*. pp. 305-368, John Wiley & Sons, Inc., New Jersey 2005.
- [149] Craggs MD, Edirisinghe N, Leaker B, Susser J, Al-mukhtar M and Donaldson N, *Conditional neuromodulation using trans-rectal stimulation in spinal cord injury*. *Neurology and Urodynamics* 28, 836-837 (2009).
- [150] Wyndaele JJ, *Correlation between clinical neurological data and urodynamic function in spinal cord injured patients*. *Spinal Cord* 35, 213-216 (1997).
- [151] Balasubramaniam AV. Neurophysiological assessment of the bladder guarding responses in spinal cord injury. 2007. UCL.
Ref Type: Thesis/Dissertation
- [152] Macfarlane MT, *Voiding disorders*. In *Urology*. pp. 134-144, Lippincott Williams and Wilkins, Philadelphia 2006.
- [153] Chapple CR and MacDiarmid SA, *Urodynamic techniques*. In *Urodynamics made easy*. pp. 19-73, Harcourt, Toronto 2000.
- [154] Lectromed UK Ltd. Lectromed 5361 isolated biopotential amplifier user manual. 1995.
Ref Type: Catalog
- [155] Digitimer. Digitimer Constant Current Stimulator Operator's Manual. 9. 26-9-2007.
Ref Type: Catalog
- [156] Dolan L, Elnaqa A, Hosker G, Hunt D, Knight S, Lucas M, Neale T, Parker J, Ramage C, Singh G, Swithinbank L, Tooze-Hobson P, Townsend J and Webb R. Joint statement on minimum standards for urodynamic practice in the UK. 1, 7-31. 2009.
Ref Type: Report

- [157] Dalsome AL, Rijkhoff NJM, Kirkeby HJ, Nohr M, Sinkjaer T and Djurhuus JC, *Conditional stimulation of the dorsal penile/clitoral nerve may increase cystometric capacity in patients with SCI*. *Neurology and Urodynamics* 22, 130-137 (2003).
- [158] Walters-Williams J and Li Y, *Comparative study of distance functions for nearest neighbors*. In *Advanced techniques in computing sciences and software engineering*. (Ed. Elleithy K) pp. 79-84, Springer science, Bridgeport 2009.
- [159] Previnaire JG, Soler JM, Perrigot M, Boileau G, Delahaye H, Schumacker P, Vanvelcenaher J and Vanhee JL, *Short-term effect of pudendal nerve electrical stimulation on detrusor hyperreflexia in spinal cord injury patients: importance of current strength*. *Paraplegia* 34, 95-99 (1996).
- [160] Vereecken RL, De Meirman J, Puers B and Van Mulders J, *Electrophysiological exploration of the sacral conus*. *Journal of Neurology* 227, 135-144 (1982).
- [161] Prévinaire JG, Soler JM, Perrigot M, Boileau G, Delahaye H, Schumacker P, Vanvelcenaher J and Vanhée JL, *Short-term effect of th epudendal nerve electrical stimulation on detrusor hyperreflexia in spinal cord injury patients: importance of current strength*. *Paraplegia* 34, 95-99 (1996).
- [162] Shah NC, Knight SL, Shah PJ and Craggs MD, *Optimisation of stimulation for conditional neuromodulation of detrusor hyperreflexia*. *European Urology* 35, 16 (1999).
- [163] Schalow G, Zach GA and Warzok R, *Classification of human peripheral nerve fibre groups by conduction velocity and nerve fibre diameter is preserved following spinal cord lesion*. *Journal of the Autonomic Nervous System* 52, 125-150 (1995).
- [164] Kestenbaum B, *Screening*. In *Epidemiology and biostatistic:an introduction to clinical research*. pp. 121-138, Springer Science, Washington, USA 2009.
- [165] Koldewijn EL, Van Kerrebroeck PE, Rosier PF, Wijkstra H and Debruyne FM, *Bladder compliance after posterior sacral root rhizotomies and anterior sacral root stimulation*. *Journal of Urology* 151, 955-960 (1994).
- [166] Ogino K and Kozak W. *Spectrum analysis of surface electromyogram (EMG)*. *Acoustics, Speech, and Signal Processing, IEEE International Conference. ICASSP '83*. 8, 1114-1117. 1983. Ohio University Athens, Ohio.
Ref Type: Conference Proceeding

- [167] Rangayyan RM, *Introduction to biomedical signals*. In *Biomedical signal analysis*. (Ed. IEEE press) pp. 1-59, Wiley-Interscience, Alberta, Canada 2002.
- [168] Bartlett R, *The anatomy of human movement*. In *Introduction to sports biomechanics: Analysing human movement patterns*. pp. 223-280, Routledge, New York 2007.
- [169] De Luca CJ. *Surface Electromyography: Detection and recording*. Electronic publication . 2002.
Ref Type: Electronic Citation
- [170] Mewett DT, Reynolds KJ and Nazeran H., *Reducing power line interference in digitised electromyogram recordings by spectrum interpolation*. *Medical and Biological Engineering and Computing* 42, 524-531 (2004).
- [171] Mewett DT, Nazeran H and Reynolds KJ. *Removing power line noise from recorded EMG*. *Engineering in Medicine and Biology*. 23rd Annual International Conference of IEEE 3, 2190-2193. 2001.
Ref Type: Conference Proceeding
- [172] Lu G, Brittain JS, Holland P, Yianni J, Green AL, Stein JF, Aziz TZ and Wang S, *Removing ECG noise from surface EMG signals using adaptive filtering*. *Neruoscience Letters* 462, 14-19 (2009).
- [173] D. T. Mewett, *Reducing power line interference in digitised electromyogram recordings by spectrum interpolation*. *Medical & biological engineering & computing* 42, 524-531 (2004).
- [174] Schweitzer TW, Fitzgerald JW and Bowden JA, *Spectral analysis of human inspiratory diaphragmatic electromyograms*. *Journal of applied physiology: Respiratory, environmental and exercise physiology* 46, 152-165 (1979).
- [175] Lectromed. *Lectromed 5361 Isolate Bio-potential Amplifier*. 2006. Lectromed UK Ltd, Herts.
Ref Type: Catalog
- [176] CED. 1401plus. 1997. Cambridge, UK.
Ref Type: Catalog
- [177] Nagel JH, *Biopotential Amplifiers*. In *The Biomedical Engineering Handbook* vol. 2. pp. 70-1-70-15, Florida 2000.
- [178] Berson AS and Pipberger HV, *Skin-electrode impedance problems in electrocardiography*. *The American heart journal* 76, 514-525 (1968).

- [179] Casas O and Pallas-Areny R, *Optimal bias circuit for instrumentation amplifiers*. Proceeding of 14th IMEKO world conference 4, 143-148 (1997).
- [180] Burr-Brown Corporation. INA 118 - Precision, Low Power Instrumentation Amplifier. 1998.
Ref Type: Data File
- [181] Spinelli E and Haberman M, *Insulating electrodes: a review on biopotential front ends for dielectric skin–electrode interfaces*. Physiological Measurement 31, 183-198 (2010).
- [182] Galjan W, Hafkemeyer KM, Tomasik JM, Wagner F, Krautschneider WH and Schroeder D. Highly sensitive biomedical amplifier with CMRR calibration and DC-offset compensation. EUROCON 2009. IEEE Xplore , 152-155. 2009. IEEE Xplore. 18-5-2009.
Ref Type: Conference Proceeding
- [183] Radio-Electronics. Operational amplifier / op amp notch filter circuit. Radio-Electronics.com . 2010.
Ref Type: Electronic Citation
- [184] Graf RF, *Filters (Notch)*. In *Converter and Filter Circuits*. pp. 77-89, Butterworth-Heinemann, 1996.
- [185] Kumngern M, Lerkvaranyu S and Dejhan K. Wide-band CMOS precision rectifier circuit. Communications and Information Technologies, 2008. ISCIT 2008. International Symposium on. 315-320. 21-10-2008.
Ref Type: Conference Proceeding
- [186] Antoniou A., *Design of precision rectifiers using operational amplifiers*. Electrical Engineers, Proceedings of the Institution of 121, 1041-1044 (1974).
- [187] Elliott R. Precision rectifiers. Website . 2009. Elliott sound products. 24-7-2010.
Ref Type: Electronic Citation
- [188] Jones D and Stitt M. Precision absolute value circuit. Burr-Brown application bulletin . 1997. Burr-Brown.
Ref Type: Electronic Citation
- [189] Ballou G. AC 2 DC. Millimeter . 2001.
Ref Type: Electronic Citation
- [190] Rectification and smoothing. Lecture note - EM08 . 2010.
Ref Type: Electronic Citation

- [191] Bronzite M, *Simple active filters - design procedure*. Wireless world 117-119 (1970).
- [192] Webster JG, *Basic concepts of electronics*. In *Bioinstrumentation*. pp. 28-91, John Wiley & Sons, Inc, 2004.
- [193] De Lima JA and Cordeiro AS. A simple constant-current neural stimulator with accurate pulse-amplitude control. 23rd Annual EMBS International Conference. IEEE proceedings , 1328-1331. 2001. 25-10-2001.
Ref Type: Conference Proceeding
- [194] Digitimer Research Instruments. Stimulators. Digitimer website . 2010.
Ref Type: Electronic Citation
- [195] Philips Semiconductors. Dual retriggerable precision monostable multivibrator. 1993.
Ref Type: Data File
- [196] Kumar V, *Astable and monostable multivibrator*. In *Digital electronics - theory and experiments*. pp. 93-104, New Age International (P) Ltd, New Delhi, India 2006.
- [197] Texas Instruments. TLC251 LinCMOS programmable low-power operational amplifiers. 1983. Dallas, Texas.
Ref Type: Data File

Appendix 1 – Patient consent form



CONSENT FORM

Agreement to participate in a clinical investigation

Investigators: Professor MD Craggs, Director of Spinal Research
Dr A Gall FRCP, Consultant Rehabilitation Physician
Mr PJR Shah FRCS, Consultant Urological Surgeon
Mr J Woodhouse MRCS, Clinical Research Fellow, Urologist
Sr J Susser, RGN, Clinical Nurse Specialist

1. I have read the information sheet concerning this study and I understand what will be required of me if I take part in this study.
2. My concerns regarding this study have been answered by
.....
3. I understand that at any time I may withdraw from this study without giving a reason and without affecting my normal care and management.
4. I understand that the information from this study may be published in scientific journals, but that I will not be identified.
5. I agree to take part in this study.

Patient's signature or independent witness.....

Name in BLOCK LETTERS

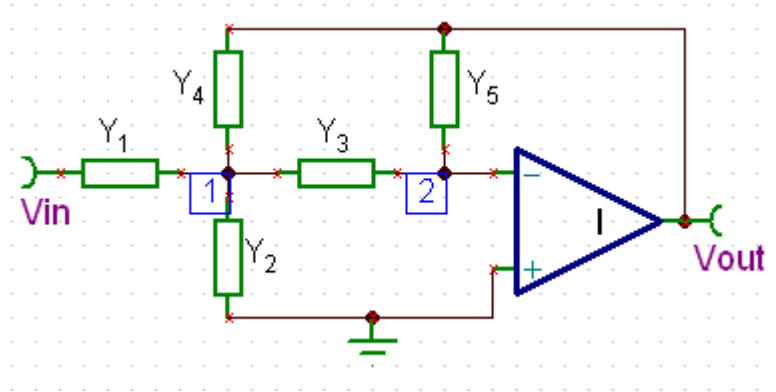
Date

Doctor's signature

Name in BLOCK LETTERS

Date

Appendix 2 – Multiple feedback filter design



Nodal analysis at node 1

$$(V_1 - V_{in})Y_1 + V_1Y_2 + V_1Y_3 + (V_1 - V_{out})Y_4 = 0 \quad \text{Eq. 1}$$

Rearranging, gives

$$V_1(Y_1 + Y_2 + Y_3 + Y_4) - V_{out}Y_4 - V_{in}Y_1 = 0 \quad \text{Eq. 2}$$

Nodal analysis at node 2

$$V_{out}Y_5 + V_1Y_3 = 0 \quad \text{Eq. 3}$$

Rearranging, gives

$$V_1 = -\frac{V_{out}Y_5}{Y_3}$$

Substituting V_1 in equation 2,

$$-\frac{V_{out}Y_5}{Y_3}(Y_1 + Y_2 + Y_3 + Y_4) - V_{out}Y_4 - V_{in}Y_1 = 0$$

Finally,

$$\frac{V_{out}}{V_{in}} = \frac{-Y_1Y_3}{Y_5(Y_1 + Y_2 + Y_3 + Y_4) + Y_3Y_4}$$